

# **Electrocardiogram Analysis for Robust Optimal Thresholding System Design**

*Thesis submitted in fulfilment of the requirements for the Degree of*

**DOCTOR OF PHILOSOPHY**

By

**NAVDEEP PRASHAR**



Department of Electronics and Communication Engineering  
JAYPEE UNIVERSITY OF INFORMATION TECHNOLOGY  
WAKNAGHAT, DISTRICT SOLAN, H.P., INDIA

December, 2020

*Dedicated to*  
*My*  
*Beloved Parents, Wife*  
*and*  
*Sons*

# TABLE OF CONTENTS

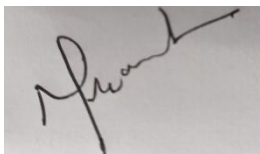
Contents	Page No.
DECLARATION BY THE SCHOLAR .....	vi
SUPERVISOR’S CERTIFICATE .....	vii
ACKNOWLEDGEMENT .....	viii
LIST OF ABBREVIATIONS AND ACRONYMS .....	x
LIST OF FIGURES.....	xiii
LIST OF TABLES .....	xv
ABSTRACT .....	xvii
<b>CHAPTER 1</b> .....	<b>1</b>
<b>INTRODUCTION</b> .....	<b>1</b>
1.1 Heart Anatomy .....	3
1.2 ECG Events and Segments.....	4
1.3 Acquisition on ECG .....	7
1.4 Distinct noises in ECG Signals .....	9
1.5 Heart Related Diseases.....	11
1.5.1 Cardiac Arrhythmia.....	12
1.6 ECG Database .....	18
1.7 Software Used .....	19
1.8 Performance Evaluation Parameters .....	19
1.9 Motivation .....	20
1.9.1 Scope of Research Work.....	21
1.10 Research Gaps.....	21
1.11 Objectives Framed .....	23

1.12 Organization of Thesis .....	23
<b>CHAPTER 2.....</b>	<b>24</b>
<b>REVIEW OF STATE-OF- THE-ART-TECHNIQUES .....</b>	<b>24</b>
2.1 Review Based on Removal of Artifacts .....	26
2.2 Review on Event Detection .....	35
2.3 Review on Noise Estimator .....	37
<b>CHAPTER 3.....</b>	<b>44</b>
<b>BIO-SIGNAL PROCESING FRAMEWORK FOR ECG SIGNALS .....</b>	<b>44</b>
3.1 Bio-signals.....	45
3.2 Bio-signal Processing .....	47
3.3 Removal of Artifacts .....	48
3.3.1 Frequency Domain Filtering .....	49
3.3.2 Optimal Filtering .....	56
3.3.3 Proposed Cascade Digital Filter Design.....	62
3.3.4 Time-Frequency Domain Filters.....	65
3.4. Event Detection .....	76
3.5 Summary .....	86
<b>CHAPTER 4.....</b>	<b>87</b>
<b>DESIGN OF ROBUST DENOISING SYSTEM.....</b>	<b>87</b>
4.1 Introduction .....	88
4.2 Optimal Threshold Denoising Method .....	88
4.2.1 Threshold Functions .....	89
4.2.2 Threshold Value Selection.....	91
4.3. Conventional Noise Estimator .....	92
4.4 Proposed Methodology for Denoised System.....	93
4.5 Results and Discussion.....	97
4.5.1 Results for Conventional Estimator .....	98
4.5.2 Results for Proposed Estimator .....	100

4.5.3 Optimal Threshold Tuning.....	104
4.5.4 Curve Fitting.....	107
4.5.5 Comparison with State-of-the-Art Work.....	108
4.6 Summary .....	108
<b>CHAPTER 5.....</b>	<b>110</b>
<b>DISTRIBUTION MODELLING FOR ECG DENOISING SYSTEM DESIGN</b> .....	<b>110</b>
5.1 Introduction .....	111
5.2 The Proposed Denoised Approach.....	114
5.3 Results and Discussion.....	116
5.3.1 Results of Varying Distribution Functions.....	117
5.3.2 Proposed results by introducing Downscaling Factor ( $2^n$ ).....	127
5.4 Optimal Threshold System Design.....	131
5.5 Summary .....	133
<b>CHAPTER 6.....</b>	<b>135</b>
<b>CONCLUSION AND FUTURE SCOPE.....</b>	<b>135</b>
6.1 Conclusion.....	136
6.2 Future Scope .....	138
LIST OF PUBLICATIONS .....	139
REFERENCES.....	142
APPENDICES.....	156

## **DECLARATION BY THE SCHOLAR**

I hereby declare that the work contained in the Ph.D thesis entitled “**Electrocardiogram Analysis for Robust Optimal Thresholding System Design**” submitted at **Jaypee University of Information Technology, Wagnaghat, India** is an authentic record of my work carried out under the supervision of **Dr. Shruti Jain and Dr. Meenakshi Sood**. I have not submitted this work elsewhere for any other degree or diploma. I am fully responsible for the contents of my Ph.D. thesis.



**Navdeep Prashar**

Enrollment No.: 166005

Department of Electronics and Communication Engineering

Jaypee University of Information Technology,

Wagnaghat, Solan, H.P-173234

Date: 29-12-2020



# JAYPEE UNIVERSITY OF INFORMATION TECHNOLOGY

(Established by H.P. State Legislative vide Act No. 14 of 2002)  
P.O. Wagnaghat, Teh. Kandaghat, Distt. Solan - 173234 (H.P.) INDIA

Website: [www.juit.ac.in](http://www.juit.ac.in)

Phone No. (91) 01792-257999

Fax: +91-01792-245362

## SUPERVISOR'S CERTIFICATE

This is to certify that the work reported in the Ph.D. thesis entitled “**Electrocardiogram Analysis for Robust Optimal Thresholding System Design**”, submitted by **Navdeep Prashar** at **Jaypee University of Information Technology, Wagnaghat, India**, is a bonafide record of his original work carried out under my supervision. This work has not been submitted elsewhere for any other degree or diploma.

*Shruti Jain*

**Dr. Shruti Jain**  
**Associate Professor**  
Department of ECE  
Jaypee University of Information  
Technology, Wagnaghat, Solan  
H.P, India

*Meenakshi Sood*

**Dr. Meenakshi Sood**  
**Associate Professor**  
Department of CDC  
National Institute of Technical  
Teachers Training & Research,  
Chandigarh, India

## ACKNOWLEDGEMENT

*First of all, I owe and dedicate everything to the **Almighty GOD** for the strength, wisdom and perseverance that he had bestowed upon me during this research project, and indeed, throughout my life. A major research project like this can never be achieved by the only person's effort. The contribution of number of people in different aspects have made this happen. I extend my sincere gratitude to everyone who stood by me during the entire course of my Ph.D. work.*

*I would like to express my special appreciations and sincere thanks to my supervisor **Dr. Shruti Jain & Dr. Meenakshi Sood** for sharing their truthful and illuminating views on a number of issues related to my topic of research and encouraging my research and allowing me to grow as a research scientist. They provided inspiring guidance for successful completion of my research work. I rate this as my privilege to work under their supervision. Your advice on both researches as well as on my career has been priceless. I have been blessed with your continuous moral support, invaluable inputs and suggestions when I needed the most.*

*My heartfelt appreciation to **Prof. M J Nigam**, the then Head of Department of Electronics and Communication, for his co-operation, support and constant encouragement. I am grateful to all the members of technical and non-technical staff especially **Mr. Pramod Kumar** for their valuable contributions.*

*I am also thankful to Dr. Hem Raj Saini, Dr. Rajiv Kumar and Dr. Shewta Pandit for their guidance and valuable suggestions throughout my research work. I wish to convey my sincere thanks to all the faculty members of Department of Electronics and Communication Engineering, for their help and guidance at the various stages of this study.*

*Life is miserable without parents and beloved ones. I can't forget the pain that my parents have taken throughout my research work. It is only because of their support, love and blessings that I could overcome all frustrations and failures. Last but not least, I would like*



*to thank my **parents, wife and relatives** for their unconditional support, both financially and emotionally throughout my Ph.D. They always stood by my decision and provided me all the resources even in difficult times to help me to achieve my goals and realize my dreams. I am also thankful to my beloved wife **Mrs. Ashima Sharma**, Sons **Aadit** and **Dhairya** for their moral support. I would also like to thanks **Dr. SC Sharma, Mr. Vineet Kumar** and **Dr. Sushil Chaudhary** from my work place (Bahra University) for their motivation and continuous support.*

*Besides, I can never ever forget my friends **Ashish Goswami, Nithin Varma, Vikas Ucharia, Gautam Kumar** and **Kamal Rana** who have helped me in numerous ways. I cherish the time spent in the Department of Electronics and Communication Engineering, JUIT, Wajnaghat.*

*I am indebted to all those people who have made this dissertation possible and because of whom this research experience and wonderful journey shall remain everlasting and cherished forever in my sweet memories.*

*All may not be mentioned, but no one is forgotten.*

***Thanks to all of you!***

***Navdeep Prashar***

## LIST OF ABBREVIATIONS AND ACRONYMS

ECG	Electrocardiogram
CVDs	Cardio Vascular Diseases
WHO	World Health Organization
AV	Atrio-Ventricular
AP	Atrial Premature
BW	Baseline Wander
PLI	Power line interference
NSR	Normal Sinus Rhythm
PJC	Premature Junctional Contractions
VT	Ventricular Tachycardia
LBBB	Left Bundle Branch Block Beat
RBBB	Right Bundle Branch Block Beat
MIT	Massachusetts Institute of Technology
BIH	Beth Israel Hospital
DCT	Discrete Cosine Transform
DWT	Discrete Wavelet Transform
CWT	Continuous Wavelet Transform
HT	Hilbert Transform
FFT	Fast Fourier transform
STFT	Short-Term Fourier transform
IDWT	Inverse Discrete Wavelet Transform

IIR	Infinite Impulse Response
FIR	Finite Impulse Response
AOLC	Adaptive Linear Orthogonal Combiner
RLS	Recursive Least-Squares
WT	Wavelet Transform
DTCWT	Dual Tree Complex Wavelet Transform
IDTCWT	Inverse Dual Tree Complex Wavelet Transform
SWT	Stationary Wavelet Transform
GA	Genetic Algorithm
WT	Wavelet Transform
ERG	Electroretinogram
MSE	Mean Square Error
PRD	Percent Root Deviation
SNR	Signal to Noise Ratio
PSNR	Peak Signal to Noise Ratio
ENG	Electroneurogram
MMG	Mechanomyogram
LMS	Least Mean Square algorithm
NLMS	Normalized Least Mean Square algorithm
MTD	Mallet Tree Decomposition
PDA	Peak Detection Algorithm
EMD	Empirical mode decomposition
MAD	Median Absolute Deviation
LMDS	Least Median Square

MP	Median Product
DB	Daubechies
ECE	Energy Contribution Efficiency
GMM	Gaussian Mixture Modeling
EEMD	Ensemble Empirical Decomposition Mode
IMFs	Intrinsic Mode Functions
BWT	Baseline Wander Tracking
MODWT	Maximal Overlap Discrete Wavelet Transform
FDM	Fourier Decomposition Method
PDF	Probability Density Function
IMFs	Intrinsic Mode Functions

## LIST OF FIGURES

<b>Figure No.</b>	<b>Title</b>	<b>Page No.</b>
1.1	Heart anatomy	4
1.2	The typical ECG wave pattern	5
1.3	Electrodes placement for ECG measurement	8
1.4	Einthoven equilateral triangle	8
1.5	(a) Normal sinus rhythm, (b) Sinus tachycardia	13
1.6	Atrial arrhythmias, (a) PAC, (b) Atrial tachycardia, (c) Atrial Flutter, (d) Atrial fibrillation	15
1.7	Junctional rhythm	15
1.8	Ventricular arrhythmias (a) PVC, (b) VT, (c) Ventricular Fibrillation	16
1.9	Atrioventricular Blocks (A) first degree, (B) Second degree, (C) Third degree	17
1.10	Bundle Branch blocks	18
2.1	Pie Chart displays the proportion of world-wide deaths owing to distinct Cardiovascular diseases	25
3.1	Representation of Bio-signal: (a) 1-D ECG Waveform (b) 2-D Human Brain (c) 3-D view of an infant of pregnant women	46
3.2	Structural Diagram of Bio-signal Processing	48
3.3	Frequency Domain Filters	49
3.4	Frequency spectrum of filtered ECG signal (a) Rectangular window, (b) Kaiser window, (c) Hanning window, (d) Hamming window, (e) Blackman window	51
3.5	Filtered ECG frequency spectrum using Notch Filter	53
3.6	ECG signal through IIR Low Pass Filter (a) Butterworth (b) Chebyshev (c) Elliptic	55
3.7	Generalized structure of Adaptive Filter	57
3.8	Analysis of ECG signal in time domain using LMS algorithm	60

3.9	Analysis of ECG signal in time domain using NLMS algorithm	60
3.10	Frequency spectrum of ECG signal using (a) LMS algorithm (b) NLMS algorithm	61
3.11	Block diagram of Proposed Cascade Digital Filter	62
3.12	Time domain analysis by Cascaded Filter	63
3.13	Spectral analysis of ECG signal filtered by Cascaded Filter design	63
3.14	Flow chart of time –frequency domain signal filtering	66
3.15	Mallet Tree Decomposition	67
3.16	Denoised ECG signal using bior3.9 wavelet	70
3.17	Dual tree complex wavelet transform	72
3.18	Reconstructed signal using DTCTWT	75
3.19	Peak detection of clean ECG signal employing PDA	80
4.1	Proposed Methodology	93
4.2	Input ECG signal	94
4.3	Removal of Low frequency component from ECG signal	94
4.4	Detail coefficients at 4 <sup>th</sup> level decomposition	95
4.5	Approximation coefficients	95
4.6	Denoised ECG signal	97
4.7	Block diagram summarizing the results of different threshold value and threshold functions using proposed estimator	105
4.8	Curve Fitting Plot	107
5.1	Methodology Adopted for ECG denoising using Different Distribution Functions	115
5.2	Performance analysis for different distribution function using conventional and proposed estimator	122
5.3	Proposed robust noise estimator for distinct value of $n$	128
5.4	Optimal Threshold System Design	131

## LIST OF TABLES

<b>Table No.</b>	<b>Title</b>	<b>Page No.</b>
1.1	ECG interval with duration	6
3.1	SNR Evaluation of Window based FIR filters	52
3.2	SNR Evaluation using Approximation based Low Pass IIR filter	56
3.3	SNR Evaluation of Adaptive filter using different algorithm	61
3.4	SNR computation of Cascade Digital Filter	64
3.5	Comparison of Cascade Filter with state-of-the- art-work	64
3.6	Performance evaluation of distinct wavelet families	69
3.7	Coefficients of Detail and Approximation at each sub band assuming sampling frequency ( $f_s$ ) 360 Hz	73
3.8	Comparison of DTCWT with State -of- the-Art-Work	76
3.9	Different Peaks and Intervals of distinct ECG records using Proposed Cascade Digital Filter Design	81
3.10	Different Peaks and Intervals of distinct ECG records using Mallet Tree Decomposition	82
3.11	Different Peaks and Intervals of distinct ECG records using DTCWT Technique	83
3.12	Impact of Arrhythmias on Peak Morphology	84
3.13	Calculation of R-R Intervals for different Techniques	85
4.1	Different types of Threshold value selection rules	91
4.2	Evaluation of SNR values for Conventional estimator	98
4.3	Evaluation of MSE values for Conventional estimator	99
4.4	Evaluation of PRD values for Conventional estimator	99
4.5	Evaluation of SNR values for proposed estimator	100
4.6	Evaluation of MSE for proposed estimator	101
4.7	Evaluation of PRD for proposed estimator	101
4.8	SNR computation of distinct threshold value selection and threshold function using proposed estimator	102

4.9	Comparative Analysis of conventional and proposed estimator	104
4.10	SNR Comparison of 100 -109 records arrhythmia database	106
4.11	Comparison of Proposed estimator with State of Art Work	108
5.1	SNR Evaluation of Proposed estimator with $n =1$ using Normal distribution	117
5.2	MSE Evaluation of Proposed estimator with $n =1$ using Normal distribution	118
5.3	PRD Evaluation of Proposed estimator with $n=1$ using Normal distribution	118
5.4	SNR Evaluation of Proposed estimator with $n = 1$ using Exponential distribution	119
5.5	MSE Evaluation of Proposed estimator with $n=1$ using Exponential distribution	120
5.6	PRD Evaluation of Proposed estimator with $n = 1$ using Exponential distribution	120
5.7	Performance Analysis of Proposed estimator with $n = 1$ using Gaussian distribution	121
5.8	Comparison Table of performance metrics using different distribution functions	121
5.9	Performance Evaluation for MIT-BIH Arrhythmia Database for Normal and Gaussian distribution functions with proposed estimator	123
5.10	Proposed noise estimator downscaled by $2^n$ using normal distribution	127
5.11	PSNR Evaluation of Proposed Estimator using $2^3$ factors for 100-107 record	129
5.12	Comparison with State-of-the- art- techniques	130
5.13	Event Detection employing Optimal Threshold System	132
5.14	Computation of Heart Beat Rate	133



## **ABSTRACT**

The Electrocardiogram (ECG) is a most prominent and economical technique that has been used as the standard approach for diagnosis of cardiovascular disease through the investigation of the heart rate and the morphological analysis. Presence of different noises in ECG signals designated as Baseline wander, Power-line interference, Burst noise and Electromyography degrades the perceptual quality and performance that results into false interpretation of ECG by clinicians. The denoised ECG signals and accurate event detection of signals can be used for design of automated heart diseases analysis model.

The different Bio-signal Processing methods are examined in this research for removal of artifacts and event detection. For ECG denoising and signal quality improvement the Frequency domain filtering, optimal filtering and Time–Frequency domain filtering techniques are used. Frequency domain filtering involves design of High pass FIR Filter using windowing techniques; Notch Filter and Low pass IIR Filter using approximation methods. The analysis of these approaches depicts that High pass FIR Filter using Blackman window is more effective for elimination of low frequency Baseline wander noise whereas Low pass IIR filters Elliptic approximation method is found to have more potent for removing high frequency electromyography noise and IIR Notch filter for suppression of Power-line interference persists at 50 Hz. Optimal filtering includes the design of adaptive filters using LMS and NLMS algorithm for removal of burst noise. An NLMS algorithm introduces less error in the signal while the weight equation of LMS algorithm continuously update to recent input data. By employing high performance filters (both frequency domain filtering and optimal filtering), a cascade digital filter design is proposed that eliminates distinct noises present in the ECG signal which exhibits significant SNR improvement of 7.75dB at the cost of more computational complexity, large memory requirement that restricts its use for analysis of non-stationary signals. In this regard, time-frequency domain filtering is used for evaluation and refining of signals, since it distributes the energy of the signal in space (time and frequency). Time-Frequency domain filtering includes Mallet Tree Decomposition (MTD and Dual tree Complex Wavelet Transform (DTCWT) techniques for noise reduction. The performance evaluation metrics depicts that DTCWT outperforms in comparison to MTD and distinct state of art strategies as it reduces the distortion in the output

signal by providing shift-invariance and directional selectivity and restrict the aliasing effect. Further, detection of principal peaks ( $P, Q, R, S, T$ ) and their intervals are executed employing Peak Detection Algorithm (PDA) to extract clinical significant information from the filtered ECG signal for Proposed Digital Cascade Filter, MTD and DTCWT. The DTCWT technique perceives its efficiency in computing the  $R-R$  interval as compared with MIT-BIH Arrhythmia Database (Gold Standard).

Enhancement of non-stationary ECG signals by suppressing background noise is very important in signal processing. The additive background noise deteriorates the perceptual features of the original signal. The noise may be inherited to these non-stationary signals during recording or communicating from one place to other place. A robust noise estimation approach is proposed using optimal threshold tuning for ECG denoising. The proposed and conventional noise estimator is used to apply and evaluate eight distinct sets of threshold value selection rules along with six distinct threshold functions on MIT-BIH arrhythmia database. The optimal threshold tuning is achieved by using Non-negative Garrote threshold function with universal modified level-dependent threshold value selection that overcomes the limitation of over-killing the useful information. The proposed noise estimator accomplished magnificent performance evaluation results as 54.98dB SNR,  $2.03e-07$  MSE and 0.005 PRD in comparison to the conventional noise estimator having 45.67 dB SNR and  $1.73e-06$  MSE and 0.005 PRD that signifies 20.38% SNR improvement of proposed robust noise estimator than conventional estimator. Further, Curve fitting plot for conventional and proposed noise estimator for verification are plotted and analyzed for distinct records of MIT-BIH Arrhythmia database.

To supervise the trade-off between distortion of signal and residual noise for removal of estimated noise in highly non-stationary and distinct noisy environments, the proposed robust noise estimator is empowered with  $2^n$  downscaling factor to restrict spurious high frequency information from ECG signal. Further, applying the threshold limits without model fitting for non-stationary ECG signals have demonstrated a significant difference between the data sets of similar parameters measured over a different time period. Different probability distribution functions (Gaussian, Normal and Exponential) are exploited for signal measurement that contains random noise and gross error. Different performance metrics such as SNR, MSE, and PRD are determined which reflects the signal denoising by applying a finer downscaling factor for  $n = 1, 2, 3$  and 4 values and selecting the best distribution function and collaterally evaluating the signal quality by analyzing the PSNR value. The computational outcomes

depicts that the proposed robust noise estimator with  $n = 3$  downscaling factor by employing Normal distribution delivers high SNR 80.72 dB, sharp PSNR 92.63dB, low MSE  $5.45e-10$  and small PRD  $9.21e-05$  that signifies the considerable reduction of noise by subsequently improving the quality of the signal.

Finally, an *Optimal Threshold System* is designed to compute accurate Heart rate for precise detection and diagnosis of Cardiac Arrhythmias.

**Keywords:** Electrocardiogram, Denoising, Peak Detection Algorithm, Dual Tree Complex Wavelet Transform, Threshold Values, Threshold Functions, Noise Estimator, Distribution Functions.

# **CHAPTER 1**

## **INTRODUCTION**

# CHAPTER 1

## INTRODUCTION

Cardio Vascular Diseases (CVDs) has been identified as one of the main issues for health care and associated medical diagnostic advancements in 21<sup>st</sup> century. World Health Organization (WHO) raised their concern regarding the consequences of CVDs as a leading cause of global mortality. It constitutes about 31% of global deaths in 2012 [1]. WHO has set a global goal to reduce the overall mortality by 25% that occur due to some life-threatening diseases like CVD, cancer and chronic respiratory till 2025 drawing serious attention towards prevention and cure of CVDs. In this regard, an electrocardiogram (ECG) plays an important role in depicting the Cardiac disorder.

An electrocardiogram is a graphic record provided by an electrocardiograph that tracks the heart's electrical activity over a time frame [2]. By measuring the electrical potential between the body's various location ECG signal is acquired. ECG signals have wide applications in the field of medical sciences to assess the heart functioning. Any disruption in the heart rhythm or variation in physiological pattern indicates CVDs symptoms, which are examined through the ECG. ECG simulates the electrical activity by polarizing and depolarizing the cardiac tissue and converting it into a waveform. ECG is classified as non-stationary signal therefore the emergence of aperiodic irregularities and their occurrence at indefinite intervals. This waveform tests the heart rate, heart size and chamber position [3]. In general, the ECG signal consists of [4]

- i. Rhythm of the heart and heart rate
- ii. Impulse origin and its transmission
- iii. Variability in the concentration of electrolytes

As a consequence, ECG is commonly used by practitioners around the world as a primary tool for assessing the heart condition as it provides substantial data on the valuable parts of the cardiovascular system. Early diagnosis of heart disease can improve lifetime as well as raise the quality of living through specific care. This chapter broadly describes the ECG signal description, frequently found artifacts during its acquisition, transmission and classification of different heart related disease.

## **1.1 HEART ANATOMY**

The Heart is the principal component of human cardio-vascular system [6]. It pumps oxygenated blood through circulatory systems into the entire human body. Heart uses veins for collection of deoxygenated blood from other parts of body for blood purification. This vital organ is located in the chest midst to the lungs beyond the sternum and over the diaphragm. The anatomy of heart comprises four chambers: two atrium and two ventricles (right and left) along with number of Atrio- Ventricular (AV) and Sino- Atrial (SA) nodes. The right atrium and right ventricle are accountable for blood circulation among the heart and lungs. Impure blood from the body to the right atrium is carried through two large veins defined as superior and inferior venacava. During the contraction of right atrium, the blood streams to the right ventricle through tricuspid valve. This tricuspid valve is remained open as long as the right ventricle is filled. With the contraction of right ventricle the blood pumps out of heart via pulmonic valve to enter the lungs through pulmonary artery to perform oxygenation process [7]. The left atrium and the left ventricle are accountable for circulating the blood rich in oxygen between the heart and rest body parts. During the contraction of left atrium, the blood moves from left atrium towards left ventricle via mitral valve. [7]. At the time of left ventricle contraction the oxygenated blood moves out of the heart via aortic valve into the blood vessels. The entire process of blood circulation is classified into two phases named as systole and diastole phase. Systole is expressed as the heart ventricular muscle phase of the contraction whereas the diastole is described as the phase of heart ventricular muscle relaxation allowing the chambers to fill up with blood [8]. Generally; the cardiac muscles have negative polarity. The cross-sectional view of human heart as depicted in Fig.1.1 [9].

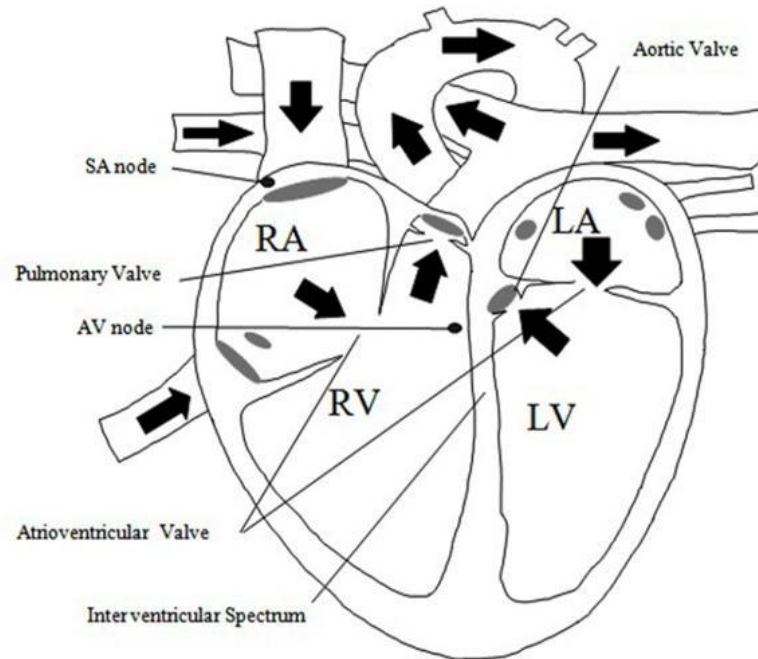


**Figure 1.1:** Heart anatomy [9]

Throughout the diastolic phase of the ventricle, the pure blood move into the left ventricle via mitral valve from left atrium and impure blood move into the right ventricle via tricuspid from the right atrium. During the systolic cycle of the ventricle, pure blood moves out of the left ventricle to the whole body via aortic valve opening through the aorta, and impure blood moves out of the right ventricle to the lungs via semi-lunar valve opening through the pulmonary artery. The main task of human heart is to perform rhythmic contraction and to assist the blood movement for oxygenation and to the entire body. This ideal rhythm is constantly sustained by the electrical impulse produced by the sino-atrial node.

## 1.2 ECG EVENTS AND SEGMENTS

ECG depicts the electrical representation of the contractile behavior of the human heart [10]. The heart rhythm is appraised as beats per minute (bpm). The standard ECG pattern is depicted in Figure 1.2. The ECG signal comprises of five waves *P*, *Q*, *R*, *S*, *T* that provides the valuable information to diagnose the disorders and heart rhythm's rate. It records electrical

pulses that are generated at different parts of the human heart. These features provide the important information about the presence of different diseases that affects the human heart [11].

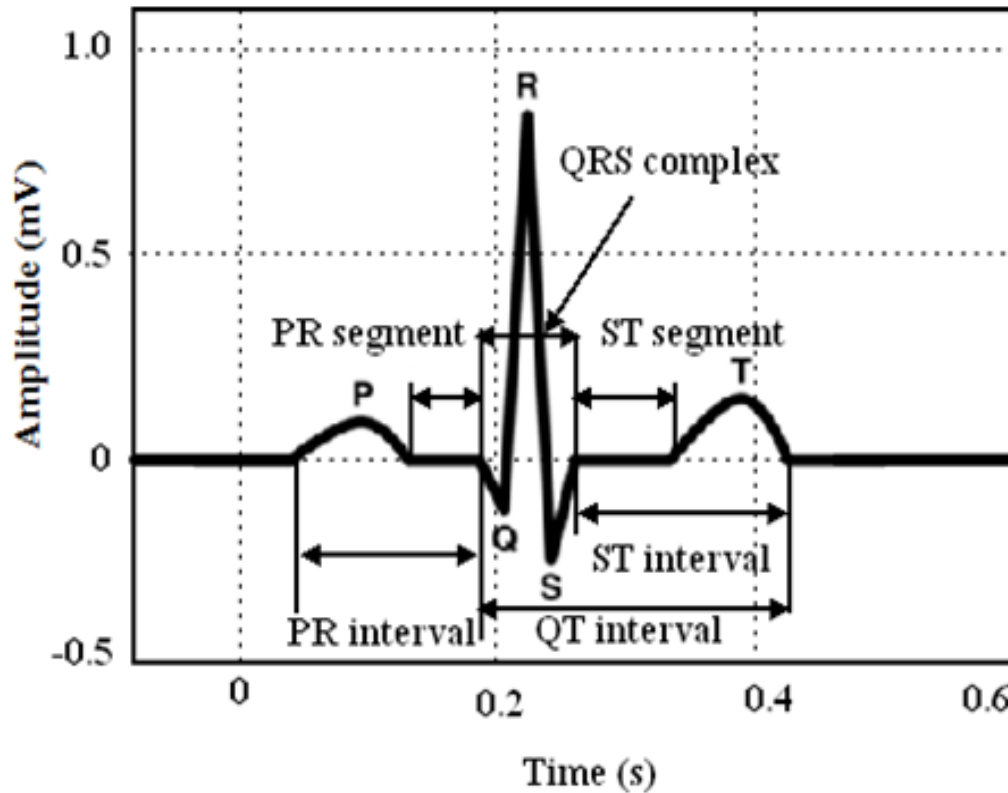


**Figure 1.2:** The typical ECG wave pattern [10]

Each portion of a heartbeat extended a diverse sweep across the ECG. A brief overview of the ECG waves is as follows:

*P Wave* – The first slight deflection of pulse is known to be *P* type wave. The low amplitude of this wave is depicted due to the atrium depolarization and contraction. The upward or downward deflection of wave is dependent the electrical activity is going towards or away from the lead.

*Q Wave* - It is the initial downward deflection after the occurrence of *P* wave that defines the depolarization of the ventricle.

*R Wave* - *R* wave determines the foremost upward deflection after the occurrence of *P* wave. It shows ventricular depolarization.



*S Wave* - *S* wave determines the initial negative deflection after the occurrence of *R* type wave. This shows the depolarization of the ventricle.

*T Wave* - *T* wave reflects the ventricle repolarization. This type of wave has large values that represent ischemia and Hyperkalaemia.

*U Wave* - *U* wave is depicted after the occurrence of *T* wave produced in the midst of the late repolarization of Purkynje filaments in ventricles.

Detection of ECG peaks and their intervals have clinical significance in the field of cardiology. Variations in ECG peaks and their interval represent the heart condition of subjects. Different segments of ECG along with their normal duration values [12] are shown in Table 1.1.

**Table.1.1** ECG interval with normal duration [12]

Interval	Interpretation	Normal Duration
RR interval	The intervening time between two consecutive R waves. Heart normal resting rate is 60-100 bpm.	0.6 to 1.2s
PR interval	The interval PR is computed from the emergence of the P wave to the initiation of the QRS complex. This interval represents the time needed for the electrical impulse to pass across the AV node from the sinus node and into the ventricles. So this interval is an indication of the function of the AV node	0.12 to 0.20s
QRS complex	This is used to measure the rate of muscle contraction in the heart and to detect issues with heart rate regularity. R wave represent the highest point in QRS complex.	0.06 to 0.12s
ST interval	The ST interval is determined from the point J to the onset of T wave.	0.05 to 0.15s
QT interval	The interval QT is determined from the origin of the QRS complex till the ending of T wave. A prolonged duration of QT contributes towards premature death and ventricular tachyarrhythmia's.	0.33to 0.46s

Analysis of these segments and intervals are useful for early detection of cardiovascular diseases [13]. These events and segments are able to predict the individual's health and provide the cardiologists an upper edge to diagnose the heart related problems.

### 1.3 ACQUISITION OF ECG

Human heart electrical behaviour is specified as the total sum of electrical impulses belongs to all cardiac cells. This can be examined as variations to the signal voltage occur on the body surface. The heart has unique mechanism for producing and performing action potentials by a dynamic shift of ion concentration through the membrane of cells. [14]. The heart cell consists of an ion conductor differentiated through semi-permeable membrane that serves as a ion filter selector. Fluids of ionic body surround the cells that bring bioelectric signal conduction. These fluids compose mostly of sodium ( $Na^+$ ), potassium ( $K^+$ ) and chloride ( $Cl^-$ ) salts. The membrane vary its attributes because the cell is stimulated by external stimuli or ionic currents which allow the entering  $Na^+$  ions into a cell that induces an effect called as avalanche due to the difference in the membrane characteristics. As  $Na^+$  ions migrate through the cell equally responding the  $K^+$  ions attempts to exit the cell due to their higher concentration in the cell, but are impotent to travel due to their slower movement relative to the  $Na^+$  ions movement [15]. The electrical activity of the lead is conveyed between the reference point and the electrode. This clinical information is essential for the selection of the electrode position [16]. Once the surge of  $Na^+$  ion ceases, an equilibrium state comes into account. This transition marks the initiation of potential of around +20 mV peak value. The action potential produced by the excited cells leads to the depolarization process. With due course of time, these depolarized cell is again polarized and returns to the resting position by a mechanism defined as repolarization. This repolarization cycle is equivalent to depolarization, except to the condition that the dominant  $K^+$  ions are considered for repolarization than  $Na^+$  ions. As a consequence, the process of polarization and depolarization related to cardiac tissue produces the electrical impulses which later transformed into a waveform called an

ECG signal. The Right Leg (*RL*), Right Arm (*RA*), Left Leg (*LL*), Left Arm (*LA*), and Chest (*C*) are the five different electrodes used for ECG monitoring [17, 18] as seen in Fig.1.3.

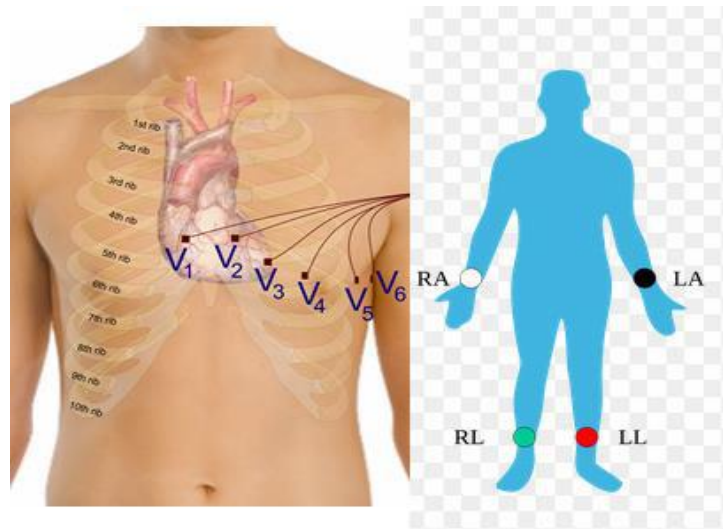


**Figure 1.3:** Electrodes placement for ECG measurement [18]

All of these electrodes are attached to the differential amplifier inputs through a lead selector switch. Six leads in the chest are categorized as precordial and six leads in the limbs are known as extremity. Fig 1.4 shows the Einthoven equilateral triangle which depicts the Bipolar recordings for standard limb lead configurations [19].

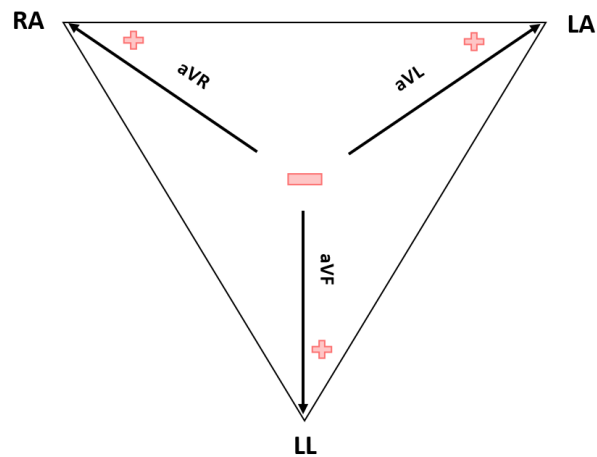


**Figure 1.4:** Einthoven equilateral triangle [19]

The potential record for chest leads and limb leads is transferred to the horizontal plane and frontal axis, respectively. The six limb leads are classified into triad bipolar leads specified as lead *I*, lead *II*, and lead *III*; and triad augmented leads / unipolar leads known as *aVR*, *aVL*, and *aVF*. The unipolar leads in the chest are analyzed as *V1* to *V6* [19]. Positive deflection in the *P*-wave is normally found for lead *II*, whereas negative deflection is normally found for lead *aVR*. Right atrial depolarization shows a positive component followed by a small negative component ( $< 1 \text{ mm}^2$ ) representing left atrial depolarization, which signifies that normal *P* wave is biphasic in lead *V1*.

*QRS* poles ranges from  $-30^\circ$  to  $+100^\circ$ . The axis more negative than  $-30^\circ$  is referred to as the left axis deviation, while the axis more positive than  $+100^\circ$  is referred to as right axis deviation. Depending on its electrical axis, which determines the mean orientation of its vector with regard to the sextet frontal plane leads, the *QRS* pattern in the extremity leads varies from one normal subject to another. The precordial lead is referred to as the transition region (usually *V3* or *V4*) where the *R* and *S* waves are nearly equal in amplitude. The *T*-wave vector is centered about  $45^\circ$  in the frontal plane, with the mean *QRS* vector. Positive deflection is observed when the wave of depolarization for negative deflection is applied to the positive pole of the lead and vice versa. If the vector mean orientation of depolarization is  $90^\circ$  to the lead axis, a biphasic (equally positive and negative) is observed. Depolarization occurs in two forms- Normal Atrial Depolarization (NAD) and Normal Ventricular Depolarization (NVD). NAD is downward driven that indicates the depolarization from the SA to the right and later to the left atrial myocardial, while NVD precedes a continuous and rapid distribution of wave front activation. NAD includes *P*-wave, and NVD is for *QRS* complex [17, 18]. During its acquisition, the ECG signal is corrupted by distinct noises that are categorized in next section.

#### **1.4 DISTINCT NOISES IN ECG SIGNALS**

An Electrocardiogram (ECG) diagnostic system outperforms when the ECG recording is free from disruptions like muscle defects, issues with the handling of electrodes etc. These noises and artifacts undergo the variations in the ECG signal characterization and presence of these noises and artifacts provide main obstruction for extraction of crucial information from the signal. Hence noise estimation of ECG signal allows the cardiologist to analyze the ECG

recording more precisely [20]. ECG signal becomes contaminated during acquisition by multiple factors that behave as noise. Such disruptive results impair both visible and computerized interpretation efficiency. The reduction of noise therefore is an essential task in order to enable further processing.

The various noises [21] exists in ECG signal are-

- i. *Base line Wander*- This type of noise exist in lower frequency band usually less than 1.0 Hz emerges due to electrode-skin impedance variation, patient agitation and breathing that pose difficulties in detecting signal peaks. As the electrode-skin impedance shoots, a smaller relative impedance variation is required to bring about a significant base line shift. When the impedance to the skin is extremely large, a precise feature detection of ECG signal become tedious. Instant variations in the electrode-skin impedance cause sharp transition which further leads the exponential decay to the baseline that happens repeatedly over a time. The characteristic of this kind of noisy signal includes the initial transition amplitude and time constant decay.
  
- ii. *Power line interference (PLI)* – PLI is induced in medium frequency spectrum usually occurs at 50 Hz to 60 Hz due to electromagnetic frequency interference in transmission lines. Power line interference exhibits capacitive and inductive coupling mechanisms. The energy shift due to the presence of coupling capacitance among two circuits results in Capacitive coupling while the phenomenon of mutual inductance results in Inductive coupling. The reduction in the value of coupling capacitance is due to the circuit separation. The flow of current is channelized through wires that produce magnetic flux induces a current in adjacent circuits. The mutual inductance is determined by the proximity of conductor and thus level of inductive coupling. Capacitive coupling is the main cause of high frequency noise whereas inductive coupling results low frequency noise. These two mechanisms results into the emergence of PLI in electro-cardiology. To restrict the extent of PLI, electrodes should attach in proper way ensuring no loose connection with an adequate shielding of all components.

- iii. *Burst noise* – Classification of Burst noise as White Gaussian noise (WGN) and instrumentation noise that exists at the entire frequency band of ECG signal when transmitted through channels. Most often the electrical equipments needed for ECG measurements also introduce the noise. Electrode probes, cables, amplifying circuits and converters are the main cause leading burst noise. Unluckily, the elimination of instrumentation noise can't be feasible because of the electronic parts, but possible to minimize through fine equipments and precise circuit design. ECG data belongs to low frequency that brings the inclusion of flicker noise which contaminates the entire ECG signal. The energy traps lying between the two material interfaces are the main root cause of persistence of burst noise. The charge carriers are assumed to be unexpectedly trapped / released that leads to flicker noise.
- iv. *Electromyography (EMG) noise*- High frequency noise arises as a result of muscles contraction having frequency greater than 100 Hz. Electromyography noise is due to the contraction of certain muscles in addition to the heart. When these muscles contract in the vicinity of the electrodes, leading the waves of depolarization and repolarization that sense by the ECG recorder. The magnitude of the crosstalk relies on the quantity of muscle contraction, and probe quality. The amplitude of the EMG signal is random in nature assuming zero mean of noise and variance lies on the environmental variables. The standard deviation of EMG noise is approximately 10% of the ECG peak-to-peak amplitude. It is also observed that the muscle electrical activity throughout the contraction phase generates surface potentials at par to that of the heart and may muffle the entire signal of interest.

Presence of these types of noises may restrict the cardiologists to identify the various heart related problems effectively.

## **1.5 HEART RELATED DISEASES**

Cardiac disease is the foremost reason of mortality in India as well as all over the world. Heart disease is a collection of disorders and conditions that give rise to cardiovascular problems.

Making efforts for early detection of these issues leads to priority research in biomedicine. Some of the common heart problems [22] that ECG can detect are Cardiomegaly (It refers to cardiac enlargement results from hypertension or coronary artery disease), Congenital heart defects affecting the (electrical) conduction mechanism, Abnormal rhythm (arrhythmia), Cardiac mutilation, Atherosclerosis, Abnormal Heart Location, Cardiac inflammation, Cardiac arrest during critical care treatment, Disruption in heart's conduction system etc.

Derived from current trends and review of cardiac related statistics, the WHO has predicted about the future of Heart disease till 2030. Their mortality forecasts signifies the annual escalation in CVD deaths to 18.1 million in 2010, 20.5 million in 2020 and as high as 24.2 million by 2030 worldwide. These represent 30.8%, 31.5% and 32.5% respectively of all worldwide deaths. Among them cardiac arrhythmia is a prime source of morbidity and mortality that leads to more than a quarter of a million deaths worldwide [23].

### **1.5.1 Cardiac Arrhythmias**

Cardiac arrhythmias are a cardiac disease, characterized by an irregular heart beat pattern. It is one of the substantial and diverse ranges of condition determining an abnormal electrical activity is pertaining in the heart [24]. The pulse can be either too fast or too slow, and can be regular or irregular. Arrhythmias emerge due to inadequate functioning of the electrical impulses to the heart that regulate heartbeats. For example, certain people have erratic heartbeats that can sound like a racing heart or flutter. Generally the following disorders are caused by abnormalities in the rhythmicity-heart conduction system [25]:

- i. Abnormal rhythm of pacemakers
- ii. Abnormal pacing for pacemakers.
- iii. Change the sinus node pacemaker to another location of the heart.
- iv. Blockages of the transmission of an impulse in the heart at different stages.
- v. Irregular cardiac impulse transmission mechanisms.
- vi. Skipped beats that occur in atria and ventricles of the Heart.

Arrhythmic symptoms often include dizziness, breathlessness and palpitations. The major causes of arrhythmia are diabetes, mental stress, and smoking.

In normal heart rhythm the morphology of the ECG signal does not contain any disease or disorder known to be Normal Sinus Rhythm (NSR). NSR heart rate exists in the range (60-100) bpm. The R-R interval changes significantly according to the respiratory process. A sinus tachycardia rhythm came into existence when the heart rate shoots above 100 bpm. This is not an arrhythmia but a natural heart response that demands higher circulation of the blood [26]. Slow rate of heart identifies the bradycardia which critically affects vital organs. The high heart rate condition restricts the ventricle to be filled properly with blood ahead of contraction resulted to a reduction in the pumping capabilities that critically affecting the perfusion. Fig1.5 (a) depicts the Normal sinus rhythm of ECG recording and Fig 1.5 (b) shows the Sinus tachycardia.

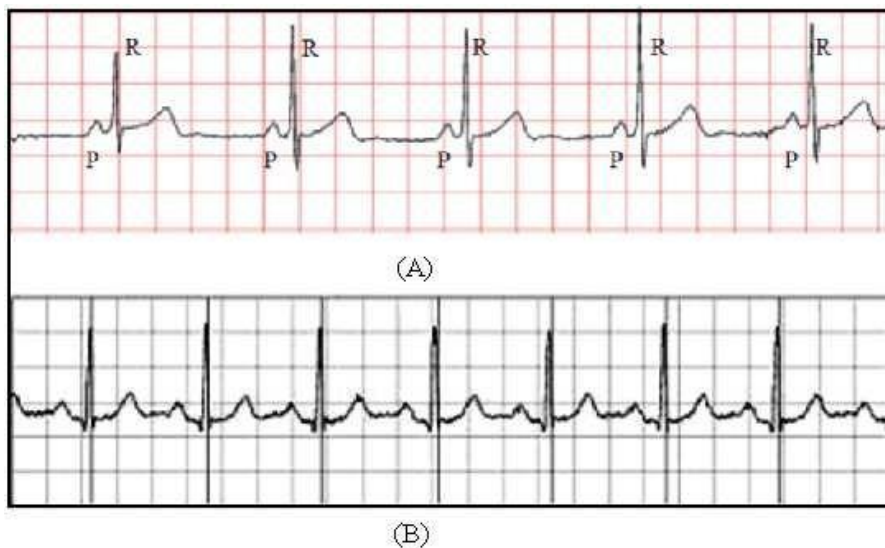


**Figure 1.5(a)** Normal sinus rhythm, (b) Sinus tachycardia

Different types of Cardiac Arrhythmias [27] are:

**Sinus Node Arrhythmias-** This form of arrhythmia originates from the S-A node. The electrical impulse is generated from the normal pacemaker. The characteristic feature of these arrhythmias depicts the normal P wave morphology. These arrhythmias are sub classified as Sinus arrhythmia, Sinus bradycardia, and Sinus arrest.

**Atrial Arrhythmias-** Atrial arrhythmias emerge outside the S-A node but inside the atria in the shape of electrical impulses. Figure 1.6 illustrates different types of Atrial Arrhythmias.



- a. *Premature Atrial Contractions (PAC)* -These arrhythmias cause irregular shape of the *P*-wave accompanied by a regular complex of the *QRS* along with *T* wave as shown in Figure 1.6 (a). This is due to an ectopic pacemaker firing in front of S-A node. PACs exists as a couplet producing two consecutive PACs. The rhythm associated with the occurrence of three or more consecutive PACs known to be atrial tachycardia.
  
- b. *Atrial Tachycardia*- Heart rate of Atrial tachycardia (as shown in Figure 1.6 (b)) lies between 160 -240bpm. Some common symptoms of Atrial tachycardia often include palpitational feelings, nervousness and anxiety.
  
- c. *Atrial Flutter*- The heart rate associated to atrial flutter is extremely high and lies in the range of 240-360 bpm. In this case, the appearance of abnormal *P*-wave is presumed to be more rapid and regularly such that it attains the morphology of the saw-tooth waveform identified as waves of flutter (*F*) as shown in Figure 1.6 (c).
  
- d. *Atrial Fibrillation*-In this kind of arrhythmias the atrial heart rate surpass 350 bpm. This arrhythmia transpires as a result of disordered activation and compaction of distinct tissues of the atria as shown in Figure 1.6 (d). The higher heart rate and disordered compaction may contribute to the inadequate blood supply into the ventricles. These arrhythmias mostly take place in short bursts.

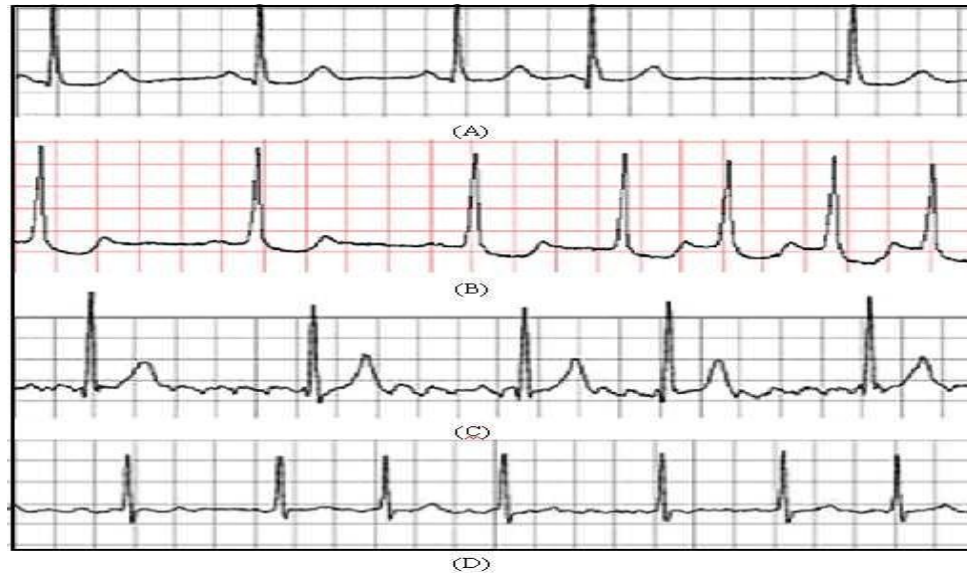


**Figure.1.6** Atrial arrhythmias, (a) PAC, (b) Atrial tachycardia, (c) Atrial flutter, (d) Atrial fibrillation

**Junctional rhythm-** Inside the A-V junction, Junctional rhythm arise as an impulse that incorporate the A-V node, and its Bundle. Because of this rhythm the irregularity in P wave morphology exists. The abnormal P-wave polarity is contrary to that of normal P type wave due to the opposite propagation of depolarization as from the A-V node to the atria. Premature Junctional Contractions (PJC) is one of the types of Junctional rhythm. It defines ventricular contraction in the AV node, inducted by an ectopic pacemaker. A normal-looking *QRS* complex appears prematurely in premature junctional escape contraction without proceeding *P* wave while *T* wave remain normal. Fig.1.7 shows the graphical view of Junctional rhythm.



**Figure 1.7** Junctional rhythm

**Ventricular arrhythmias-** The impulses in this form of arrhythmias originated from ventricles and later transferred to remaining parts of the heart. The *QRS*-complex in this type

of arrhythmia is large and peculiar in shape. The ventricular arrhythmias are classified as Premature Ventricular Contractions (PVC), Ventricular Tachycardia (VT) and Ventricular Fibrillation and are shown in Fig.1.8.

- a. *Premature Ventricular Contractions (PVC)* - The abnormality in PVC emerges from ventricles. PVCs under normal condition can't depolarize the atria either the S-A node, and thus the morphology of P-waves preserves its underlying rhythm that occurs at the specific duration. PVCs can exist in any location of entire cycle of heart beat.
- b. *Ventricular Tachycardia (VT)* -In Ventricular tachycardia heart rate lies between 110 – 250 bpm. In VT, the QRS complex is nasty wide, out of shape, and follows different direction relative to normal QRS. VT is considered life endangering as it can obstruct the proper blood filling in ventricular that leads to the declination of heart performance.
- c. *Ventricular Fibrillation* -Ventricular fibrillation is life threatening cardiac arrhythmia occurs due to the uncoordinated waves of depolarisation and producing ineffective contraction of ventricular myocardium. It exhibits extremely high ventricular rate representing the ECG waveform as a saw-tooth wave.

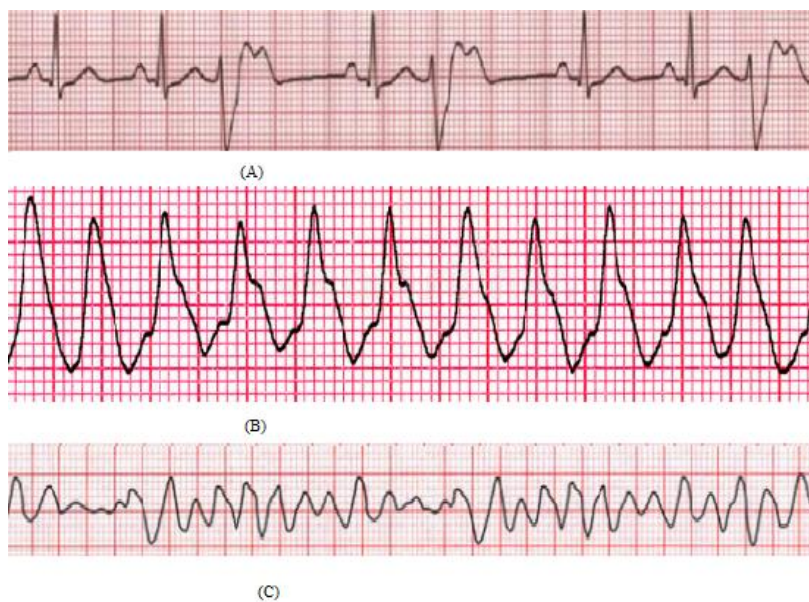


**Figure 1.8** Ventricular arrhythmias (a) PVC, (b) VT, (c) Ventricular Fibrillation

**Atrioventricular Blocks-** The standard transmission of electric impulse to the ventricles using conduction path medium but the presence of these blocks may restrict the spread put of these impulses to the entire conduction system. Figure 1.9 shows the Atrioventricular Blocks of first, second and third degree. First degree AV block exists when all P waves propagates to the ventricles resulted into a prolongation of P-R interval. The second degree AV block occurs when there is intermittent atrial to ventricle conduction. Second-degree AV blocks can be further classified into Mobitz type 1 (Wenckebach) and Mobitz type 2. In second-degree Mobitz type 1 AV block, there is a progressive prolongation of the PR interval, which eventually culminates in a non-conducted P wave. In second-degree Mobitz type 2 AV block, there are intermittent non-conducted P waves, whereas in third-degree AV block the overall dissociation of P wave rhythm with respect to QRS complex rhythm is observed.

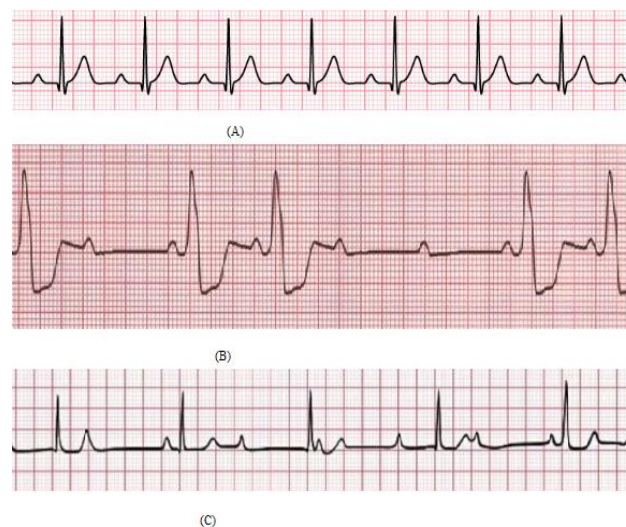


**Figure 1.9** Atrioventricular Blocks (a) first degree, (b) Second degree, (c) Third degree

**Bundle Branch blocks** –Presence of Bundle branch block restricts the transmission of impulse from the AV-node to the entire conductivity framework. Because of this block myocardial infarction or cardiac surgery will occur. Fig.1.10 shows the waveform of the Bundle Branch blocks as projected in the ECG waveform. The bundle branch block beat is categorized as Left Bundle Branch Block Beat (LBBB) and Right Bundle Branch Block Beat (RBBB). LBBB prevents the natural depolarization of the left ventricular myocardium by the electrical impulses deriving out of the A-V node. The RBBB persists when the electrical

impulse deriving out of the AV node restricts its propagation to the conduction lattice for depolarization of the right ventricular myocardium.

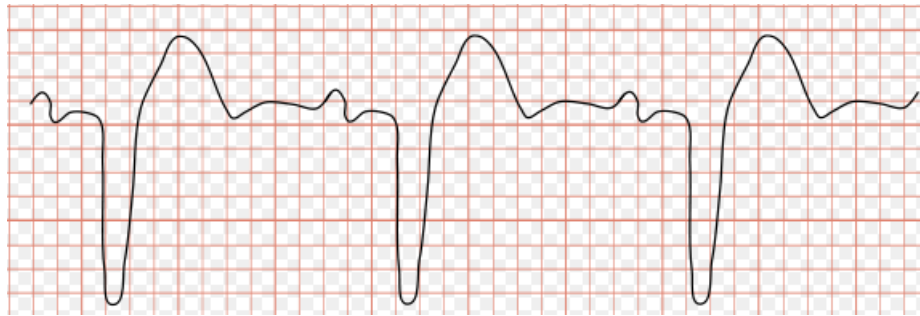


**Figure. 1.10** Bundle Branch blocks

Arrhythmias can be diagnosed using Electrocardiogram (ECG) that records the electrical activity of human heart and assist the cardiologists to procure the individual from life threatening issues such as cardiac arrest or stroke. In order to examine the above arrhythmias, MIT-BIH Arrhythmia Database is utilized in this research.

## 1.6 ECG DATABASE

MIT-BIH Arrhythmia database [28] is coordinated by the Massachusetts Institute of Technology (MIT) and Beth Israel Hospital (BIH) to direct investigation on the assessment of arrhythmia and various heart activities. The collection consists of 48 sets of two-channel ambulatory ECG recordings, acquired from 47 participants tested by the MIT-BIH Arrhythmia Lab. The data was drawn from 25 men of age group 32-89 years and 22 women of age group 23 -89 years. There is inclusion of two leads in each recording as the modified limb lead II and one of the modified leads V1, V2, V4 or V5. First Twenty-three recordings incorporate routine samples of clinical recordings and last 25 recordings incorporate some arrhythmias of complex ventricular, junctional, and supraventricular categories. The duration of each record of MIT-BIH Arrhythmia database [28] is 30 minutes, and 5.556 seconds that are used in the form of discrete samples sampled at the rate of the 360 samples/sec. The following steps are used (i) Click Physio Bank ATM (ii) In the input column select MIT- BIH arrhythmia database (iii) Select the signals in record (have number of signals) (iv) In the signals, select any one either V5 or MLII (v) In the toolbox column select the export signals as .m or text file. (vi) Load the

file in the Matlab software. The statistical description of each record ranging from 100-234 is broadly described in Appendix 1.1.

## 1.7 SOFTWARE USED

The whole process of implementation is performed in MATLAB R2016a environment in an Intel i5 2.4 GHz processor with 16 GB RAM specification and 64 bit operating system.

## 1.8 PERFORMANCE EVALUATION PARAMETERS

The efficacy of the proposed methodology is assessed using different performance parameters such as SNR, MSE, PRD, and PSNR. These parameters are evaluated using their mathematical expression.

- i. *Signal -to- Noise Ratio (SNR)* express the proportion of signal power to the noise power. This compares signal level expected to background signal level. SNR is expressed in decibel (dB). SNR is mathematically modelled in Eq. (1.1).

$$\text{SNR} = 10\log\left(\frac{S}{N}\right) \quad (1.1)$$

where  $S$  represents signal power and  $N$  is noise power.

- ii. *Mean Square Error (MSE)* calculates the average square of errors and described as average squared difference among the original signal and reconstructed signal. MSE is expressed in Eq. (1.2).

$$\text{MSE} = \frac{1}{N} \sum_{n=1}^N [x(n) - y(n)]^2 \quad (1.2)$$

- iii. *Percent Root Deviation (PRD)* is defined to compute the distortion in the signal. PRD is expressed in Eq. (1.3).

$$\text{PRD} = \sqrt{\frac{\sum_{n=1}^N [x(n) - y(n)]^2}{\sum_{n=1}^N x(n)^2}} \quad (1.3)$$

where  $x(n)$  is the original signal and  $y(n)$  is the reconstructed signal

iv. *Peak Signal-to-Noise Ratio (PSNR)* is determined as the ratio of maximum signal strength to the noise strength which effects the fidelity of their representation. PSNR is expressed by Eq.(1.4).

$$PSNR = 10 * \log \left( \frac{Maxi^2}{MSE} \right) \quad (1.4)$$

where  $Maxi^2$  denotes the maximum amplitude of the signal and MSE represents the mean square error.

## 1.9 MOTIVATION

The functionality and behavior of heart is reflected by its morphological representation and heart beat rate. ECG, if appropriately examined, can deliver the crucial findings about heart related diseases [29]. The clinical observation of ECG recording is very tedious and time consuming task. In addition, its visual analysis depicts a strong possibility of missing vital information due to the presence of different noises. ECG Contamination with different noises and artifacts brings serious issue for precise detection of cardiac diseases. Therefore noise reduction is a critical task in signal processing [30]. A clean signal is acquired after all noise suppression strategies by considering noise estimation range that existing in the raw input signal. The efficiency of the optimized algorithms to deliver high quality signal are dependent on noise estimation. The least value of estimated noise depicts the presence of residual noise whereas its high value resulted into the intelligibility loss [31]. Biomedical signal processing allows the scientists to discover a latest approach to examine the crucial issue designated as noise encountered in many applications. Noise has a time and recurrence space property that distinguishes it from the signal. Uniform noise bears constant probability density over a defined interval while Gaussian noise is characterized by two factors defined as average and spread over an infinite interval. As consequences of these noises, the vital information contained in the signal gets misinterpreted.

### **1.9.1 SCOPE OF RESEARCH WORK**

The main focus of this research is to establish an optimal thresholding system design for an ECG signal. This system design comprised of efficient Bio-signal Processing method for removal of artifacts associated with robust noise estimator utilizing optimal thresholding for different distribution functions to attain high SNR at the output. The thresholding technique is implemented on MIT-BIH arrhythmia ECG database using distinct threshold values and their functions and different performance parameters were evaluated. In this thesis, eight distinct types of threshold value selection rules accompanying six different threshold functions are determined to attain the finest combination among them. The proposed noise estimator is designed by introducing the considerable modification in scaling factor and a parameter that rely on distinct probability distribution functions to examine their significance on evaluation parameters and quality of the reconstructed signal. The valuable information from the reconstructed signal is extracted using Peak Detection Algorithm. This research helps to discover the following:

- i. Physical health of a patient
- ii. Detection of different Events
- iii. Heart rate computation
- iv. Wearable health monitoring system

### **1.10 RESEARCH GAPS**

Detection of Arrhythmias is observed through ECG recording of an individual that are supported with an instrument that monitors their heartbeat for a long time. This results in an immense volume of data containing noise due to movements and other interactions that require preprocessing before any valuable information can be extracted. In this regard, different methods of ECG preprocessing have been developed named as Discrete Wavelet Transform (DWT), Continuous Wavelet Transform (CWT), Hilbert transform (HT), Fast Fourier transform (FFT), Short-Term Fourier transform (STFT).



After examining the current challenges that hinder the precise interpretation of ECG signal and the state-of-the-art methodologies are designed to address these problems, we identified some research gaps that are addressed in this research.

### **1. ECG contamination during acquisition**

Electrocardiogram signals are classified as non-stationary having intermittent linear drifts and noise trends that integrate with signal frequency range to produce distortion. Noise and artifacts introduce the distortion and limit the precision of the resulting signal processing analysis. The presence of these artifacts leads to performance degradation of visual as well as computerized analysis. Therefore, it is essential to execute the denoising process without affecting the principal features. Also, it is extremely important when the noise lies in the same frequency band as the signal of interest. Therefore, Traditional filtering strategies cannot perform well, because they cannot discriminate between the preferred signal and the noise.

### **2. Degradation in the perceptual quality of reconstructed signal**

The denoising effect of the wavelet threshold approach relies on the determination of a threshold value selection and its function. If the selected threshold is too high, certain useful information is filtered out. Also, a fixed amount of noise is retained if corresponding value of threshold is too low. The flaw in the traditional strategies is that uniform thresholds are always set too high, which can lead to over killing of the useful information. Moreover the conventional estimator exhibit low efficiency and views the dispersion of symmetric distribution. Due to these multiple interferences in the ECG signal that generate spurious high-frequency details that further leads to degradation in the quality of reconstructed signal.

### **3. Probability distribution modeling of noise estimator**

Threshold limit setting for ECG signal in the absence of model fitting has observed a significant difference among the data sets of similar parameters measured over a varying time period. This challenge has prompted researchers to consider the execution of Probability distribution modeling which can reduce the discrepancies among the data over varying time periods.

## **1.11 OBJECTIVES FRAMED**

Focused on above research gaps, the following objectives are framed -

1. Implementation of Bio-signal Processing methods to extract Clinically Significant Information from the ECG Signal
2. Design and Implementation of Robust Denoising System for ECG Signal using Optimal Thresholding Tuning.
3. Probability Distribution Modeling for Enhanced Denoised Electrocardiogram System.

## **1.12 ORGANIZATION OF THESIS**

The rest of thesis structured as follows:

*Chapter 2* overviews of the research carried out by numerous researchers in the areas of ECG analysis. This section lists some of the related papers which helped to achieve the targeted outcomes.

*Chapter 3* explains the Bio-signal Processing Methods for successive elimination of artifacts and extraction of clinically significant information from the ECG signal.

*Chapter 4* proposes a Robust denoising System for ECG Signal using Optimal Thresholding Tuning. The performance analysis is also carried out by incorporating the statistical analysis with the existing state of art work.

*Chapter 5* provides Probability Distribution Modeling for Electrocardiogram System Design for achieving better efficiency by implementing finer downscaling factor employing distribution functions.

*Chapter 6* summarizes the conclusion and gives the future scope of this dissertation.

**CHAPTER 2**

**REVIEW OF STATE-OF-THE-ART-  
TECHNIQUES**

## CHAPTER 2

### REVIEW OF STATE-OF-THE-ART- TECHNIQUES

An Electrocardiogram (ECG) signal plays a crucial role in the identification, analysis and prognosis of Cardiovascular (CVD) disease [32-34]. Fig 2.1 shows the percentage of global mortality rate due to distinct cardiovascular diseases.

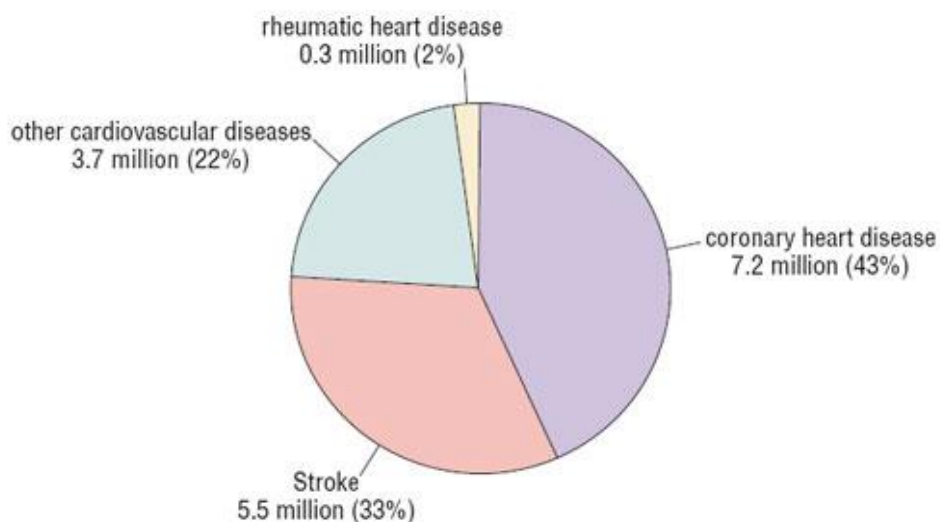


**Figure 2.1** Pie Chart displays the proportion of world-wide deaths owing to distinct Cardiovascular diseases [34]

Fig 2.1 clearly indicates that CVD is leading cause to global deaths, killing nearly about 17.9 million people every year. Therefore, early detection of CVD is essential to prevent these deaths. In this aspect, ECG is a well known tool for early detection of cardiovascular diseases.

This chapter provides a description of the work that has been performed from time to time in the domain of ECG signal processing. The thought process behind the study of the existing literature is to fetch the information associated with the topic inside and getting the inspiration for cutting edge inquiry. Over the last few years, advancements in signal processing techniques have brought massive improvements in the identification and removal of artifacts.

Various methods had been introduced for detection and elimination of various artifacts from ECG signal.

Artifacts are unwanted signals that arise from experimental, environmental, and physiological aspects. The existence of artifacts in signal degrades signal quality and that makes it difficult to interpret physiological signals for diagnostic purposes [32]. The identification of these artifacts and their exclusion from the signals has therefore been an important area of research. ECG examination contains important and vital knowledge about heart disease. In a clinical environment, there are several sources of noise that leads to degradation in the quality of ECG signal. Instrumentation amplifiers, recording system, cable picking of ambient EM signal etc are the primary sources that leads to the high frequency noise in an ECG [34]. Coughing or breathing resulted into a large movement of the chest that leads to Low-frequency artifacts and base-line drift in chest-lead ECG signals or by raising an arm or leg in the case of limb-lead ECG acquisition [34].

There are several techniques of Bio signal processing that have been used to emphasize for removing artifacts utilizing time, frequency and time-frequency domain and an event detection approach. The motive explicitly involves the filtering process to eliminate noise; most signal processing methods effectively include some framework for distinguishing desired from undesired signal content.

## **2.1 REVIEW BASED ON REMOVAL OF ARTIFACTS**

Many techniques have been accounted in the historical backdrop of ECG signal processing. In the context of ECG signal analysis, different methods have been taken into account for the elimination of noise and artifacts.

**Thakor and Zhu** (1991) presented a recurring adaptive filter structure for the regular QRS complex impulse response. For the impulse response of the regular QRS complex, an effective recurrent filter configuration is proposed. The filter's primary input is the ECG signal to be evaluated, while a reference input is an impulse train which concurs with the QRS complexes.

This approach is applicable to different concerns regarding the diagnosis of arrhythmias: P-waves recognize, premature ventral complexes and conduction block identification, atria fibrillation [35].

**Jain. R et al.** (1992) introduced an adaptive cascade filter for suppression of noise categorized as Baseline wander while preserving the component of low frequency ECG signal. This technique comprises of two stages. In first stage constitutes an adaptive notch filter operated at 0 Hz frequency and second stage consist of an impulse correlated adaptive filter with QRS performed the ECG signal estimation [36].

**SC Pei and Tseng C.** (1993) in their research, An IIR adaptive notch filter of second order is investigated using the least-mean-p-power criterion to remove 60 Hz interference in the ECG recording. The performance evaluation parameters indicate that the adaptive algorithm outperforms the LMS algorithm and has better statistical accuracy [37].

**SC Pei and CC Tseng** (1995) proposed a technique that utilizes the vector projection to eliminate the filter's transient states by providing fine initial values for notch filters. This technique delivers better performance than that of conventional notch filter with a limitation of additional computational load [38].

**A Sander et al.** (1995) designed a notch filter of frequency 50/60 Hz for elimination of PLI for high resolution ECG signal. An integer coefficient filter techniques is applied that reduces the computational complexity [39].

**Donoho** (1995) proposed a de-noising technique employing DWT by applying the proposed threshold on detail coefficients that restrict the coefficients below a specified value followed by implementation of inverse DWT (IDWT). With this de-noising method, the output SNR at output up to 8.26 dB is achieved [40].

**PS Hamilton** (1996) investigated the design and performance of 60 Hz notch filter using adaptive and non adaptive algorithm in terms of complexity, adaption rate and complexity.

Analysis of both type of filters indicate that implementation of adaptive filter is least complex and more noise resistant as compared to non adaptive filter [41].

**Norden E. Huang *et al.*** (1998) developed an Empirical Mode Decomposition method (EMD) for exploration of nonlinear and non-stationary signals with which complex data set decomposed in to intrinsic mode functions. These intrinsic mode functions yields instantaneous frequencies utilizing Hilbert transform that delivers sharp identification of features. This method eliminates the spurious harmonics form nonlinear and non-stationary signal that effects the energy-frequency –time distribution [42].

**S Olmos and Laguna P.** (2000) evaluated the convergence of steady state MSE by using deterministic functions as reference inputs for LMS adaptive algorithm filters. A specific linear adaptive combiner is introduced where set of orthogonal base functions- adaptive linear orthogonal combiner (AOLC) is considered as reference input. A more comprehensive analysis that uses the determinist existence and time-varying correlation vector of the reference parameters. The research addresses two different situations: complete orthogonal expansions and pAtrial expansions. The steady-state misalignment is measured using two separate methods with similar results: the classical method (MSE transient analysis behavior) and the residual noise at the output of the corresponding time-varying function of the system [43].

**SS Dhillon and S Chakrabarti** (2001) the infinite impulse response (IIR) second-order filter was introduced using a simplified adaptive algorithm to eliminate PLI from the ECG signals on the power lines. The efficiency of this filter is more effective for ECG real time recordings than a notch filter [44].

**Ziarani and Konrad** (2002) new approach to the reduction of noise as power line interference for ECG signals has been introduced. The method proposed uses a newly-developed signal processing framework that extracts the specific element of a signal and monitors its time variations. The reliability of the proposed system is tested using computer simulations.The

suggested approach that offers a simpler and reliable structure with fewer computing resources and low sampling frequency [45].

**YVR Rao and N. Venkateswaran** (2003) a second order DC notch filter with a lattice structure is designed to eliminate frequencies close to DC successively to provide a sharp transition. It is a basic filtration system with 1Hz cut-off frequency and 800 Hz sample rate [46].

**Bai Y-W et al.** (2003) suggested using a linear phase property for finite impulse response filter to achieve noise reduction without distortion of the phase. This design consists of a comb notch filter and the equiripple-size filter, which uses the Parks-McClellan algorithm to remove 60 Hz noise [47].

**M.S.Chavan and R.A. Agrawala** (2005) introduced digital elliptical approach filters for ECG signal for elimination of noise and artifacts. In contrast to Butterworth, Chebyshev I & II, elliptical filter outperforms with certain limitations [48].

**L Chmelka and Kozumplik J** (2005) introduced wiener filter based on wavelet theory to eradicate the high frequency electromyography noise from ECG signal. Degradation in quality of ECG signal due to presence of noise hinders the precise diagnosis of cardiac disease [49].

**Pomsathit A et al.** (2006) introduced a novel adaptive algorithm with variable step size for second order lattice type structure IIR notch filter that achieves the filter coefficient optimization by varying the notch frequency and bandwidth. The Performance evaluation of proposed algorithm delivers fast convergence rates, low square error and high noise to remove 50 Hz of ECG signal interference [50].

**Martens SMM et al.** (2006) presented an enhanced adaptive canceller for electrocardiogram (ECG) recording to eliminate PLI section and harmonics. The device records the amplitude, phase and frequency of all interference elements up to approximately 4 Hz for power line frequency deviations. The enhanced adaptive canceller depicts a signal-to-power line-



interference ratio of up to 30 dB higher for the fundamental portion than from other methods [51].

**Tinati Mohammad Ali and Behzad Mozaffary** (2006) presented a WT based search algorithm for ECG signal by utilizing the signal energy in various scales to separate baseline wandering noise. During the measurement of ECG parameters, the baseline wanderers generated due to the electrode movements can affect inaccurate data. By means of the proposed algorithm, the baseline drifts have been successively removed from the ECG signal without any signal deformation without losing any clinical significance [52].

**Kim KJ et al.**(2007) proposed a FIR notch filter utilizing modified alpha- scaled sampling kernel. The proposed technique provides formulae of closed-form filter coefficient, resulting in an effective structural design for sharp notch filters with provided specifications Simulation outcomes indicate that the proposed design achieves high efficiency in eradicating the PLI from ECG signals [53].

**Alfaouri and Daqrouq** (2008) presented a decomposition based DWT method for raw ECG signals employing db4 wavelet. A new threshold value is proposed where an optimum threshold is determined by having a minimal error between the noisy and original signal. This approach performs better than Donoho's thresholding method by attaining output SNR of 9.07 dB. This strategy can efficiently detect and eliminate the PLI from the ECG, even for the frequency of the varying powerline, without the supervision of the human operator [54].

**Zhang Wei and Linin Ge** (2008) presented the application of adaptive filters based on wavelet employing Johnstone and Silverman level-dependent threshold estimator. This method gives better results than Donoho's method based on DWT. This technique incorporates wavelet theory and adaptive filter property that delivers the minimum error (0.006324) between expected and actual output signal. This approach has enhanced precision, speed and efficient for noisy environment. [55]

**Saritha et al.** (2008) presents the ECG denoising when the corresponding wavelet coefficients is removed at higher scales. Many methodological aspects such as selection of mother wavelet and value of scaling parameters are needed to be examined to enhance the clinical usefulness [56].

**Lin and Hu** (2008) proposed a novel algorithm for PLI detection and suppression from the ECG signal. A distinctive characteristic of the proposed algorithm is the capability to detect PLI on the ECG signal before using the PLI suppressor algorithm. If PLI is not detected, no PLI removal operation is carried out. A PLI detector is proposed using an optimum linear discrimination (LDA) algorithm to decide the presence of the PLI. For PLI removal, an adaptive notch filter is developed using RLS algorithm. By evaluating the various performance metrics, the experimental results show the superiority of the proposed algorithm [57].

**Dai M and Lian SL** (2009) introduced a modified moving average filter to identify and eliminate the baseline wandering noise to attain the clean ECG. When measuring the moving average the interval sampling data is taken into account to limit the loss of usable ECG signals and distortions. Experimental findings suggest the success of the proposed moving average filter over the traditional one in suppressing the baseline wandering without any interference from the ECG signals [58].

**Mohammad Zia et al.** (2009) proposed an effective Fast Block LMS (FBLMS) algorithm to eliminate artifacts while preserving the ECG components of low frequency and delicate features. The implementation of this proposed design is well suited for the applications where high SNR with fast convergence rate is main prospective. As the solution for the steepest descent technique to minimize the MSE, the FBLMS algorithm is seen to be unbiased and with a smaller variance than the LMS algorithm. The findings reveal that the FBLMS algorithm is superior than LMS algorithm [59].

**Qawasmi and Daqrouq** (2010) proposed a new technique that employs Wavelet Transform for ECG signal filtration. Adaptation of DWT is implied for ECG enhancement. This method

outperforms than other conventional method such as Donoho's discrete wavelet thresholding and FIR filter for attaining clean ECG signal [60].

**J Piskorowski** (2010) presents a novel digital IIR notch filters with time-varying quality factor. The transient can be decreased considerably due to a sudden adjustment in the quality factor. Simulations of proposed Q-varying IIR notch filter are examined and compared to the output of the standard Q-constant filter using real ECG signals [61].

**Bhavani Sankar et al.** (2010) focused on two aspects (i) second order Auto Regressive mechanism with respiratory signal model. (ii) Elimination of artifacts and PLI at 50 Hz frequency from respiratory signal employing distinct adaptive algorithms. Performance evaluation between these adaptive algorithms on the basis step size depicted the tradeoff between step size and mean square error [62].

**Mbachu C.B et al.**(2011) designed Kaiser Window based Digital FIR filters to suppress distinct artifacts. This method considered three filters namely low pass high pass and notch filter in a cascade structure for ECG filtration. The output of cascade design indicates its superiority to attain a clean signal with optimal filter order [63].

**Khan M et al.** (2011) presents Signal-Noise Residue approach that defines a novel wavelet-ECG denoising algorithm that provides improved efficiency relative to traditional wavelet-based techniques [64].

**Awal A et al.** (2011) introduced a Savitzky-Golay filter to smoothen the ECG signal without affecting its physiological characteristics. Performance of Savitzky-Golay relies on two parameters-frame size and polynomial degree. The results are evaluated by depicting the variations between these two parameters. The best denoising of ECG signal is achieved when the polynomial degree is inversely proportional to frame size [65].

**Vullings R et al.** (2011) A sequential average filter, based on ECG characterization, was developed which significantly changed the number of complexes included in the average. The

filter is expected to have an efficient Kalman filter architecture. The adaptive evaluation process and noise covariance measurements was carried out by optimizing the Bayesian evidence functions of the sequential ECG estimation and investigating the spatial correlation of many concurrently recorded ECG signals. The resulting noise covariance estimates allow the filter to assign more weight to newer data with morphological variability, and to reduce the weight if the morphological variability is not present. To measure the accuracy of the adaptive noise-covariance estimation, the filter's output is compared to that of a Kalman filter with a fixed optimized noise covariance. The comparison result reveals that the filter with adaptive noise estimation performs closer to the filter with optimized fixed noise covariance by using a prior knowledge on signal characteristics, thereby favors the adaptive filter in the circumstances where prior information is not necessary [66].

**Dewangan and Kowar** (2011) presented a denoising technique that based on DWT for elimination of three distinct noises from the ECG signals. Signal Decomposition is performed using mother wavelet. In the end, a reconstructed signal is obtained without high frequency noise, PLI and baseline drift. A comparative analysis of different wavelets has been performed to select the wavelet that delivers high SNR, correlation coefficient and low computation time [67].

**Piskorowski J** (2012) presented ECG denoising method for the time-efficient suppression of PLI employing notch IIR filter having minimum transient response. Minimum transient response is delivered by realizing the non-zero initial conditions. Simulation results shows the superiority of the proposed algorithm as compared to the conventional filters with zero initial conditions [68].

**Smital L et al.** (2013) concentrated on the elimination of broadband myopotentials (EMG) from ECG signals by Wiener wavelet filter using stationary wavelet transform (SWT). Realization of appropriate filter bank and selection of certain Wiener filter parameters is determined to obtain SNR. Experiment is carried out on artificial noisy signal at 500 Hz sampling rate. The performance of filtration is improved by setting adaptive parameters

according to the interference level in ECG signal. This proposed techniques outperforms than the classical Wiener filter [69].

**Mbachu,C.B and Nwosu A. W** (2014) introduced triad set of filters classified as high pass, low pass and adaptive noise canceller to eradicate inherit noise from the signal. It presents the ECG acquisition, processing and interpretation [70].

**S Kocon and Piskorowski J** (2014) proposed a all-pass model based multi-band stop time-varying IIR filter to eliminate PLI from ECG signal. The parameters of the all-pass prototype filter are momentarily time varying to minimize the length of the transient state of the proposed IIR multi-notch filter. The performance of proposed filter is evaluated using simulations and output indices show that the proposed technique has stronger properties than conventional IIR time-invariant filter [71].

**Jayant HK et al.** (2015) designed a second order digital IIR notch filter to suppress PLI. For minimization of root mean square error (RMSE), a minimax optimization approach is utilized. The proposed minimax-based notch filter system is a successful solution for elimination of PLI as depicted by the computational outcomes [72].

**Razzaq N et al.** (2016) proposed the adaptive noise rejection filter without the need for the auxiliary reference data for suppression of PLI and its harmonics. The device proposed will self-adjust the monitoring frequency of the first, third and fifth harmonics of PLIs to ensure high-precision filtration. It is based on the recursive state space model, computationally less complex and outperforms in a non-stationary framework [73].

**Tseng C and Lee S** (2017) designed a notch filter that relies on approximation of Bernstein polynomial for elimination of PLI. The approach is straightforward having empirical solution. For ECG signal, the efficiency of the method was demonstrated by removing 60 Hz PLI [74].

## 2.2 REVIEW ON EVENT DETECTION

QRS complex detection is the most prominent step of ECG analysis. During the ventricular contraction, the QRS method reflects the heart electric activity. The heart contraction and morphology offers the crucial information of heart current state. It provides the basis for an automated heart rate determination initially for classifying the cardiac cycle and frequently utilized in ECG data compression algorithms. The QRS detection is thus the basis for almost all automated ECG analysis [75].

**Daskalov and Christov** (1999) predict the complications for ECG interpretation for automatic detection of QRS onset and offset with an extreme accuracy. This issue is complicated additionally by existence of PLI, EMG artifacts, and baseline fluctuations, particularly in multi-phase complexes, with small waves of q, r, r9 or s9 waves. A proposed method of pre-processing is proposed that ensured the correct maintenance of QRS limits, even when strong PLI or EMG noise is present [76].

**Mahmoodabadi et al.** (2005) developed multi-resolution wavelet transform utilizing Daubechies based feature extraction system. The ECG signal is de-noised in the first step by eliminating the appropriate wavelet coefficients on a higher scale. Later, individual peaks and QRS complexes are detected along with the inclusion of onset and offset of P and T waves for one cardiac period. Ripples belong to high and low frequencies are separated at these stages. The extremes, which were previously observed, suggest P and T peaks prior to and after the null crossings on the R peak [77].

**Sumathi and Sanavullah** (2009) DWT based method is proposed to decompose signal to level 4, with the QRS complex dominant on this approximate level and detection of R-peak corresponds to highest amplitude points. To suppress PVC sounds, an adaptive threshold is used. The R detection compares for cubic spline, Haar and db4 wavelets [78].

**Banerjee and Mitra** (2010) The algorithm for denoising is introduced, along with precise detection of R peaks and QRS complexes employing DWT, with db6 mother wavelet. The denoising of ECG is performed by decomposition and selective reconstruction. For QRS complex detection, thresholding is used together with slope inversion method. The 10<sup>th</sup> level signal decomposition is performed with orthogonal db6 that generates 10 approximation coefficients. The baseline drift can be easily remedied as a lowest frequency signal. Due to signal decomposition, the detection of comparatively high-frequency QRS is much easier [79].

**Narayana and Rao** (2011) utilized derivative based / PanTompkins / wavelet based algorithms for the QRS complexes detection. A specific ECG signal from the data base MIT / BIH Arrhythmia is utilized with MATLAB tools to validate the different algorithms. Comparative analysis is done among the wavelet-based algorithm and AF2 algorithm for ECG denoising and QRS complex detection, while the wavelet baseline algorithm provided better results. The QRS complexes are then identified and further utilized for P and T wave location [80].

**Sasikala and Wahidabanu** (2011) concentrated on P wave and T wave detection due to its low amplitude the determination of the location of wave P and T is challenging. WT is an effective tool for transient signal analysis and ECG feature extraction. P and T wave positioning is the desired performance. The signal analysis, diagnosis, authentication, and identification, the precision of the location of the features is essential for ECG processing. MT-BIH Arrhythmia data base is used to evaluate the process [81].

**Dewangan and Kowar** (2013) proposed DWT based ECG denoising algorithm, along with a precise detection of the R peaks and thus of the ECG-signal QRS-complex. Noise such as EMG, PLI and BLD is eliminated by subtraction of 8<sup>th</sup> level denoised signal from denoised signal. When 5<sup>th</sup> level denoised signal is subtracted from 3<sup>rd</sup> level denoised signal that determines the QRS complex [82].

## 2.3 REVIEW ON NOISE ESTIMATOR

This section explains the review of different existing threshold functions, value selection and noise estimators.

**Shafiullah AZM and Khan J A** (2011) developed a robust Median Product (MP) correlation estimator that achieves computational efficiency by diminish the impact of outliers. The outcomes verified its superiority in terms of less computing time over the classical estimator as robust correlation estimator does not use iterative algorithm [83].

**Rahman MZU et al.** (2012) introduced simple and effective nonlinearity-based adaptive filters with free weight update loops are used for noise suppression in ECG signals, which are computationally superior. The proposed design is ideal for biotelemetry applications where high SNR are required with lower computational complexity. Such schemes often employ addition, shift operations and substantial speed relative to LMS realization. Simulation outcomes reveals that the proposed method is efficient as delivers high SNR and low computational complexity as opposed to other existing approaches [84].

**NiranjanaMurthy HS and Meekashi M** (2013) proposed an Electrocardiogram (ECG) signal detection algorithm for myocardial Ischemic events using the Daubechies Wavelet transform technique. Discarding the associated wavelet coefficients at a higher scale delivers the denoised ECG signal. Two test cases were used to assess the algorithm i.e. for healthy subjects and another for myocardial ischemia. ECGs are acquired from MIT-BIH Arrhythmia Database that is annotated manually and established further for validation purposes. Result outcomes depict that Daubechies wavelets are ideally suited for datasets and can clearly discern the healthy and unhealthy subjects [85].



**Jablonski A et al.** (2013) proposed a procedure for automatic threshold calculations in wide monitoring system and presented the several distribution functions and their comparison on different data sets are evaluated [86].

**AlMahamdy M and Riley HB.** (2014) introduced five standard and significant denoising approaches namely DWT applying universal and local thresholding, adaptive algorithm using LMS and RLS algorithm, Savitzky-Golay filtering and NeighBlock wavelet algorithm is performed on real ECG signals with distinct artifacts. The comparison result reveals that the NeighBlock wavelet algorithm is more efficient than the other denoising technique [87].

**Usman Seljuq et al.**(2014) presents the comparison of distinct wavelet functions along with the selection of convenient mother wavelet for ECG filtration by retaining the desired diagnostic information. The analogy is based on measurement of MSE, SNR, and correlation. The analytical results obtained showed the suitability of order 9 Daubechies wavelet is efficient for denoising the ECG signals. Specific mother wavelets have been studied to improve denoising procedures. In addition to SNR, MSE and correlation, the wavelet selected is also best suited to preserve critical characteristics [88].

**Ghombavani FM and Kiani K** (2015) proposed a novel noise removal strategy rely on the Dual Tree Complex Wavelet Transform (DTCWT) to retain ECG diagnostic information. DTCWT offers substantially different levels of time- and frequency information on the nature of the data. It handle the issue of variance in discrete wavelet transforms (DWT).For evaluating the noise content, Signal Energy Contribution Efficiency (ECE) and Kurtosis in wavelet sub-bands is essential. The proposed approach is presented using these factors at baseline level and Donoho threshold is for remaining levels. The performance evaluation parameters PRD, SNR and MSE are evaluated for proposed technique. It is found that the approach suggested not only extracts the signal differently than the other prominent approaches but also aims to preserve diagnostic knowledge effectively [89].

**Can He et al.** (2015) presented an interscale correlation that rely on Wavelet coefficients propagation characteristics for ECG denoising. The results reveal the efficiency of proposed

method to achieve denoising when applied on distinct types of signals, noise intensity and thresholding functions [90].

**Singh B et al.**(2015) presented the various techniques which aim to eliminate distinct noises that disrupt the ECG signal. Multiresolution discrete wavelet transformation (DWT) has been found to be the better alternative for eliminating PLI while for elimination of EMG noise and motion artifact, a discrete Meyer wavelet along with hard and soft thresholding properties is considered. Advanced Algorithms, such as EMD, DWT or both techniques hybrid method, produce better results in removing artifacts and noises [91].

**Afkhami RG et al.**(2016) proposed a new approach for accurate diagnosis of heart arrhythmias. To train a classifier, the morphological and statistical attributes of each heartbeats are employed. Throughout this analysis, two RR interval features are used as for time-domain information. A Gaussian mixture modeling (GMM) with an improved expectation maximization (EM) approach is implemented to fit the PDF of heartbeats. GMM parameters are also used in the function vector along with shaping parameters such as skewness, kurtosis, and 5th moment to evaluate the performance then an ensemble of decision tree is train using these features. Evaluation of algorithm is performed using MIT-BIH arrhythmia database. The overall accuracy is achieved in "class-oriented" scheme of 99.70 percent and in "subject-oriented" scheme of 96.15 percent. Both cases demonstrate a significant increase in accuracy as compared with other approaches [92].

**Jebaraj J and Arumugam R.** (2016) introduced an optimized algorithm rely on ensemble empirical decomposition mode (EEMD) for suppression of PLI from the ECG signal. An algorithm with computational efficiency is the essential criteria for tracking cardiac movements and diagnosing arrhythmias in real-time. EEMD having Computational complexity is minimized considerably by introducing EMD in preprocessing stage. Employing EMD the ECG noisy signal is subdivided into IMFs. ECG signals affected by PLI is recognized automatically on the basis of a simple zero crossing ratio of IMF components. EEMD is employed for ECG decomposition of noisy IMF. The proposed algorithm is evaluated by ECG signals in the MIT-BIH arrhythmia database for signal-to - noise ratio and

root mean square errors. This new paradigm is tested statistically using profiling functions from MATLAB and compared to wavelet-based approaches including EMD, EEMD and adaptive sign-based approaches [93].

**Niederhauser T** *et al.* (2016) presented a system known to be baseline wander tracking (BWT) which simultaneously detect and discard the baseline disturbances while eliminating the analog front-end saturation. The proposed algorithm shifts the ECG signal's baseline point into the center of the dynamic input range. Due to fast shifting offsets, which produce far higher portion of signal than normal ECG, the true ECG signal can be retrieved offline and filtered using computationally intensive algorithms. Monte Carlo simulations found reconstruction errors induced mostly by the DAC's non-linearity inaccuracies. However, when using a synthetic ECG signals, BWT is able to diminish the offset potentials without inserting long transients the BWT 's signal-to-error ratio is higher than an analog front end with dynamic input range of 15 mV. Because of its device stability, memory durability and DC coupling capacity, the BWT is dedicated to the higher integration and low power ECG recording systems [94].

**Gong Yet al.** (2017) an improved cardiopulmonary resuscitation (CPR) adaptive filtering technique is introduced in real time. Data with 183 shocking and 453 non-shockable parts of ECG and the reference signal for CPR were used in 233 patients treated as cardiac arrests in hospitals. In a sequence of 98 shocking and 242 non-shockable data that was tested on a test set, the approach was extended for training. Compared mite-disrupted ECG signals and precision between 74.1% and 92.0% later, the SNR was increased from  $-9.8 \pm 12.5$  to  $11.2 \pm 11.8$  dB [95].

**Rodrigues et al.** (2017) presents a new noise detection approach and artifacts based on ECG time series clustering. The algorithm begins by extracting features that characterize signal form and conduct most effectively over time and group samples through a clustering process. [96].

**Nagai et al.** (2017) Stationary wavelet transform algorithm (SWT) is employed for motion artifact elimination that overlaid on ECG data. In the context of median before and after motion removal, the correlating coefficients of the ECG clean signal have been improved from 0.71 to 0.88, demonstrating the effectiveness of proposed SWT-based algorithm. [97]

**Shanti Chandra et al.** (2018) in order to extract useful diagnostic features, an approach was introduced using rule-based algorithms for ECG analysis. Different noise types are eliminated using the maximal overlap discrete wavelet transform (MODWT) and universal thresholding [98].

**Kumar S et al.** (2018) the efficacy of empirical decomposition mode (EMD) with non-local mean (NLM) approach is investigated through the use of the differential standard deviation for ECG signal denoising. FOR ECG noise reduction, the EMD paradigm is utilized in the proposed methodology. The output of the EMD is transmitted via NLM to preserve the edges [99].

**He H and Tan Y** (2018) ECG signal enhancement adaptive wavelet thresholding (AWT) method is proposed. In order to prevent the ECG signal from various noises, the vector universal threshold (VarUniversal) is used for distinct decomposition levles. To attain smooth cut-off transition, an identical correlation shrinking function (Ico Shrinkage) is introduced [100].

**Zubair AR et al.** (2018) introduced Modified Garrote Threshold Shrinkage Function for removal of high frequency noise. A tuning constant  $\alpha$  optimizes the universal threshold. The performance of MGTSF is examined and further comparison is done with current threshold shrinkage approach [101].

**Alyasseri et al.** (2018) presented as a new approach for denoising of ECG signal as hybrid of hill climbing metaheuristic algorithm and wavelet transform.  $\beta$ -hill climbing is used to identify the best wavelet parameters that can achieve the minimum MSE [102].

**Alan S. And Majd S** (2018) introduced the Arrhythmia ECG denoising process using Genetic Algorithm (GA) with Wavelet Transform (WT). WT parameters are used as a inputs for GA to eliminate white gaussian noise for ECG denoising [103].

**Wang Di et al.** (2019) proposed a new approach appropriate for detecting short-term ECG signal. In order to reduce the influence of HR variability during heartbeats processing, an improved HR-free resampling strategy was introduced. To assess the potential difference between subjects, the principal component analysis network (PCANet) is used to extract features [104].

**Li W** (2019) set description and categorization based on deep analysis of their methodological characteristics and a full overview of systematic categorization of the various DWT methods for singularity detection, signal denoising and classification of arrhythmias. This study demonstrates how to use wavelet-based approaches to evaluate the ECG and also the modeling concepts they can adopt [105].

**Amit Singhal et al.** (2020) presents a methodology for the separation of BW and PLI from the reported ECG signal simultaneously and to achieve clean ECG results, based on the Fourier decomposition method (FDM). For processing the signal, the proposed technique uses either the discrete Fourier transform (DFT) or the discrete cosine transform (DCT) [106].

After examining the current challenges that hinder the precise interpretation of ECG signal and the state-of-the-art methodologies are designed to address these problems, we identified some research gaps that are addressed in this research. Through an extensive literature review following research gaps has been found based on which objective for this research work has been framed.

### **1. ECG contamination during acquisition**

Electrocardiogram signals are classified as non-stationary having intermittent linear drifts and noise trends that integrate with signal frequency range to produce distortion. Noise and

artifacts introduce the distortion and limit the precision of the resulting signal processing analysis. The presence of these artifacts leads to performance degradation of visual as well as computerized analysis. Therefore, it is essential to execute the denoising process without affecting the principal features. Also, it is extremely important when the noise lies in the same frequency band as the signal of interest. Therefore, Traditional filtering strategies cannot perform well, because they cannot discriminate between the preferred signal and the noise.

## **2. Degradation in the perceptual quality of reconstructed signal**

The denoising effect of the wavelet threshold approach relies on the determination of a threshold value selection and its function. If the selected threshold is too high, certain useful information is filtered out. Also, a fixed amount of noise is retained if corresponding value of threshold is too low. The flaw in the traditional strategies is that uniform thresholds are always set too high, which can lead to over killing of the useful information. Moreover the conventional estimator exhibit low efficiency and views the dispersion of symmetric distribution. Due to these multiple interferences in the ECG signal that generate spurious high-frequency details that further leads to degradation in the quality of reconstructed signal.

## **3. Probability distribution modeling of noise estimator**

Threshold limit setting for ECG signal in the absence of model fitting has observed a significant difference among the data sets of similar parameters measured over a varying time period. This challenge has prompted researchers to consider the execution of Probability distribution modeling which can reduce the discrepancies among the data over varying time periods.

Focused on above research gaps, the following objectives are framed -

1. Implementation of Bio-signal Processing methods to extract Clinically Significant Information from the ECG Signal
2. Design and Implementation of Robust Denoising System for ECG Signal using Optimal Thresholding Tuning.
3. Probability Distribution Modeling for Enhanced Denoised Electrocardiogram System.

# **CHAPTER -3**

## **BIO-SIGNAL PROCESSING FRAMEWORK FOR ECG SIGNALS**

## CHAPTER -3

# BIO-SIGNAL PROCESSING FRAMEWORK FOR ECG SIGNALS

This chapter involves the description of distinct Bio-signal Processing method for analysis of ECG to impart crucial information to the clinicians for precise decision making. The Bio-signal Processing method involves various filtering techniques for removal of artifacts accompanied by Peak Detection Algorithm for detection of various events, segments and intervals present in the ECG signal.

### 3.1 BIO-SIGNALS

Bio-signals are physiological signals that provide the information of any biological system by exhibiting the variation in the electric current originates due to the sum of potential difference. The common Bio-signals are [107]-

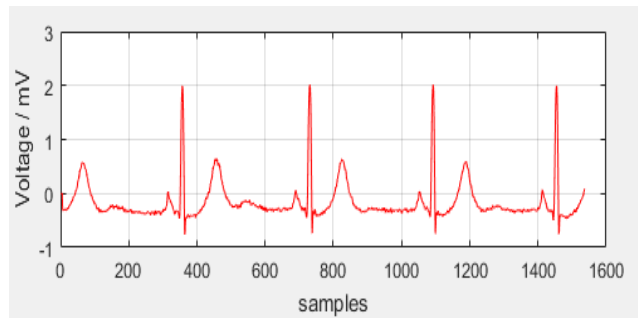
- i. Electrocardiogram (ECG)
- ii. Electroretinogram (ERG)
- iii. Electroneurogram (ENG)
- iv. Mechanomyogram (MMG)

These Bio-signals are represented in time (one dimensional (1-D)), space (two dimensional (2-D)) and time-space (three dimensional (3-D)) domain [108]. Some of the examples of Bio-signals defined in different dimensionality are

- i. In *time domain* – Electrocardiogram (ECG) measures the heart activity by monitoring the changes associated with muscle contractions as shown in Fig. 3.1 (a). It helps to detect the different diseases and abnormalities related to heart. Accurate analysis of an ECG signal assists the cardiologists to prevent many premature deaths [109].
- ii. In *space domain*- A non-invasive technique known as Magnetic Resonance Imaging (MRI) is one of the finest examples of 2-D domain Bio-signals as shown in Fig. 3.1(b).



This technique measures the brain activity by detecting the variations associated with the flow of blood. MRI technique provides assistance to the radiologist and specialist for the diagnosis and prognosis of many life-threatening diseases such as Brain tumors, Clotting and Brain stroke etc [110].



(a)



(b)



(c)

**Figure 3.1** Representation of Bio-signal: (a) 1-D ECG Waveform (b) 2-D Human Brain (c) 3-D view of an infant of pregnant women

- iii. In *time-space domain*- Ultrasound (Sonography) measures the structural movements in internal organs by detecting the variations in the reflection of the sound waves on the tissues as shown in Fig. 3.1 (c). Ultrasound utilizes transducer as a small probe and a gel that straightly spread on the subject's skin. From a transducer probe, high-frequency sound waves are infiltrated through the gel approaching the tissue. As a result bouncing back sounds are generated which are collected by the probe. These particular sound waves are accessed by the computer system to create an image. Ultrasound tests are radiation free procedures (as found in X-rays). Ultrasound imaging categorized as a noninvasive medical procedure that assists clinicians to detect and

diagnose various medical problems. This technique helps to identify the growth, position and computation of cardiac pulsations of infant inside the mother womb [111].

The analyses of Bio-signals are examined through Bio-signal Processing methods explained in next section. Bio-signal Processing involves assessing the measurements in order to provide valuable knowledge for clinician's decision making. Scientists are formulating novel mathematical formulae and algorithms to find new ways to process such signals. Employing advanced methods to evaluate the body behaviour, non-invasive interventions will theoretically assess the state of an individual health. This research is carried out in time domain Bio-signal an ECG signal.

### **3.2 BIO-SIGNAL PROCESSING**

Bio-signal Processing aims to impart clinical significant information flows from Physiological signals [112]. At early stage, analysis of bio-signals was observed manually. A low-level signal processing approach was performed for elimination of noise followed by feature extraction and their classification using conventional classifiers. The implementation of these systems introduced some drawbacks like large time consuming process and experienced an inconsistent accuracy [113]. To overcome these limitations models defining time-series and supervised expert frameworks are introduced. The primary goal of Bio-signal Processing is –

- i. Noise Removal from the signal.
- ii. Feature extraction for function evaluation.

Introducing the Bio-signal Processing methods assists the clinicians with more precise analysis of Bio-signals by removing the noise to overcome the technical deficiencies of the recordings along with extraction of different features to analyze the information contained in the signal and then improving the measurement accuracy and reproducibility of reconstructed signal. These all aspects can be achieved by an efficient Bio-signal Processing techniques and robust algorithms. The proposed diagram of Bio-signal Processing technique is illustrated in Fig. 3.2.

It consists of primary block *Removal of artifacts* followed by *Event Detection*. Bio-signal Processing involves various filtering techniques along with advanced algorithms for detection of different Peaks and their intervals from ECG signal.

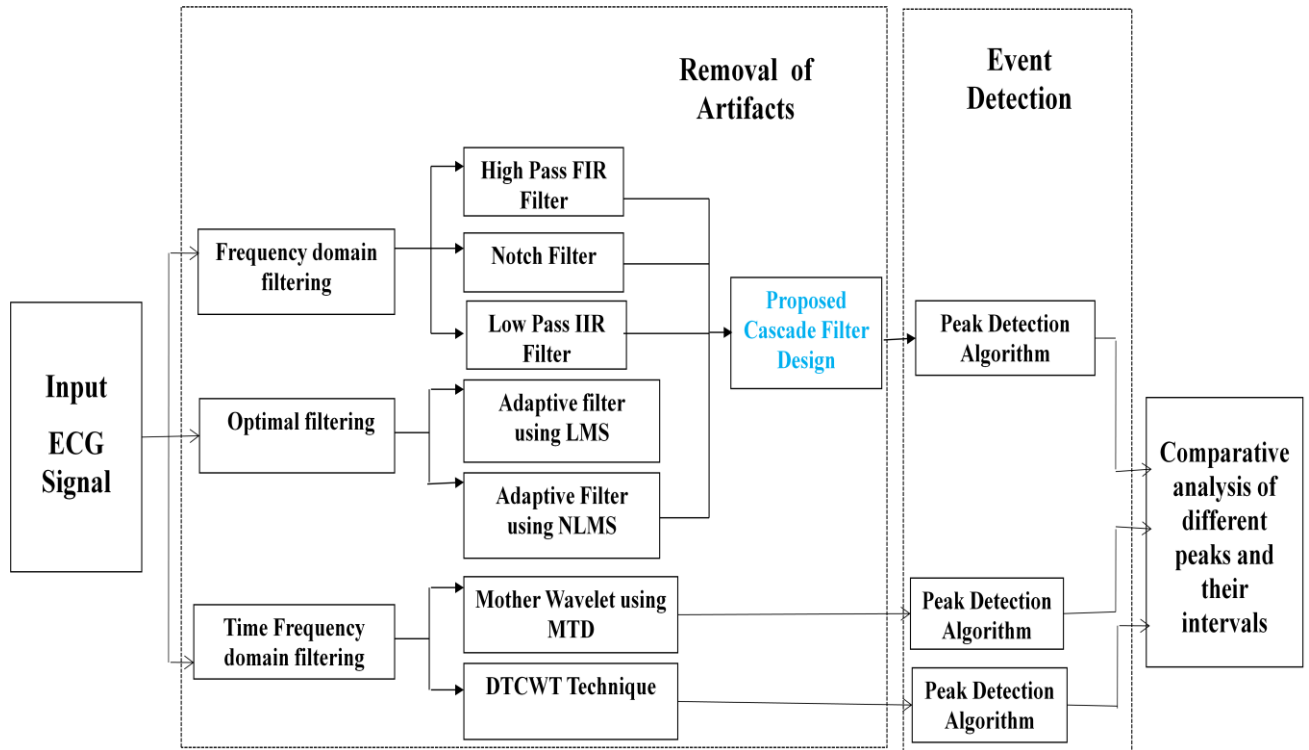


**Figure 3.2** Structural Diagram of Bio-signal Processing

### 3.3 REMOVAL OF ARTIFACTS

Removal of artifacts is accomplished by introducing different filtering techniques such as Frequency domain filtering, Optimal filtering and Time -Frequency domain filtering. The primary concern of this block is suppression of artifacts and noise components from the corrupted signal effectively. For this purpose filters with different characterization are implemented.

### 3.3.1 Frequency Domain filtering

Frequency Domain Filters are utilized for smoothing as well as sharpening of signal by evacuating the high or low frequency noisy components. Frequency domain filters are centered on the frequency of the signal. Distinct frequency domain filters are implemented using Finite Impulse Response (FIR) filters or Infinite Impulse response (IIR) digital filters [114]. Details are explained in *Appendix 2.1 and 2.2*.

The Frequency domain filters are implemented to eliminate distinct noises from ECG signal as illustrated in Fig 3.3.

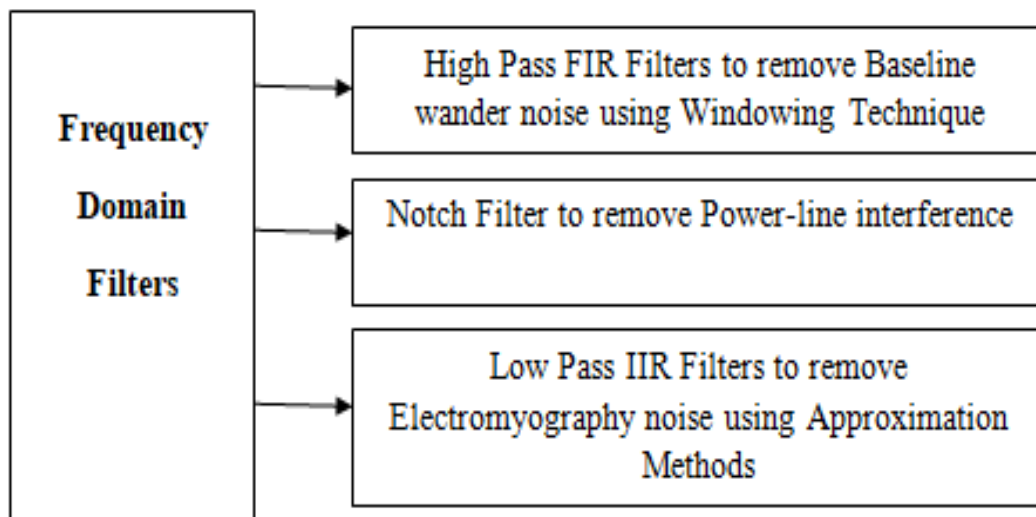


**Figure 3.3** Frequency Domain Filters

High Pass FIR Filter, Notch Filter, and Low Pass IIR Filter are different frequency domain filters that helps in removing inherit noises exist at different frequency levels of ECG signal. A High Pass FIR Filters are designed to eliminate low frequency Baseline wander noise, Notch Filter for Power-Line Interference (PLI) removal and Low Pass IIR filter using Approximation methods for removal of high frequency Electromyography noise.

- i. *High Pass FIR filter* - A high pass FIR filter is designed utilizing window method. In window method, infinite impulse response has been cropped by multiplying it with finite length window function. The various functions used in this thesis are Rectangular

window, Kaiser window, Hanning window, Hamming window, and Blackman window [115] as described in Appendix 2.3 With an increase in the length of window function  $M$ , the width of the main lobe is decremented which lessens the transition band width, but also involves some ripples in the frequency response [116] that can be overcome by introducing the window function it successively eradicates the ringing effects at the band edge and results in lower side lobes at the cost of an expansion of filter's transition band width [117].

A high pass FIR filter is designed to eradicate the low frequency artifacts from the signal. The input signal is sampled ( $f_s$ ) at the rate of 360 Hz. The cut-off frequency ( $f_c$ ) of the filter is set at 0.5 Hz that allows the signal above 0.5 Hz frequency and attenuates the signal less than 0.5 Hz frequency.

The following specifications are considered for designing of High Pass FIR filter utilizing distinct windowing techniques:

- a) Cut-off frequency = 0.5Hz
- b) Sampling frequency = 360 Hz
- c) Window length =  $N + 1$
- d) Order of Filter ( $N$ ) = 10

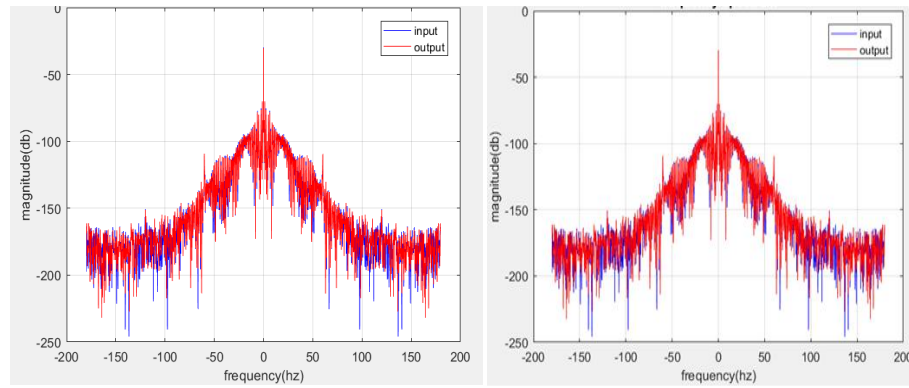
The normalized frequency ( $f_n$ ) for FIR High pass filter has been calculated using Eq. (3.1) and Eq. (3.2).

$$\omega_n = f_n \times f_s \quad (3.1)$$

$$2 \pi (0.5) = f_n \times 360 \quad (3.2)$$

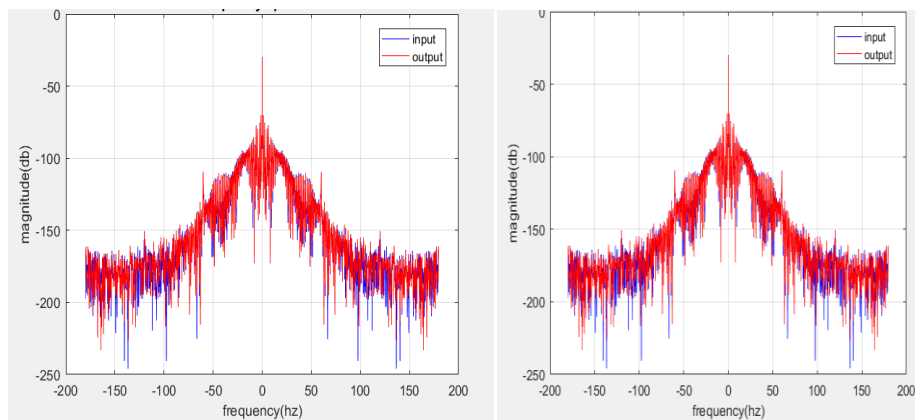
The calculated normalized frequency for digital FIR High pass filter is  $0.002\pi$  rad/sample.

High pass FIR filter implementation using windowing technique removes baseline wander noise from the ECG signal. Fig. 3.4 depicts the frequency spectrum of the filtered ECG signal by employing different windowing based high-pass FIR filters.



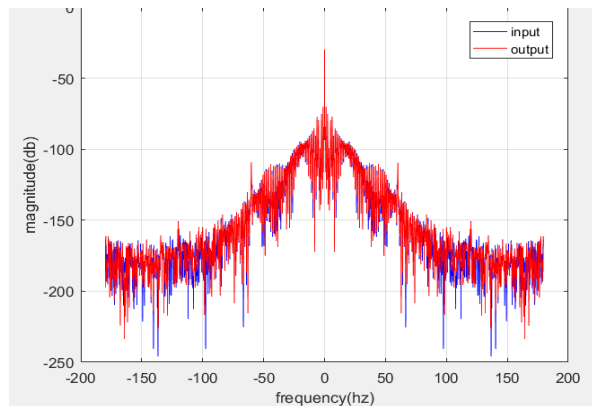
(a)

(b)



(c)

(d)



(e)

**Figure 3.4** Frequency spectrum of filtered ECG signal (a) Rectangular window, (b) Kaiser window, (c) Hanning window, (d) Hamming window, (e) Blackman window

In Fig. 3.4 (a), spectral analysis of Rectangular window based high pass FIR filter is represented which indicates the high resolution and low dynamic range of spectrum. This window function is best to distinguish components of identical amplitude in close frequencies, but worst to distinguish components of different amplitude even if the frequencies are distant, that results into the induction of ripples in the frequency response characterization. Figure 3.4 (b) indicate the designing of high pass FIR filter using Kaiser Window that signifies the reduction in the frequency resolution of ECG signal that noticed the overlapping of noise with signal spectrum. Figure 3.4 (c) indicates the successive reduction in the ripples after applying Hamming window in a High Pass FIR filter. Figure 3.4 (d) depicts the finer frequency resolution along with least spectral leakage of filtered signal using Hanning window function. Finally, in figure 3.4 (e) represents the frequency spectrum of filtered ECG signal using Blackman window function which reveals its smoothness and efficiency.

### Quantitative Analysis:

To evaluate the performance of High pass FIR filters based on window techniques, SNR is determined in the Table 3.1.

**Table 3.1.** SNR Evaluation of Window based FIR filters

High Pass FIR Filter based Window Method	SNR prior to filtering (dB)	SNR ensuing filtering (dB)
Hamming window	-5.5313	6.0130
Hanning window	-5.5313	6.0212
Kaiser window	-5.5313	5.9340
Rectangular window	-5.5313	5.9156
Blackman window	-5.5313	<b>6.0315</b>

From Table 3.1, it is observed that Blackman window based high pass FIR filter performed better than other window based filters as it delivers smooth truncation of ideal impulse response accompanied by linear phase response and high stability.

- ii. *Notch filter* : A notch filter is a band rejection filter that allow the most frequencies unaltered, but attenuates frequencies that fall within a specific range. It is basically a narrow stop band filter which achieves high Q factor [118]. An IIR notch filter is designed to eliminate 50 Hz PLI from an ECG signal with a 49.5 Hz -50.5 Hz frequency band. The ST segment of ECG signal is affected by PLI that limit the precision of arrhythmias diagnosis. It is essential to eradicate the 50 Hz PLI from the recorded ECG signal to attain a clean ECG signal for the arrhythmias diagnosis. The frequency spectrum of the filtered ECG signal passing through the notch filter is shown in Fig. 3.5.

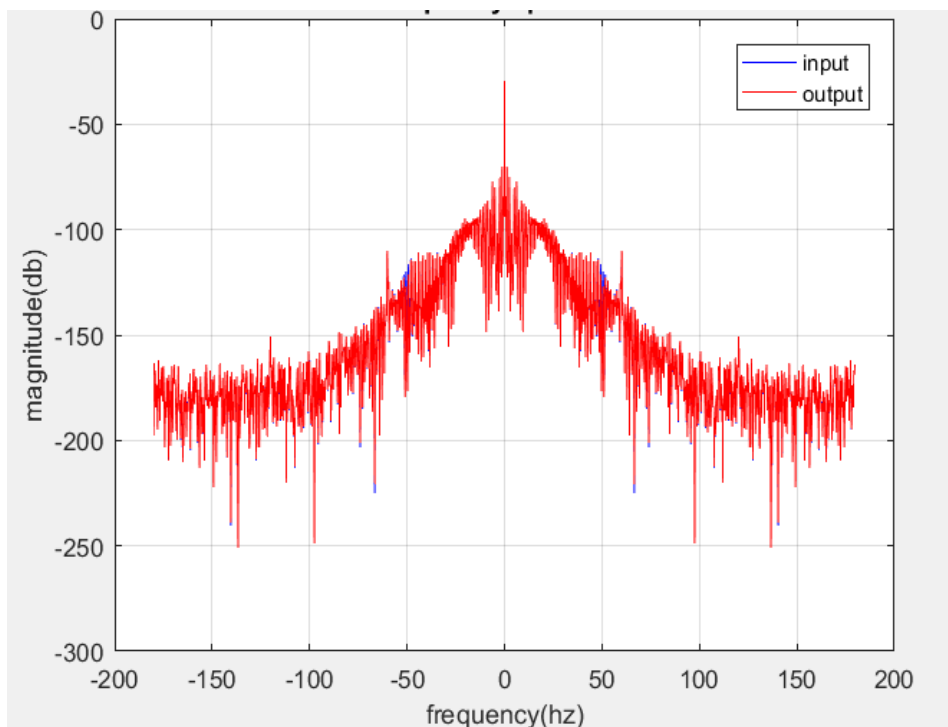


**Figure 3.5** Filtered ECG frequency spectrum using Notch Filter

Fig. 3.5 delineates the successive elimination of noise designated as PLI using notch filter that occurred in the specific frequency range of (49.5-50.5) Hz while passing the remaining signal unalterably.

- iii. *Low Pass IIR filter* – A low pass IIR filter is designed to remove the High frequency Electromyography noise from the ECG signal [119]. The design of low pass IIR filter is based on different approximation methods like Butterworth, Chebyshev I and Elliptic [120]



as described in Appendix 2.4. The cutoff frequency ( $f_c$ ) for low pass filter is 100 Hz. The design of Low Pass IIR Filters using approximation method can be done using bilinear transformation, which maps analog low-pass prototype to the desired filter. The following specifications are taken into the consideration for Low Pass IIR Filter design using different approximation methods.

- a) Cut-off frequency = 100 Hz
- b) Sampling frequency = 360 Hz
- c) Order of Filter ( $N$ ) = 7

The normalized frequency for specific filter design is computed using Eq. (3.3).

$$2 \pi (100) = f_n \times 360 \quad (3.3)$$

Normalized frequency for digital low pass IIR filter is  $0.55\pi$  rad/sample.

IIR filter designs have fast computation speed and require less memory as compared to their counter parts FIR filters. IIR filters exhibits high sensitivity and less delay than FIR filters. Moreover, IIR filters with least filter order delivers the similar performance as attained by high order FIR filters. Implementation of low pass filter utilizing approximation methods eliminates the High frequency electromyography noise from the ECG signal. Figure 3.6 shows the frequency spectrum of filtered ECG signal by employing Butterworth, Chebyshev I and Elliptic based Low Pass IIR Filter respectively.

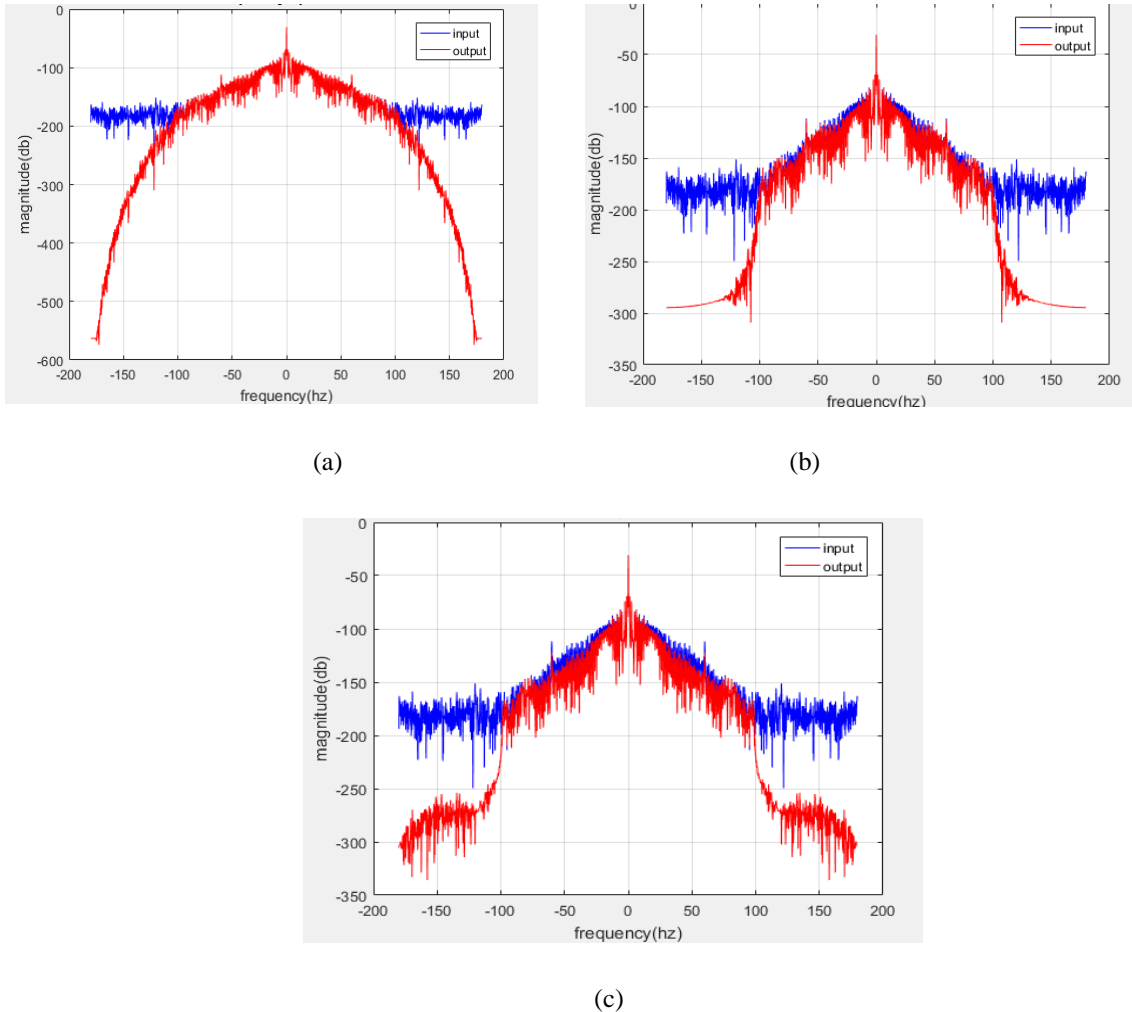


**Figure 3.6** Filtered ECG signal through IIR Low Pass Filter (a) Butterworth (b) Chebyshev (c) Elliptic

Fig.3.6 (a) depicts the suppression of high frequency noise by low pass IIR Butterworth filter. The quality factor ' $Q$ ' of respective filter is 0.707 which determines that the higher frequencies above the cut-off point roll down to zero in the stop band at 20dB/decade. From Fig. 3.6 (b) it has been observed that low pass Chebyshev I filter has steeper roll-off as compared to low pass Butterworth filter design. Fig.3.6 (c) represents the frequency spectrum of filtered ECG signal obtained through low pass Elliptic filter which signifies its steeper roll-off characteristics than Butterworth and Chebyshev filters i.e. best suited for elimination of Electromyography noise beyond the cut-off frequency. Further performance evaluation of low pass filter designs using different approximation methods has been evaluated in Table 3.2.

**Table 3.2.** SNR Evaluation using Approximation based Low Pass IIR filter

<b>Distinct IIR Filter Design</b>	<b>SNR prior to filtering</b>	<b>SNR ensuing filtering</b>
	<b>(dB)</b>	<b>(dB)</b>
Butterworth Filter	-5.5313	11.8139
Chebyshev I Filter	-5.5313	9.0951
Elliptic Filter	-5.5313	<b>12.2930</b>

The best value of SNR is achieved using Elliptic low pass filter which justify its superiority for suppression of electromyography noise from desired signal.

These frequency domain filters able to eliminate the distinct artifacts and noises that lies in specific frequency range of ECG signal but unable to suppress the burst noise classified as flicker and instrumentation noise that exist at entire frequency band of ECG signal when transmitted through channels. For this purpose, optimal filters are introduced to eradicate these kinds of artifacts from ECG signal.

### **3.3.2 Optimal filtering**

Optimal filtering is introduced to attain a fine estimate of desired signal from corrupted ECG records. Optimal filtering is performed to extract the signal that has been buried in random noise and can't be possible to be filtered using frequency domain filters. The optimal filters are precisely applicable at the white noise spectrum having similar amplitude at all frequency range. At these particular circumstances both signal and noise spectra overlapped, making its complicated to differentiate them for further processing. In optimal filtering, filter parameters (coefficients) vary with respect to time. The major applications concerning optimal filtering are adaptive noise cancellation, system identification, frequency tracking and channel equalization [121]. Fig. 3.7 depicts the generalized optimal / adaptive filter structure.

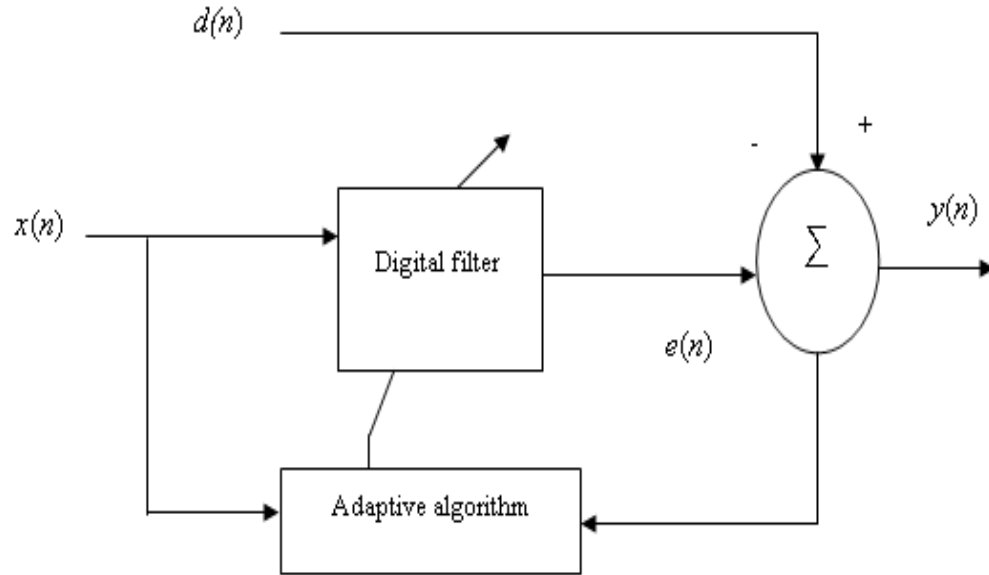


**Figure 3.7** Generalized structure of Adaptive Filter

In Fig. 3.7,  $x(n)$  represents the input signal that delivers the output signal  $y(n)$  by adjusting the filter coefficient to attain minimum error  $e(n)$ . Minimization of cost function is channelized through adaptive algorithms that update the weight vectors in adaptive filters. The different Adaptive algorithms are categorized as *Least Mean Square algorithm* (LMS), *Normalized Least Mean Square algorithm* (NLMS) and *Recursive Least Square* (RLS) algorithm [122]. In this thesis, LMS and NLMS algorithms are implemented for ECG noise reduction as RLS algorithm exhibit high computational complexity and have stability issues. Moreover, RLS is also not suited for tracking the statistical variation. Adaptive filters using LMS and NLMS algorithm are designed to remove Burst noise to achieve optimal filtering.

- i. *LMS algorithm* – LMS algorithm is based on stochastic gradient descent method in which adaptation of filter weights rely on the current time error. This algorithm adjusts the coefficients of FIR filters iteratively. The weight of the adaptive filter at the  $k^{\text{th}}$  iteration is determined by Eq. (3.4).

$$w_{k+1}(i) = w_k(i) + 2\mu e_k x_{k-1} \quad (3.4)$$

where  $\mu$  is the step size

## Algorithm for Least mean square

---

Input : Noisy ECG Signal  
Output : Filtered Output ( $\tilde{n}_k$ )

---

Initialize  $\mu$   
For each  $k$   
{  
 $e_k = y_k - \tilde{n}_k$   
 $w_{k+1} = w_k + 2\mu e_k x_{k-1}$   
}

The filter output of LMS algorithm is given as

$$\tilde{n}_k = \sum_{i=0}^{N-1} w_k(i) x_{k-i}$$

---

- ii. *NLMS algorithm*- It is modified version of standard LMS algorithm. The step size parameter in NLMS algorithm is not constant and is independent of the input signal power & number of tap weights. The weight of adaptive filter using NLMS algorithm is expressed by Eq. (3.5).

$$w_{k+1}(i) = w_k(i) + \mu e_k x_{k-1} \quad (3.5)$$

where  $\mu = \frac{\tilde{\mu}}{x_k^2 x_k + \epsilon}$  and  $\epsilon$  is smallest positive number

## Algorithm for Normalized Least mean square

---

Input : Noisy ECG Signal  
Output : Filtered Output ( $\tilde{n}_k$ )

---

Initialize  $\mu$

For each  $k$

{

$$e_k = y_k - \tilde{n}_k$$

$$w_{k+1} = w_k + 2\mu e_k x_{k-1}$$

}

The filter output of LMS algorithm is given as

$$\tilde{n}_k = \sum_{i=0}^{N-1} w_k(i) x_{k-i}$$

---

The filters are designed using following specifications:

- Filter order =10
- Step size = 0.533
- Offset value = 10
- Adaptive filter length =11
- Sampling frequency=360 Hz

The raw ECG signal of '100 record' is derived from the database of "MIT-BIH Arrhythmia" database [28] is filtered through adaptive filter using LMS and NLMS algorithms. Time domain analysis of ECG output signal by adaptive filter using LMS and NLMS algorithm is shown in Fig 3.8 and Fig 3.9 respectively.

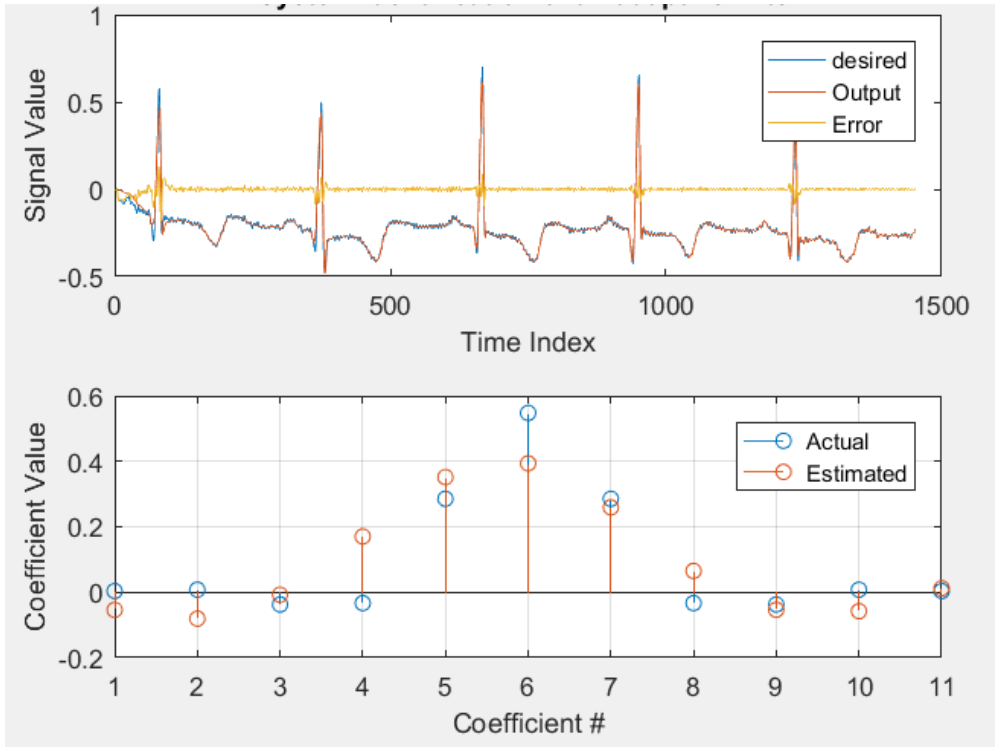


**Figure 3.8** Analysis of ECG signal in time domain using LMS algorithm

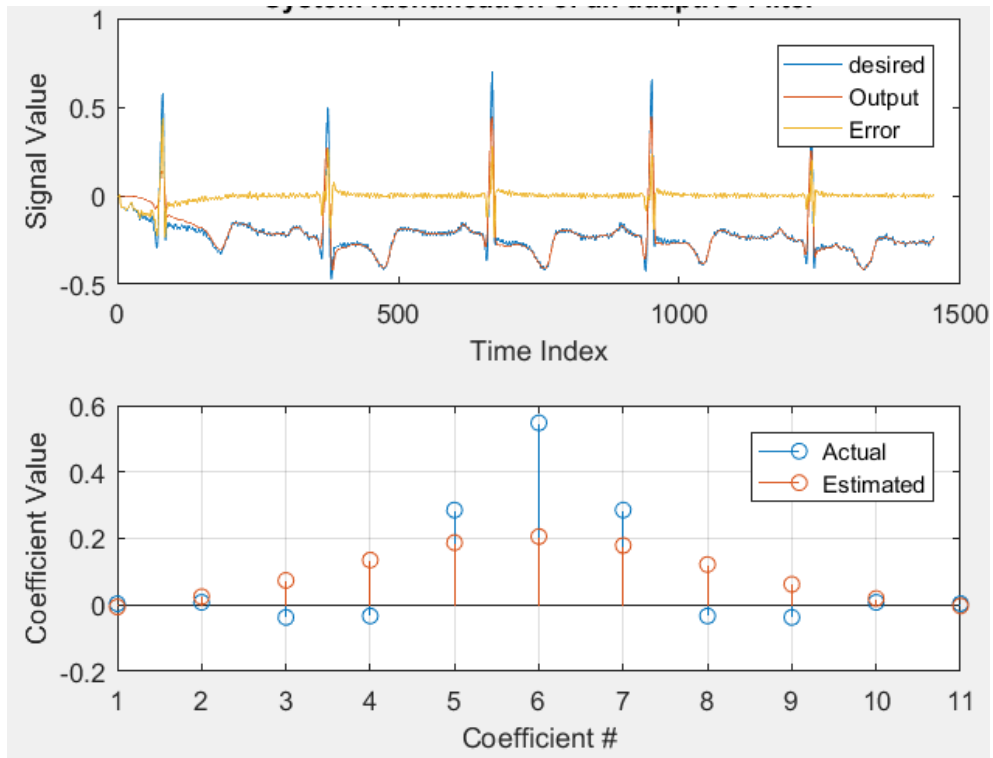


**Figure 3.9** Analysis of ECG signal in time domain using NLMS algorithm

The frequency spectrum of LMS and NLMS algorithm is evaluated and is shown in Fig. 3.10 (a) and (b) respectively. Fig.3.10 depicts that error signal obtained after filtering using NLMS algorithm is much smaller in comparison to LMS algorithm which claims its superiority to remove this particular noise from ECG signal.

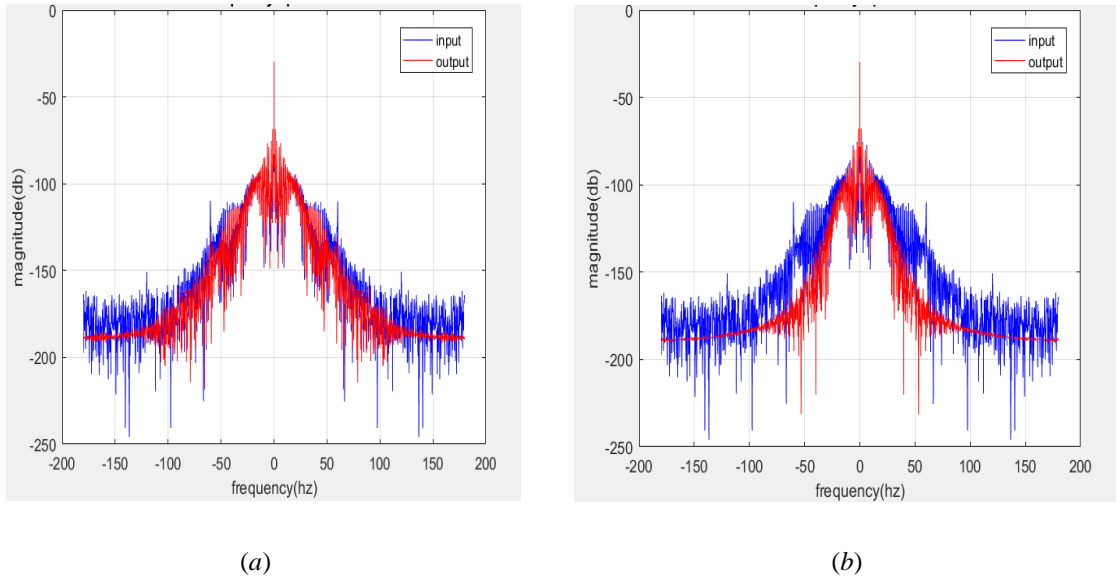


**Figure 3.10** Frequency spectrum of ECG signal using (a) LMS algorithm (b) NLMS algorithm

From Figure 3.10 it has been observed that NLMS algorithm is best suited in separating the noise from the desired signal which is further validated by evaluating the performance parameter for LMS and NLMS algorithms are tabulated in Table 3.3.

**Table 3.3.** SNR Evaluation of Adaptive filter using different algorithm

<b>Adaptive Filter</b>	<b>SNR prior to filtering (dB)</b>	<b>SNR ensuing filtering (dB)</b>
LMS algorithm	-5.5313	6.2771
NLMS algorithm	-5.5313	<b>7.1699</b>

Table 3.3 displays the computational results of obtained SNR prior and after optimal filtering. The result reveals that the best value of SNR is obtained by filtering the ECG signal using NLMS algorithm.



After evaluating the performance of different filters it has been analyzed that they remove the distinct types of noise independently. There is a need to filter the entire ECG signal that removes the overall noisy component from the signal through a single filter design. To overcome this problem, a *Cascade Digital Filter* using best performance filters is proposed.

### 3.3.3 PROPOSED CASCADE DIGITAL FILTER DESIGN

Various ECG interferences can be eradicated by design of band pass filter structure but application of this type of filter for ECG signal degrades the performance resulting into the small SNR value [123]. To tackle this particular problem, a *cascade digital filter* is using both frequency domain and optimal filters to attain clean ECG signal. The structural view of proposed cascade digital filter as depicted in Fig.3.11. The proposed cascade structure is consists of four different sets of filters : High pass FIR Filter, Adaptive Filter, Notch Filter and Low pass IIR Filter. The raw ECG input signal is contaminated by distinct artifacts which are initially fed to high pass filter designed utilizing Blackman window approach to restrict the low frequency noise from the input signal. In next step, signal obtained from high pass filter is given to the adaptive filter using NLMS algorithm to eliminate the burst noise. After elimination of burst noise signal is fed to the notch filter to suppress the PLI originated due to capacitive and inductive coupling mechanism. Finally, elimination of electromyography noise is performed through low pass filter using Elliptic approximation method.

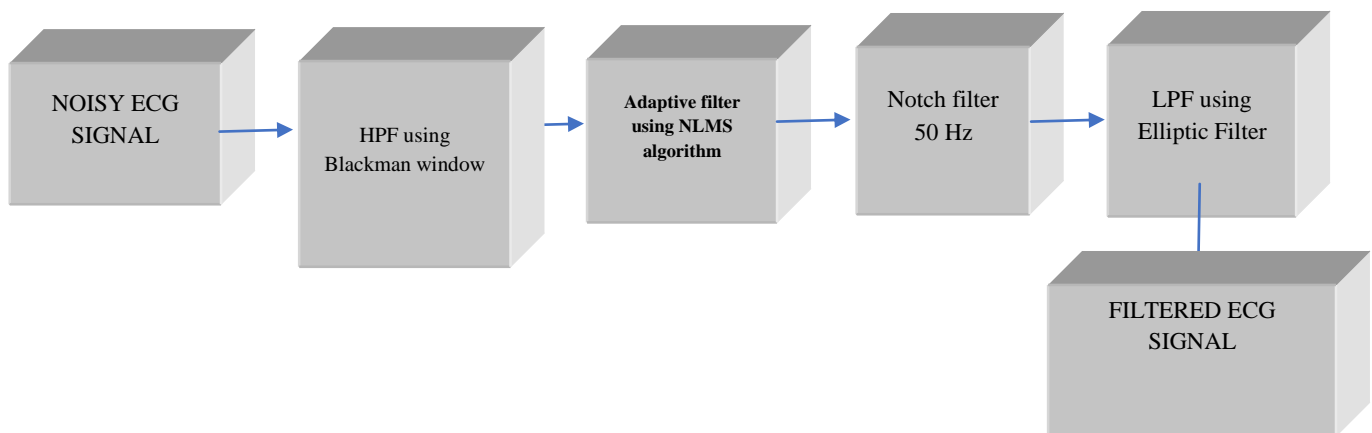


**Figure 3.11** Block diagram of Proposed Cascade Digital Filter

The output waveform of proposed cascaded Digital filter in terms of Time domain is depicted in Fig. 3.12 and its spectral analysis is represented in Fig. 3.13.

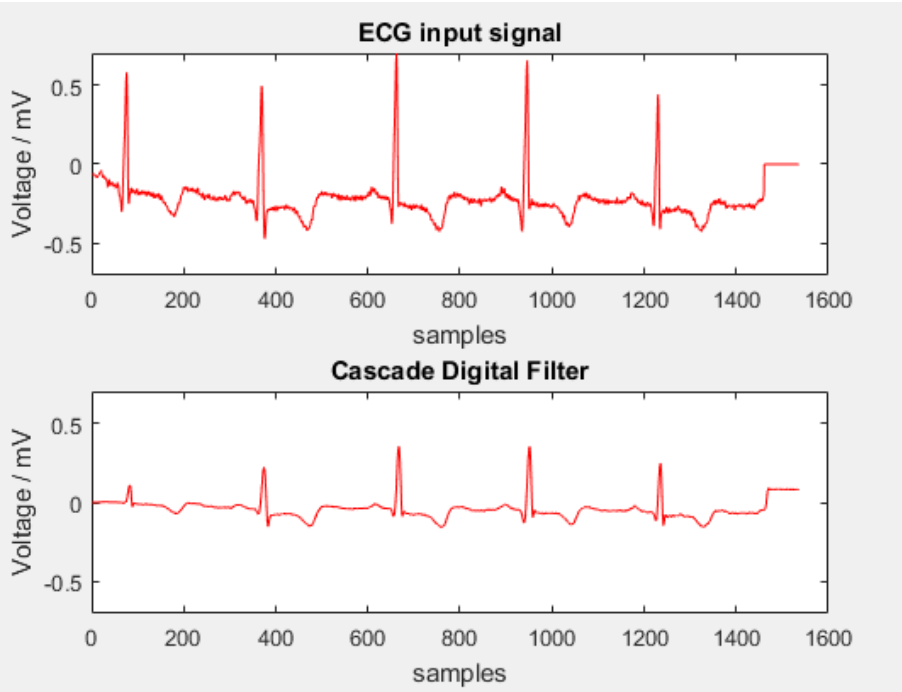


**Figure 3.12** Time domain analysis by Cascaded Filter

Fig. 3.12 clearly indicates the ECG denoising using cascade digital filter. The output using cascade digital filter is smooth and distortion less as compared to ECG input signal.

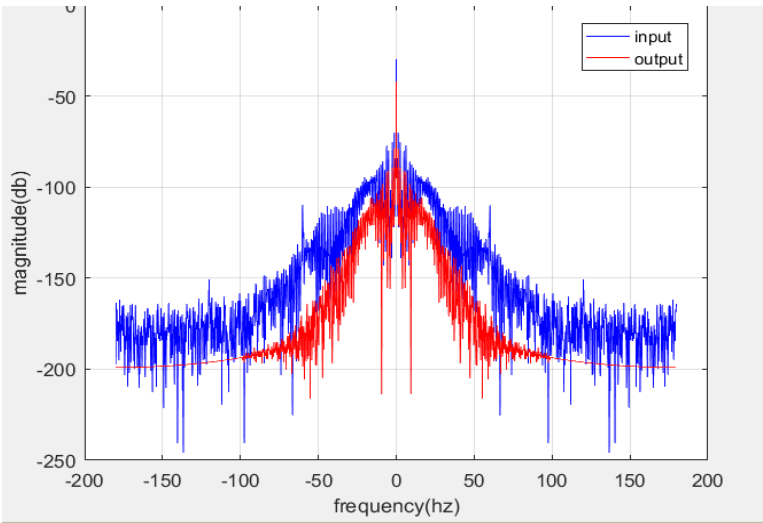


**Figure 3.13** Spectral analysis of ECG signal filtered by Cascaded Filter design.

On analyzing the spectrum it has been observed that cascade filter design successively eliminates the distinct noises present in the input ECG signal that make it suitable for further processing.

### Quantitative Results

After visual analysis of results, different performance parameters are analyzed. Table 3.4 shows the computation of SNR improvement of Cascade digital filter

**Table 3.4** SNR computation of Cascade Digital Filter

SNR prior to Filtering (dB)	SNR ensuing filtering (dB)	SNR Improvement
-5.5313	2.2226	7.7539

From Table 3.4, it has been observed that overall SNR improvement 7.7539 dB is attained by employing proposed cascade digital filter which shows the considerable improvement in denoising of ECG signal. Later, Comparison of proposed cascade digital filter with other state-of-the-art- techniques in terms of SNR improvement is depicted in Table 3.5.

**Table 3.5** Comparison of Cascade Filter with state- of-the- art- work

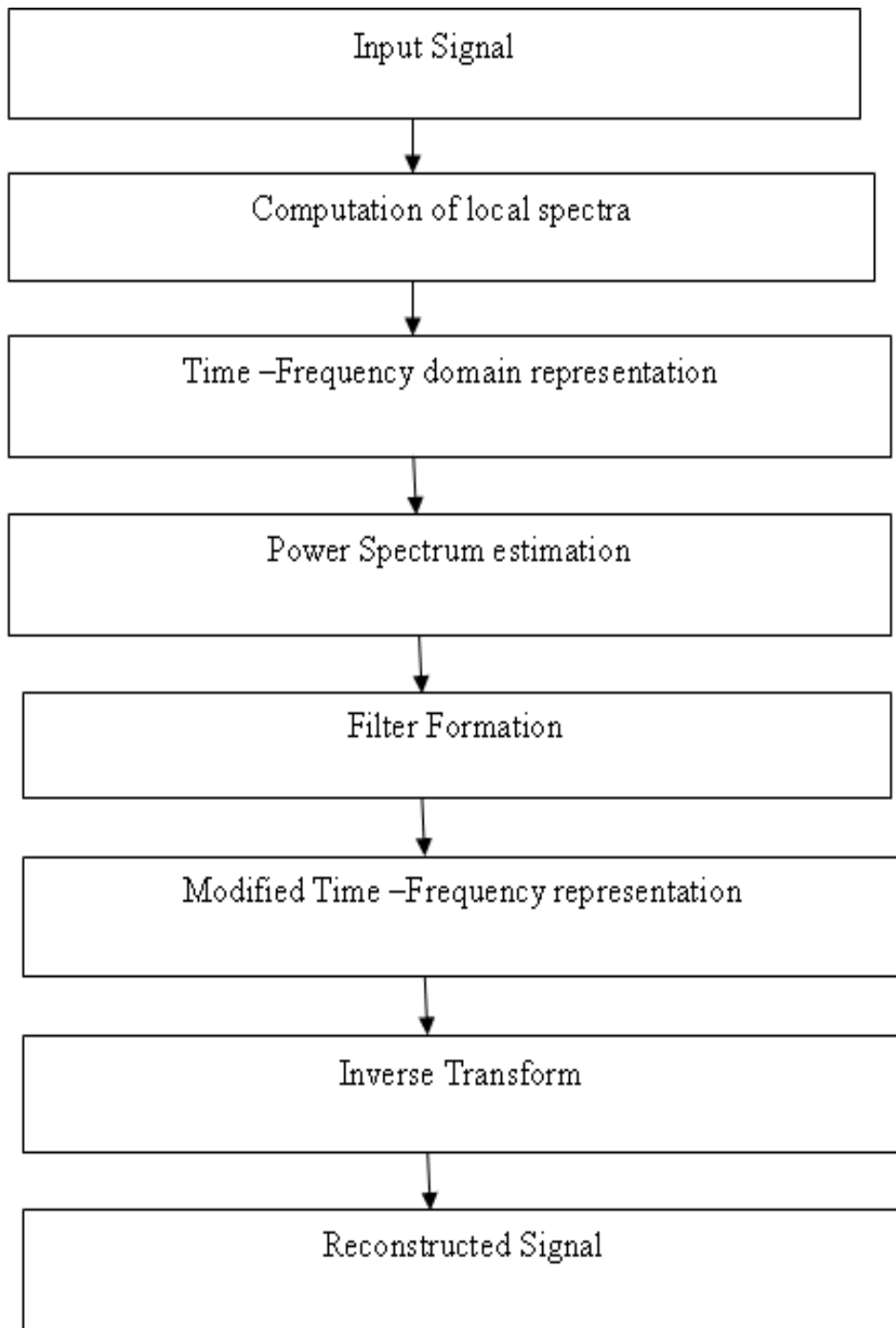
S.No.	Author name	SNR improvement ensuing filtering (dB)
1.	Patro <i>et al.</i> (2015) [124]	4.14
2.	Harshal B <i>et al.</i> (2017) [125]	2.66
3.	Cascade Digital Filter ( <b>Proposed</b> )	<b>7.75</b>

Table 3.5 depicts that the Cascade Digital Filter delivers maximum SNR improvement (7.75 dB) that restricts the influence of noise at the output signal. Deep examination of Cascade Digital Filter design depicts some shortcomings such as computational complexity, large memory requirement, Orthogonality and increase in sensitivity with the order of filter. To overcome these limitations Time- Frequency domain filters are introduced.

### **3.3.4 Time-Frequency domain filters**

The Time-frequency domain is a powerful approach for evaluation and refining of non-stationary signal that has been broadly utilized in distinct prominent fields such as communication, acoustics and medical signal analysis [126-128]. This approach exploits the time-frequency localized spectra of the information and delivers a modifying filtering procedure for non-stationary ECG signal. The time-frequency domain filtering employs a modified weight function to sort out the information from the noisy signal. The localization performed by higher weighting parts is supposed to be signal components, and the lower weighting parts predict the noise attenuation in the time-frequency domain. Reconstruction of signal is achieved by performing the inverse transform of time-frequency domain. The Time-frequency domain filtering composed of distinct stages as depicted in Fig. 3.14.

Denoising of signal is performed by segmenting the time-frequency signal into distinct regions defining signal and noise separately. In signal restoration concept modification of time-frequency signal is performed to overcome the signal degradation such as signal and image blur, signal interruptions in signaling system. This process involves exploitation of correlations patterns to enhance the reliability of signal by equally separating the noise content. A moving window signal analysis is considered where the selected transform in a window spectrum is evaluated for each window position and signal that is represented in the form of time-frequency domain followed by signal estimation leading time-frequency domain filter. The time-frequency domain filter modifies the time-frequency signal accordingly. Finally, processed signal is obtained using inverse transform. In this procedure, inverse transform of window portion are utilized to obtain the output signal either by choosing particular samples to generate the processed signal of corresponding sample or generation of sample by the suitable amalgamation of all samples in overlapped windows portion of inverse transformed signal.



**Figure 3.14** Flow chart of time -frequency domain signal filtering

The foremost prominent techniques of time–frequency domain filtering considered in the research work are Mallet Tree Decomposition (MTD) and Dual Tree Complex Wavelet Transform (DTCWT)

- i. *Mallet Tree Decomposition (MTD)* - In mallet tree decomposition the output is determined by filtering of discrete signal through successive low pass and high pass filters [129]. MTD is two-channel sub-band coder schemes that utilize quadrature mirror filters (QMFs) for signal processing as shown in Fig. 3.15.

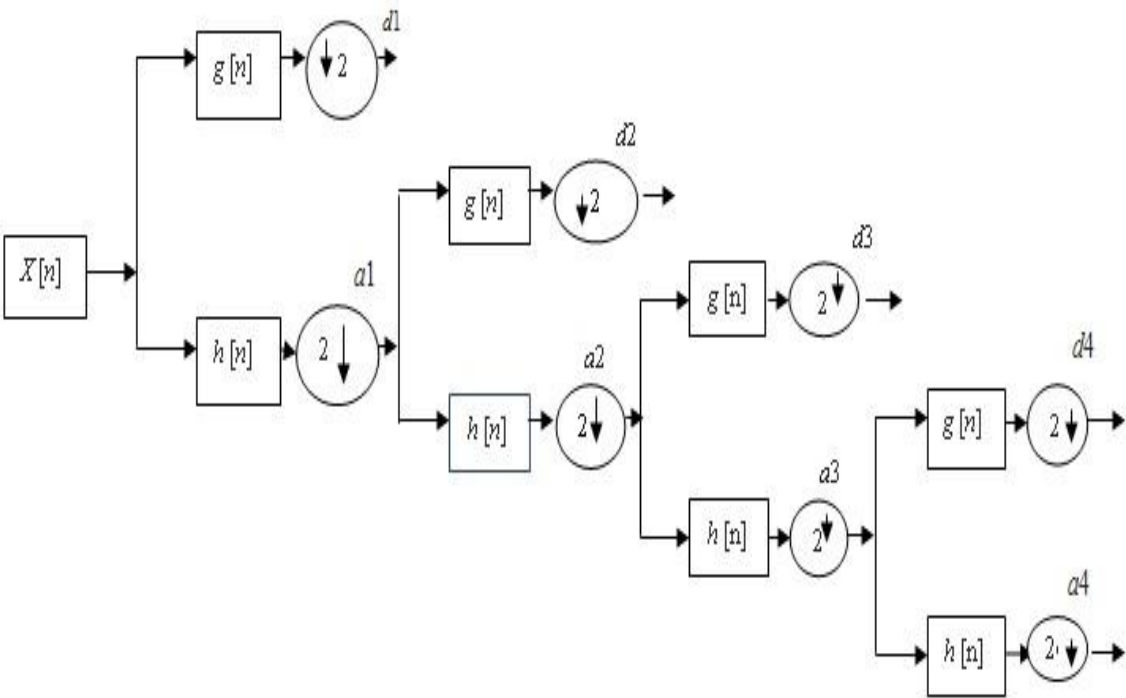


**Figure 3.15** Mallet Tree Decomposition

Fig. 3.15 display the decomposition of input signal  $x[n]$  into: high pass filter  $g[n]$  and low pass filter  $h[n]$ .The individual stage of MTD is composed of two digital filters and two down samplers (by2) that delivers frequency varying digital signals. The detail coefficient  $d1$  is extracted from the first stage output of high pass filter  $g[n]$  and approximation coefficient  $a1$  is provided by low pass filter  $h[n]$  respectively. Further decomposition of approximation coefficients is performed at every stage to deliver the new detail and approximation coefficients up to the set level of decomposition. Fourth level decomposition is performed that delivers  $(d1, d2, d3, d4)$  detail coefficients and  $(a4)$  approximation coefficient.

MTD is implemented utilizing mother wavelets that are most effective to deliver fast computation results of discrete wavelet transform (DWT). The design implementation of DWT is very simple and requires less number of resources with least computational delay [130]. Representation of digital signal with DWT in time scale is determined by utilizing digital filtering techniques. The input signal is proceed through the filters of distinct cut-off frequencies at multiple scales. In DWT, multi-resolution analysis is obtained by varying both the time and frequency resolutions in time-frequency domain by performing the signal decomposition into mutually orthogonal set of wavelets.

The Discrete Wavelet Transform function is defined by Eq. (3.6)

$$W_{\psi}(j, k) = \frac{1}{\sqrt{m}} \sum x(n) \psi_{j,k}(n) \quad (3.6)$$

where  $x(n)$  denotes the input signal,  $1/\sqrt{m}$  known as normalizing term,  $m$  determines the number of samples in the sequence and  $n$  describes the integer values as  $0, 1, 2, \dots, m-1$ .

The wavelet coefficients are extracted utilizing distinct mother wavelets by executing MTD and smoothing of coefficients are obtained by Global thresholding technique followed by denoising procedure. Decomposition level is chosen in such a manner that the denoising process is performed without removing important features from the ECG signal. Decomposition level ( $D_L$ ) of MTD is calculated by Eq. (3.7)

$$D_L = \log_2 N \quad (3.7)$$

where  $N$  defines the number of samples.

Distinct families of DWT have been explored to perform the signal denoising process [131] *described in Appendix 2.5.*

The analysis of result with distinct mother wavelets are determined using MTD and their performance parameters are computed in terms of SNR, PRD and MSE as described in Table 3.6.

**Table 3.6.** Performance evaluation of distinct wavelet families

<b>Mother Wavelets</b>	<b>Categories</b>	<b>SNR</b>	<b>PRD</b>	<b>MSE</b>
	<b>sym4</b>	24.8996	0.0569	2.0674e-04
Symlets	<b>sym5</b>	24.6218	0.0587	2.2039e-04
	<b>sym6</b>	25.2806	0.0552	1.8937e-04
	<b>sym9</b>	24.8941	0.0569	2.0700e-04
Coiflets	<b>coif 4</b>	25.1166	0.0555	1.9666e-04
	<b>coif5</b>	24.8627	0.0571	2.0850e-04
Reverse orthogonal	<b>rbio4.4</b>	24.4049	0.0602	2.3168e-04
	<b>rbio5.5</b>	24.9515	0.0565	2.0428e-04
	<b>rbio6.8</b>	25.1085	0.0555	1.9703e-04
Biorthogonal	<b>bior3.5</b>	26.3158	0.0483	1.4921e-04
	<b>bior3.7</b>	26.4652	0.0475	1.4416e-04
	<b>bior3.9</b>	<b>26.5396</b>	<b>0.0471</b>	<b>1.4172e-04</b>
Daubechies	<b>db4</b>	25.0144	0.0561	2.0134e-04
	<b>db5</b>	24.6097	0.0588	2.2101e-04
	<b>db6</b>	24.3737	0.0604	2.3335e-04
	<b>db7</b>	24.5116	0.0595	2.2606e-04
	<b>db8</b>	24.0698	0.0626	2.5027e-04



From Table 3.6, it has been observed that bior3.9 outperforms among all mother wavelets with highest SNR, lowest MSE and smallest PRD. Further, denoised ECG signal using bior3.9 wavelet is shown in Fig. 3.16.

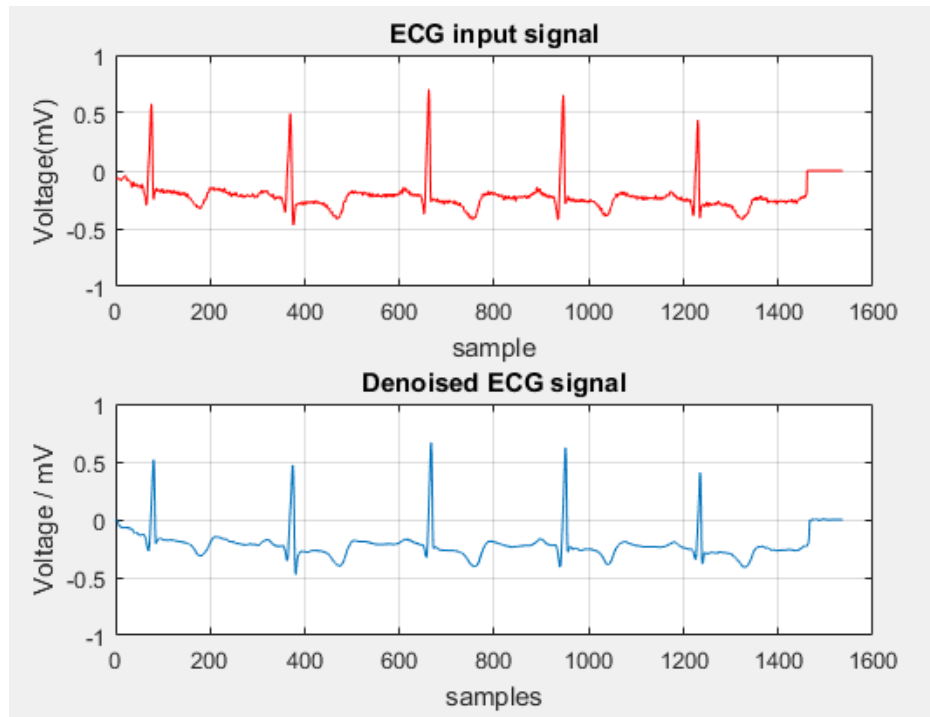


**Figure 3.16** Denoised ECG signal using bior3.9 wavelet

Fig. 3.16 shows the successful elimination of noise content from the ECG signal utilizing bior3.9 wavelet with Mallet tree decomposition (MTD). Analysis of different mother wavelets using MTD depicts some kind of distortion in the output signal due to some underlying reasons-

- a) Lacks in shift-invariance and directional selectivity which leads to much less redundancy of transform coefficients.
- b) Aliasing effect that causes diverse signals to become indistinguishable.
- c) Wavelet coefficients oscillate both in positive and negative direction around singularity that enables singularity extraction and signal modeling more tedious in real valued wavelet transform.

To overcome these challenges another technique called Dual-Tree Complex Wavelet Transform (DTCWT) is performed for further enhancement in the quality of signal.

- ii. *Dual-Tree Complex Wavelet Transform (DTCWT)* – This technique is relatively an enhanced version of DWT. This technique comprises of two DWTs structure such that real part is offered by first DWT and the imaginary part is delivered by second DWT. These two real DWTs utilized two distinct sets of filters that satisfying the Perfect Reconstruction (PR) conditions [132]. The set of two real filters are constructed together to make the wavelet is approximately analytic and the resultant coefficients are in complex form which as modeled in Eq. (3.8).

$$\mathcal{Y}(t) = \mathcal{Y}_h(t) + j \mathcal{Y}_g(t) \quad (3.8)$$

where  $\mathcal{Y}_h(t)$  represents the real and even part while  $\mathcal{Y}_g(t)$  shows the real and odd such that

$$\mathcal{Y}_g(t) \approx H \mathcal{Y}_h(t) \quad (3.9)$$

where  $H$  is the Hilbert transform.

The two filter banks compute the output for DTCWT; each filter bank comprises of two filter bank pairs of high pass and low pass as illustrated in Fig. 3.17.

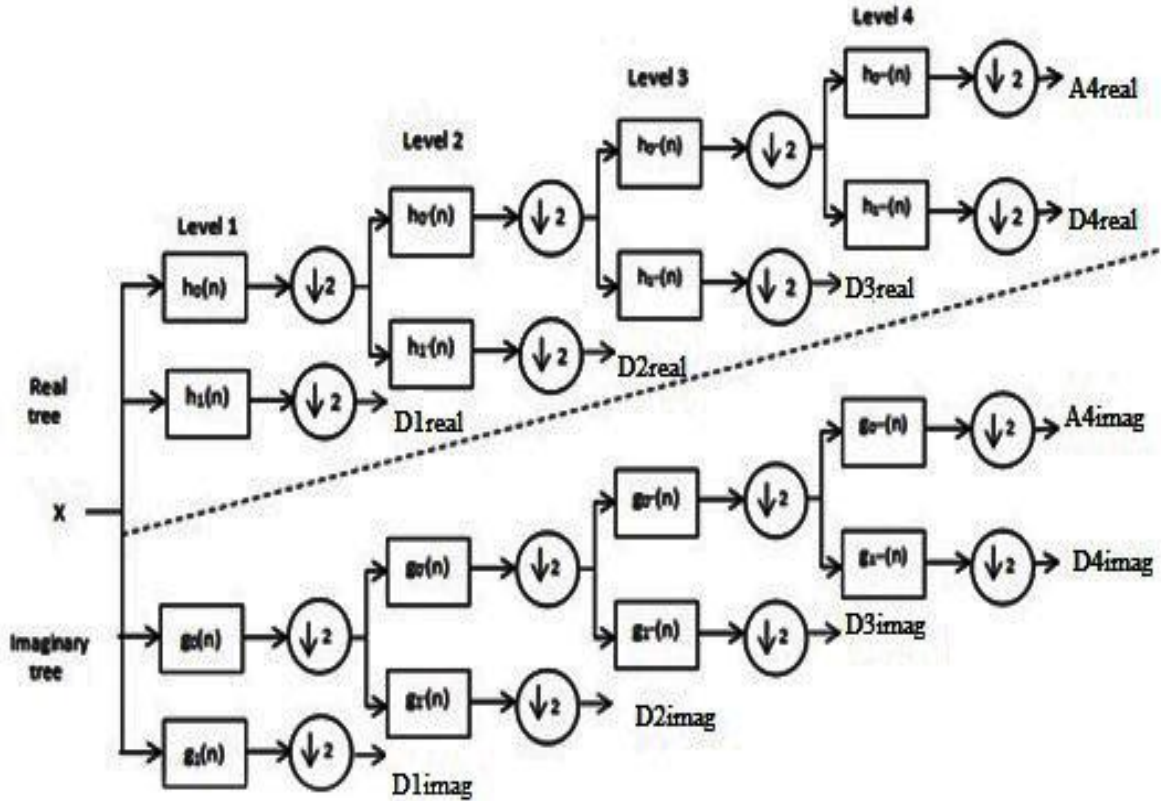


Figure 3.17 Dual tree complex wavelet transform

This technique transforms the coefficients twice that lead to the expansion of the DWT coefficients (as  $N$  coefficients in DWT converts to  $2N$  coefficients in DTCWT). In Fig. 3.17 input signal is represented by discrete value 'x',  $h_0(n)$  and  $h_1(n)$  determines the low pass filter and high pass filter for upper filter bank. Similarly, for lower filter bank low pass and high pass filter pair are represented by  $g_0(n)$  and  $g_1(n)$  respectively. Each stage consists of two digital filters that are further associated with two down samplers which down-sampled the signal by factor 2 to deliver the output signal. Approximation coefficient and detail coefficients for upper filter bank are obtained from the down-sampled output of  $h_0(n)$  and  $h_1(n)$ . Approximation coefficient are considered as low frequency components known as scaling function and is obtained at last level of decomposition whereas, detail coefficient are considered as high frequency components designated as wavelet functions extracted at each decomposition level. Similarly, for lower filter bank the approximation and detail coefficients are obtained by low pass filter  $g_0(n)$  and high pass filter  $g_1(n)$  with respective down samplers.

The whole process of decomposition up to the set level of decomposition is proceeding on the scaling function of each filter bank. The DTCWT procedure is performed to determine the absolute value of real and imaginary coefficients using 4th level of decomposition. At each level of decomposition scale, complex detail coefficients are extracted comprising four sub bands designated as ( $D1, D2, D3, D4$ ) and is represented by Eq. (3.10)

$$D1 = D1_{\text{real}} + i D1_{\text{imag}} \quad (3.10)$$

Similarly, in sub band ( $A4$ ) the complex approximation coefficient is expressed by Eq. (3.11).

$$A4 = A4_{\text{real}} + i A4_{\text{imag}} \quad (3.11)$$

Multilevel decomposition provides four detail sub bands that include complex detail coefficients and  $A4$  sub band contains complex approximation coefficient. The broad description of approximation and detail coefficients at each sub band are tabulated in Table 3.7. The level of decomposition is selected in such a manner that signal classification is preserved in the wavelet coefficient.

**Table 3.7.** Coefficients of Detail and Approximation at each sub band assuming sampling frequency 360 Hz

S.No.	Sampling Frequency at each decomposition level	Sub Bands of Detail and Approximation Coefficients (upper filter bank + lower filter bank)	Number of Coefficients (In Complex form)
1.	180	$D1 = d1_{\text{real}} + i d1_{\text{imag}}$	768
2.	90	$D2 = d2_{\text{real}} + i d2_{\text{imag}}$	384
3.	45	$D3 = d3_{\text{real}} + i d3_{\text{imag}}$	192
4.	22.5	$D4 = d4_{\text{real}} + i d4_{\text{imag}}$	96
5.	22.5 (Approximation)	$A4 = a4_{\text{real}} + i a4_{\text{imag}}$	96

Table 3.7 demonstrates that at each level of decomposition, detail coefficients are obtained to such an extent that level 1 having 768 coefficients followed by 384, 192 and 96 coefficients for level (2, 3 and 4). Also, the approximation coefficients obtained at level 4 are 96.

High frequency detail coefficients are mainly influenced to noise whereas low frequency approximation coefficients are least affected by noise. To restrict these noise contents, a conventional noise estimation method proposed by Donoho and Johnstone depend on Median Absolute Deviation (MAD) [133] is applied on the detail coefficients extracted at different levels of filter bank.

Noise level  $\delta$  is calculated by the Eq. (3.12).

$$\delta = \left( \frac{\text{median}\{|\chi_{iv}|\}}{0.6745} \right) \quad (3.12)$$

where  $\chi_{iv}$  defines the detail coefficients at finest level. Threshold value  $\lambda$  is computed by Eq. (3.13) expressed as

$$\lambda = \delta \sqrt{2 \log(k)} \quad (3.13)$$

where  $k$  defines the signal size at each detail level. The threshold value is computed for each level of decomposition and Soft thresholding procedure is employed at each level to eliminate the noise determined by Eq. (3.14)

$$Y = \text{sign}(x) \cdot (|x| - \lambda) \quad (3.14)$$

where  $Y$  denotes output, and the value of input is defined by  $x$ . In soft thresholding, the coefficients higher in magnitude than the threshold value are contracted towards zero by deducting the threshold value from coefficient value.

Finally, the inverse DTCWT technique is implemented on the modified threshold detailed coefficients ( $D-1$ ,  $D-2$ ,  $D-3$ ,  $D-4$ ) and original approximation coefficient ( $A4$ ) to achieve final signal output. The inverse DTCWT performed a reverse procedure for signal reconstruction

where the signal at each level is up sampled by factor 2 is proceed through synthesis filter and then added.

Fig 3.18 shows the reconstructed signal processed by DTCWT technique relative to ECG input signal that signifies the successive elimination of noisy content from the ECG signal.

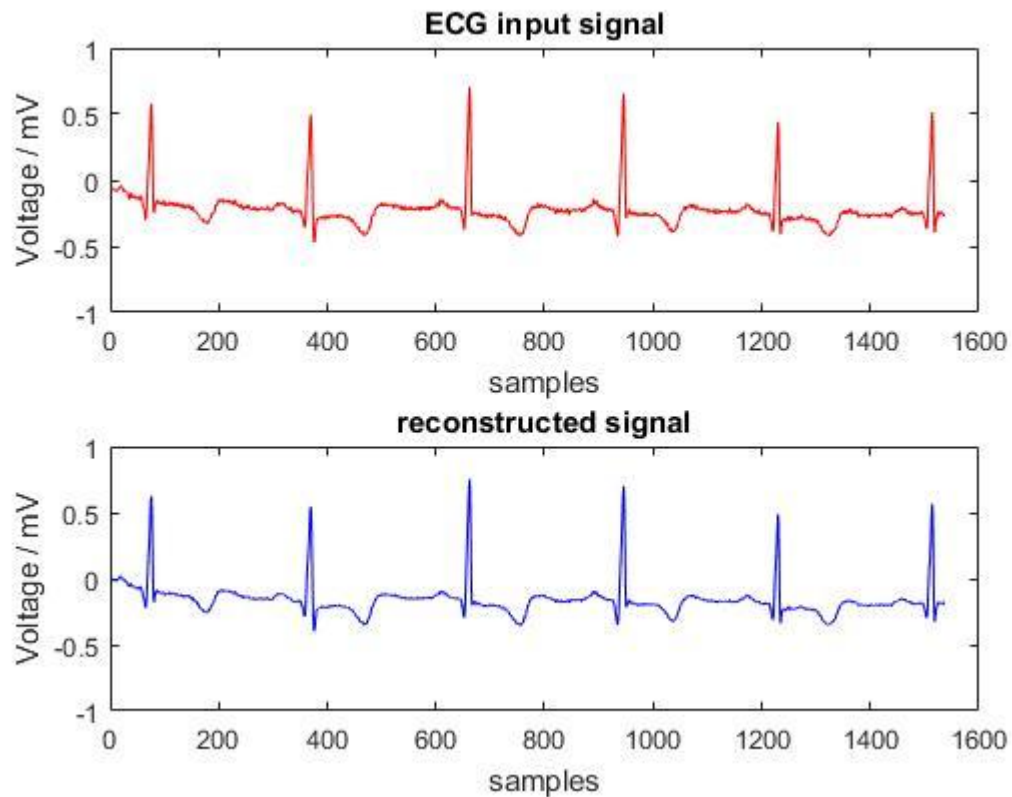


**Figure 3.18** Reconstructed signal using DTCTWT

The reconstructed signal (shown in Fig. 3.18) has good shift invariance, high directional selectivity, delivers perfect reconstruction with limited redundancy and offers less computational complexity due to the application of real valued filters.

### **Quantitative Results**

This technique is evaluated on 48 records of Modified Limb Lead II (MLII) of MIT-BIH Arrhythmia database and results for 4 MLII records are shown. The average values of SNR, MSE and PRD for MLII records are compared with state of art techniques as depicted in Table 3.8

**Table 3.8.** Comparison of DTCWT with State-of-the-Art-Work

S.No.	Technique	SNR (dB)	MSE	PRD
1.	MLII 100	32.702	6.87e-05	0.029
	MLII101	30.152	1.20e-04	0.030
	<b>DTCWT</b> MLII 106	25.639	4.29e-04	0.050
	MLII 201	22.412	3.73e-04	0.075
	<b>Average Value</b>	<b>27.750</b>	<b>1.0777e-04</b>	<b>0.0410</b>
2.	MTD	26.5396	1.4172e-04	0.0471
3.	Neigh Block [89] (2015)	4.2177	0.62052	4.8693
4.	Savitzky [89] (2015)	2.0434	1.28079	6.9956
5.	DWT using Bior 3.1 [134] (2016)	7.452	0.002	-

Table 3.8 depicts the computational assessments of DTCWT technique with other state-of-the-art-work. The remarkable results are obtained using DTCWT technique having high SNR, low PRD and Small MSE. DTCWT technique outperforms in all aspects to deliver the denoised ECG signal. After performing different filtering techniques for ECG denoising, Event Detection algorithms are implemented to extract the vital information from the reconstructed signal.

### 3.4 EVENT DETECTION

Event Detection is the most crucial step in Bio-signal Processing. Clinical information of the ECG is obtained from its features like characteristic wave peaks, amplitudes, intervals and time durations [56]. Properly recognizing cardiac rhythms includes feature vectors generation representing the original segment of the ECG. The purpose of event detection is to fetch the information from specific areas of the ECG signal and use that information as indicators of what constitutes a normal or abnormal cycle. Correct identification of these features is necessary as it can be indicators for certain medical conditions. There are some events in the signal which can be valuable for identification of certain medical conditions. For example, depolarization of the right and left ventricles of human heart constitute QRS complex. Its duration, amplitude and morphology are useful for diagnosis of arrhythmias,

abnormalities in conduction, ventricular hypertrophy, myocardial infarction, electrolyte imbalance, and other disease. Changes in PR interval can lead to some medical conditions; a first-degree heart block is presumed as PR interval over 200 ms. Prolonged PR interval can be correlated with hypokalemia, acute rheumatic fever or Lyme disease-related carditis. A prolonged duration of QT contributes towards premature death and ventricular tachyarrhythmia.

In this thesis occurrence of distinct events in an ECG signal are exploited using Peak Detection Algorithm (PDA).

### **PEAK DETECTION ALGORITHM (PDA) [135]**

Principal peaks (*P*, *Q*, *R*, *S*, and *T*) of ECG and their location along with their intervals are essentially required to be enumerated for identification of cardiovascular disease. For this purpose, Peak detection algorithm is used to detect the Morphology Analysis and Time Interval Measurements. PDA attains the correct information from specific areas of ECG signal and utilizes this information for better interpretations and diagnosis. Highest amplitude of ECG signal determines the most prominent R Peak. Measuring the RR interval of one cycle followed by the next cycle is ideal for finding the beats per minute (heartbeat) and is usually the first peak that is investigated by checking any deviations between cycles. Identification of other peaks (*P*, *Q*, *S*, *T* peaks) is done by locating positions of maximum or minimum values within the specific range from the R peaks. Specific range from the R peak is defined by expected location of a particular peak concerning distance from the R peak.

The algorithm employed for Peak detection [135] of ECG events



### Peak Detection Algorithm

---

Input- Pre-processed Signal (Y)

Output – Peak Detection

---

1. Define Sample Rate
2. Detection of  $R$  peak : The point with maximum amplitude gives the  $R$  peak location.

If  $R$  peak is located for each cycle ( $R_{peak}$ ), then different other peaks are detected by the following methods:

3. Detection of  $P$  peak :  $P$  peak location detection is given as

$$a = \left[ R_{peak} - \left( \frac{Sample\ Rate \times 25}{Beat} \right) \right] : \left[ R_{peak} - \left( \frac{Sample\ Rate \times 5}{Beat} \right) \right]$$

$P$  peak amplitude =  $\max(Y(a))$ ;

4. Detection of  $Q$  peak :  $Q$  peak location detection is given as

$$b = \left[ R_{peak} - \left( \frac{Sample\ Rate \times 10}{Beat} \right) \right] : \left[ R_{peak} - \left( \frac{Sample\ Rate \times 1}{Beat} \right) \right]$$

$Q$  peak amplitude =  $\min(Y(b))$ ;

5. Detection of  $S$  peak :  $S$  peak location detection is expressed as

$$c = \left[ R_{peak} + \left( \frac{Sample\ Rate \times 1}{Beat} \right) \right] : \left[ R_{peak} + \left( \frac{Sample\ Rate \times 5}{Beat} \right) \right]$$

$S$  peak amplitude =  $\min(Y(c))$ ;

6. Detection of  $T$  peak :  $T$  peak location detection is represented as

$$d = \left[ R_{peak} + \left( \frac{Sample\ Rate \times 10}{Beat} \right) \right] : \left[ R_{peak} + \left( \frac{Sample\ Rate \times 30}{Beat} \right) \right]$$

$T$  peak amplitude =  $\max(Y(d))$ ;

End

---

By implementing PDA different principal peaks of ECG are detected that are useful for computation of Heart Beat Rate and their intervals.

- i. *Heart Beat Rate* – One of the "vital signs" of the human health analysis framework is the heart beat rate. It measures the number of times the heart contracts or beats per minute. The heartbeat rate varies as a result of physical activity, health risks and emotional responses. Frequent monitoring of heart beat rate can help to avoid cardiac related problems. Heart beat rate is given by Eq.(3.15)

$$Heart\ Rate = \frac{Sample\ Rate \times 60}{R_2 - R_1} \quad (3.15)$$

Where  $R_2$  and  $R_1$  denotes the subsequent two R peaks on a time scale.

- ii. *Detection of Time Interval Measurements* [136] - ECG signal has distinct intervals that have crucial significance to examine the medical conditions of any individual. Some of the ECG intervals are *RR* interval, *PR* interval, *QRS* interval and *ST* interval. Measuring the RR interval of one cycle followed by the next cycle is ideal for finding the beats per minute (heartbeat) and is usually the first peak that is investigated by checking any deviations between cycles. *PR* interval represents the ventricular depolarization helpful in diagnosis of first degree AV block. *QRS* complex correlates to depolarization of the human heart's right and left ventricles. The span, amplitude and anatomy of the *QRS* complex are useful for the diagnosis of cardiac arrhythmias, conduction disorders, ventricular hypertrophy, myocardial infarction, electrolyte derangements and other diseases and *ST* interval is investigated on the ECG for the identification of myocardial ischemia, left ventricular hypertrophy, pericarditis and Brugada syndrome.

*R-R* interval is determined by Eq. (3.16)

$$R-R\ interval = (R_2 - R_1) / sample\ rate \quad (3.16)$$

where  $R_2$  and  $R_1$  are two subsequent *R* peaks locations

$P$ - $R$  interval is computed by Eq. (3.17)

$$P\text{-}R\text{ interval} = (Q_{\text{peak}} - P_{\text{peak}}) / \text{sample rate} \quad (3.17)$$

where  $Q_{\text{peak}}$  and  $P_{\text{peak}}$  are the respective peaks location in present cycle.

$QRS$  complex is computed by Eq. (3.18)

$$QRS\text{ complex} = (S_{\text{peak}} - Q_{\text{peak}}) / \text{sample rate} \quad (3.18)$$

where  $S_{\text{peak}}$  and  $Q_{\text{peak}}$  represents the respective peaks location in present cycle.

Finally,  $S$ - $T$  interval is computed by Eq. (3.19)

$$S\text{-}T\text{ interval} = (T_{\text{peak}} - S_{\text{peak}}) / \text{sample rate} \quad (3.19)$$

where  $T_{\text{peak}}$  and  $S_{\text{peak}}$  are the respective peak location in that present cycle.

The duration of the particular segment indicate certain conditions associated with different problems, therefore correct identification is required. All these intervals can be identified by correctly identifying peaks within the ECG signal. Detection of principal peaks of clean ECG signal utilizing PDA for MIT-BIH Arrhythmia ‘v5’ is shown in Figure 3.19.

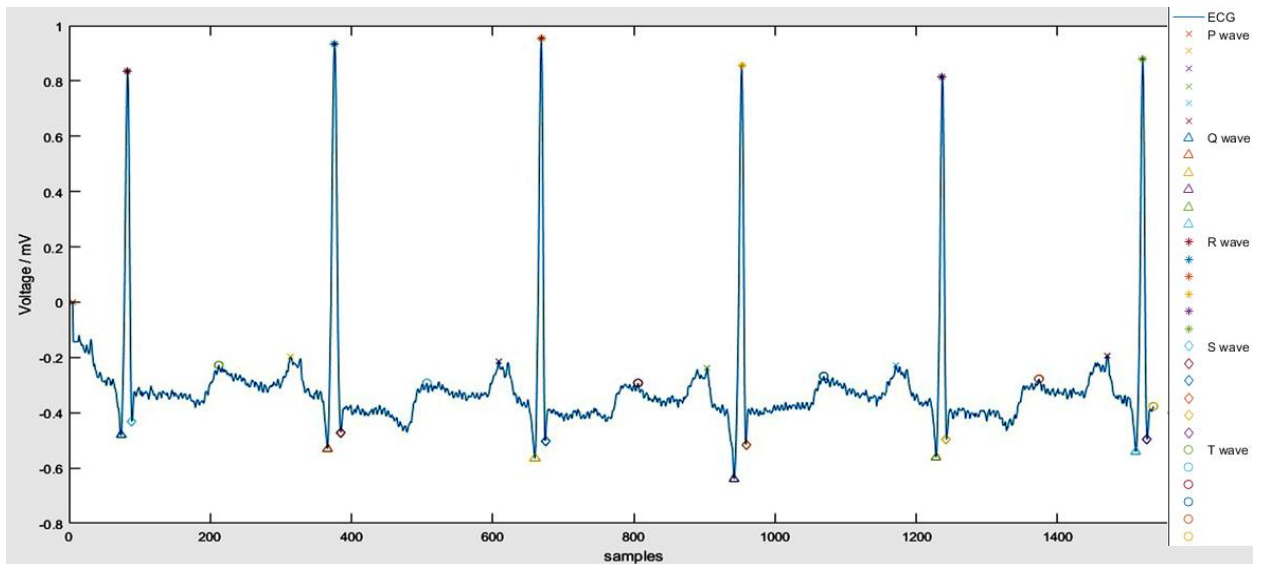


**Figure 3.19** Peak detection of clean ECG signal employing PDA

After an accurate detection of principal peaks designated as “*P*, *Q*, *R*, *S* and *T*” of ECG signal, Some important features are computed for denoised ECG signals obtained by different filtering techniques like Proposed Cascade Digital Filter, MTD and DTCWT for 100-109 record of MIT-BIH Arrhythmia database as elaborated in Table 3.9, 3.10 and 3.11 respectively.

**Table 3.9** Different Peaks and Intervals of distinct ECG records using Proposed Cascade Digital Filter Design

<b>Record</b>	<b>R wave</b>	<b>P wave</b>	<b>Q wave</b>	<b>S wave</b>	<b>T wave</b>	<b>RR interval</b>	<b>PR interval</b>	<b>QRS interval</b>	<b>ST interval</b>
MLII100	0.4101	-0.1043	-0.2765	-0.3202	-0.1808	0.7989	0.1606	0.0539	0.2819
MLII101	0.5000	-0.0838	-0.2160	-0.2573	-0.0788	0.8917	0.1656	0.0967	0.2283
V5102	0.3250	-0.1040	-0.16000	-0.0676	-0.0592	0.8243	0.3289	0.1928	0.2533
MLII103	0.9886	-0.1417	-0.3020	-0.3856	-0.0120	0.8451	0.1683	0.0550	0.2044
V5104	0.3408	-0.0662	-0.1392	-0.1914	-0.0190	0.8100	0.2917	0.1343	0.2838
MLII105	0.6397	-0.0657	-0.2084	-0.2980	-0.1250	0.7117	0.1537	0.0444	0.3051
MLII106	1.1727	0.0065	-0.2232	-0.4420	0.2346	1.0157	0.1125	0.1528	0.0285
MLII107	0.9861	-0.1285	-0.2776	-1.0421	0.4859	0.8660	0.2178	0.1817	0.2411
MLII108	0.0284	-0.1084	-0.1432	-0.1816	-0.0851	0.9861	0.3389	0.2011	0.3639
MLII109	0.2070	-0.1767	-0.3425	-0.4846	-0.0906	0.7839	0.2495	0.1394	0.2787

**Table 3.10** Different Peaks and Intervals of distinct ECG records using Mallet Tree Decomposition

---

<b>Record</b>	<b>R Wave</b>	<b>Pwave</b>	<b>Q wave</b>	<b>S wave</b>	<b>T wave</b>	<b>RR interval</b>	<b>PR interval</b>	<b>QRS interval</b>	<b>ST Interval</b>
MLII 100	0.9652	-0.1365	-0.4547	-0.2797	-0.1061	0.7914	0.1636	0.0497	0.2979
MLII101	0.7840	-0.1237	-0.3892	-0.2573	-0.0898	0.8246	0.1643	0.0914	0.2285
V5102	0.5893	-0.1243	-0.4620	-0.0676	-0.0483	0.8249	0.3273	0.1719	0.2562
MLII103	0.1274	-0.1919	-0.4381	-0.4653	-0.0282	0.8456	0.1678	0.0556	0.2365
V5104	0.6713	-0.0954	-0.19724	-0.2651	-0.0257	0.8107	0.2816	0.1435	0.2812
MLII105	0.9384	-0.0935	-0.2753	-0.3702	-0.1972	0.7116	0.1524	0.0974	0.2871
MLII106	1.9471	0.0179	-0.3532	-0.5470	0.3542	1.0154	0.1132	0.1583	0.1875
MLII107	0.9135	-0.1351	-0.2976	-1.0232	0.2152	0.8462	0.2981	0.1723	0.2524
MLII108	0.0372	-0.1241	-0.1723	-0.1312	-0.0889	0.9857	0.3381	0.1931	0.3459
MLII109	0.3630	-0.2162	-0.4265	-0.5341	-0.2186	0.7841	0.2498	0.1382	0.2719

---

**Table 3.11** Different Peaks and Intervals of distinct ECG records using DTCWT Technique

<b>Record</b>	<b>R wave</b>	<b>P Wave</b>	<b>Q wave</b>	<b>S wave</b>	<b>T wave</b>	<b>RR interval</b>	<b>PR interval</b>	<b>QRS interval</b>	<b>ST interval</b>
MLII100	0.5332	-0.1877	-0.3461	-0.3143	-0.1920	0.7989	0.1676	0.0639	0.2741
MLII101	1.1002	-0.1092	-0.4255	-0.4677	-0.1033	0.8631	0.1656	0.0989	0.2333
V5102	0.8241	-0.1869	-0.2901	-0.0305	-0.1040	0.8257	0.3233	0.1656	0.2817
MLII103	0.8458	-0.2419	0.5940	-0.5435	0.0356	0.8458	0.1661	0.0517	0.2461
V5104	0.9847	0.1139	-0.3011	-0.3017	-0.0145	0.8111	0.2708	0.1463	0.2773
MLII105	1.2009	0.0850	0.4105	-0.5086	-0.1837	0.7117	0.1495	0.1514	0.1898
MLII106	2.003	0.0499	-0.4593	-0.7494	0.4898	1.0157	0.1146	0.1451	0.2368
MLII107	1.7033	-0.2111	-0.5019	-1.5342	0.8896	0.8660	0.2117	0.1611	0.2517
MLII108	0.1218	-0.1371	-0.1653	-0.1426	-0.0785	0.8693	0.2647	0.1738	0.3157
MLII109	0.4306	-0.2756	-0.6827	-0.8637	-0.2279	0.7844	0.2588	0.1403	0.2653

Table 3.9, Table 3.10 and Table 3.11 depicts the different values of peaks (*P, Q, R, S, T*) and their intervals for different filtering techniques (Digital Cascade filter, MTD and DTCWT) to analyse most suitable filtering technique that delivers correct and accurate peaks identification. On observing the outcomes, it has found that DTCWT techniques is more powerful filtering method that provide much accurate peak and their interval values on applying peak detection algorithm.

The upper signal is obtained by placing the electrodes on the chest using modified limb lead II (MLII) and lower signal is acquired using V1, V2 or V5 of “MIT-BIH Arrhythmia” that includes distinct abnormalities in every record such as blocked Atrial Premature Complexes ‘APCs’ and ventricular flutter waves. In Tables 3.9, 3.10 and 3.11 distinct peaks and intervals

are calculated for (100-109) that suggest some abnormal values of peaks are due to the presence of certain arrhythmias in respective record [28] as described in Table 3.12

**Table 3.12** Impact of Arrhythmias on Peak Morphology

<b>Record</b>	<b>Presence of Arrhythmias</b>	<b>Impact on Peak Morphology</b>
MLII 100	Supraventricular ectopy	P wave is inverted, it is most likely an ectopic atrial rhythm is not originating from the sinus node
MLII 101	Supraventricular ectopy	P wave is inverted, it is most likely an ectopic atrial rhythm is not originating from the sinus node
V5 102	Premature Ventricular Contractions	Occurs earlier than would be expected for the next sinus impulse leads to Retrograde P wave.
MLII103	Supraventricular ectopy	P wave is inverted, it is most likely an ectopic atrial rhythm is not originating from the sinus node
V5104	Ventricular ectopy	Ectopic impulse is conducted retrogradely through the AV node, producing atrial depolarisation. This is visible on the ECG as an inverted P wave
MLII105	Premature Ventricular Contractions is present	PVC occurs earlier than would be expected for the next sinus impulse leads to Retrograde P wave.
MLII 106	Ventricular ectopy	Ectopic firing of a focus within the ventricles bypasses the His-Purkinje system and depolarises the ventricles directly that leads to abnormal morphology.
MLII107	Premature Ventricular Contractions are multiform	Occurs earlier than would be expected for the next sinus impulse leads to Retrograde P wave.

MLII108	Supraventricular ectopy	P wave is inverted, it is most likely an ectopic atrial rhythm is not originating from the sinus node
MLII109	First degree AV Block	P waves are differing in morphology from normal sinus P waves which resulted in to prolonged PR interval >0.20 sec and all P wave conduct to the ventricles.

Later, RR interval of different record 100-109 using different filtering techniques are compared with RR Interval MIT-BIH Arrhythmia Database (Gold Standard) as illustrated in Table 3.13 which further validate the proficiency of DTCWT technique.

**Table 3.13.** Calculation of R-R Intervals for different Techniques

S.No.	Types of Intervals	Cascade Filtering (sec)	MTD Technique (sec)	DTCWT Technique (sec)	R-R Interval MIT-BIH Arrhythmia Database (Gold Standard)
1.	MLII101	0.8917	0.8246	<b>0.8631</b>	0.8690
2.	V5102	0.8243	0.8249	<b>0.8257</b>	0.8259
3.	MLII103	0.8451	0.8456	<b>0.8458</b>	0.8690
4.	V5104	0.8100	0.8107	<b>0.8111</b>	0.8312
5.	MLII105	0.7117	0.7116	<b>0.7117</b>	0.7311
6.	MLII106	1.0157	1.0154	<b>1.0157</b>	1.0392
7.	MLII107	0.8660	0.8462	<b>0.8660</b>	0.8673
8.	MLII108	0.9861	0.9857	<b>0.8693</b>	0.9332
9.	MLII109	0.7839	0.7841	<b>0.7844</b>	0.6723



From Table 3.13 it has been observed that RR interval computed from denoised ECG signal using DTCWT technique that provide more accurate values closer to gold standard for MIT-BIH Arrhythmia Database than other filtering techniques.

### **3.5 SUMMARY**

Different Bio-signal Processing methods are implemented for the eradication of artifacts and noise contents from the raw input ECG signal. A cascade digital filter is proposed by choosing best performance frequency domain filters and optimal filters that eliminates the different noise from the ECG signal at the cost of large memory requirement and computational complexity. To tackle this problem different time-frequency domain filtering techniques such as MTD and DTCWT are exploited that reduces the computational complexity with less memory requirement. The Performance evaluation of different filtering techniques determines that DTCWT strategy is most effective among other specified techniques (Cascade filtering, Mallet tree decomposition) to achieve the denoising goal which is later followed by detection of principal peaks and their events to extract the crucial information for accurate analysis of ECG interpretation.

Taking its accountability, DTCWT technique is further used in designing the Robust Denoising System for ECG Signal in the next chapter of this research work.

# **CHAPTER – 4**

## **DESIGN OF ROBUST DENOISING SYSTEM**

# **CHAPTER - 4**

## **DESIGN OF ROBUST DENOISING SYSTEM**

### **4.1 INTRODUCTION**

Wavelet Thresholding is a multiscale denoising technique that delivers significant performance in processing of non-stationary signal. Wavelet thresholding exhibit good characteristic in time-frequency localization that become very effective for ECG signal processing than other denoising methods such as Kalman filtering and Empirical mode decomposition (EMD) [106]. Wavelet thresholding performs the denoising while equally preserving the complexes. In this technique shrinkage or scaling of coefficients are performed depending on the selective wavelet functions [137]. The thresholding approach are further categorised into two categories define as global threshold and level dependent threshold. Global threshold depicts single value of threshold applicable for all detail coefficients at each level of decomposition whereas level dependent threshold depicts different values of threshold for distinct decomposition level. The performance of wavelet thresholding is dependent on two parameters i.e. Selection of threshold value and Threshold functions [138]. Hard and soft threshold functions are the basic threshold functions. The major drawback of hard threshold function is the distortion of signal caused by pseudo-Gibbs effect while soft threshold function have constant deviation problem. These defects cause missing of high frequency components that influence the signal processing [139]. Further, utilization of universal threshold selection at different decomposition levels predict some limitations such that if the threshold value is small it results in the misinterpretation of useful information but if it is too large, than the residual noise remains in the signal [90]. To overcome these drawback an improved threshold functions is introduced along with the threshold value selection.

### **4.2 OPTIMAL THRESHOLD DENOISING METHOD**

ECG denoising process involves: signal decomposition by DTCWT, selection of threshold value and threshold function to calculate high frequency wavelet decomposition coefficients, and signal

reconstruction. Selections of threshold value and threshold function [138] are the key factors influencing the denoising efficiency.

#### 4.2.1 Threshold Functions

The input signal is confined by threshold functions to the desired range by suppressing the noise from detail coefficients based on the value of threshold. The prime objective of threshold function is to confine the coefficients at specific range depending on threshold value selection. It determines the coefficient value that exceeds a certain value of threshold value. Threshold function designated as Hard and Soft are categorised as classical threshold functions. In hard threshold function the coefficients below the threshold value are set to zero while the value greater than the threshold value is considered as such. This threshold function successfully preserves the local properties of the signal but observes some distortions in the reconstructed signal [140]. In soft threshold function the coefficients shrink towards zero but above threshold value it may lose some segments of high frequency coefficients [141]. To overcome these limitations, modified threshold functions are derived from soft threshold function. The different threshold functions ( $f_n$ ) [142] are defined as :

- a) *Hard Thresholding* – Hard thresholding lead to fluctuations in the output signal and is described by Eq (4.1)

$$f_H = \begin{cases} b(n), & \text{for } |b(n)| \geq \delta \\ 0, & \text{otherwise} \end{cases} \quad (4.1)$$

- b) *Soft thresholding*- Soft thresholding is specified as wavelet shrinkage as value of both positive and negative are being shrink towards zero. The soft thresholding is described by Eq. (4.2)

$$f_S = \begin{cases} \text{sign}(b(n)) (|b(n)| - \delta), & \text{for } |b(n)| \geq \delta \\ 0 & \text{otherwise} \end{cases} \quad (4.2)$$

- c) *Semi-Soft Thresholding*- It is the class nonlinearities which interpolates among hard and soft thresholding is identified. It utilizes primary and secondary values of threshold. Eq. (4.3) determines the Semi-Soft thresholding.

$$f_{\text{semi}} = \left\{ \begin{array}{ll} b(n), & |b(n)| < \delta_2 \\ \text{sign}(b(n)) \frac{(b(n) - \delta_1) * \delta_2}{\delta_2 - \delta_1}, & \delta_2 < |b(n)| \leq \delta_1 \\ 0, & |b(n)| < \delta_1 \end{array} \right\} \quad (4.3)$$

where  $\delta_1 = \sqrt{\delta_2}$  for semi-soft thresholding

d) *Trimmed Thresholding* – This threshold function depends on  $\gamma$  value. If  $\gamma$  values is equal to 1, then it leads to soft thresholding function while if  $\gamma$  tends to zero, leading hard thresholding function. Trimmed thresholding is described by Eq. (4.4).

$$f_{\text{trim}} = \left\{ \begin{array}{ll} b(n) * \frac{|b(n)|^\alpha - |\delta|^\alpha}{|b(n)|^\alpha}, & \text{for } |b(n)| \geq \delta \\ 0, & \text{otherwise} \end{array} \right\} \quad (4.4)$$

e) *Non – Negative Garrote Thresholding* – This thresholding offers advantage over both Hard ( less sensitivity to small perturbations in the data) and Soft thresholding (smaller bias) . Non – Negative Garrote thresholding is described by Eq. (4. 5)

$$f_{\text{non-neg}} = \left\{ \begin{array}{ll} \text{sign}(b(n)) \left( |b(n)| - \frac{\delta^2}{|b(n)|} \right), & \text{for } |b(n)| \geq \delta \\ 0, & \text{otherwise} \end{array} \right\} \quad (4.5)$$

f) *Hyperbolic Thresholding* : If the detail coefficients of soft threshold function are squared, leading hyperbolic threshold function. The hyperbolic thresholding is expressed by Eq.

(4.6)

$$f_{\text{hyp}} = \left\{ \begin{array}{ll} \text{sign}(b(n)) \sqrt{b(n)^2 - \delta^2}, & \text{for } |b(n)| \geq \delta \\ 0, & \text{otherwise} \end{array} \right\} \quad (4.6)$$

For all above-threshold functions, wavelet coefficients are denoted by  $b(n)$  and  $\delta$  defines threshold value.

#### 4.2.2 Threshold value selection

In the wavelet threshold denoising algorithm, the threshold value ( $\delta$ ) is a significant parameter, and the output of the denoising is affected directly by threshold selection. A minimum value is a threshold value under which all coefficients tend to be zero. These thresholds are applied to all detail coefficients [142]. Table 4.1 demonstrates the different types of threshold value selection for denoising of ECG signal.

**Table 4.1.** Different types of Threshold value selection rules

S.No	Different Threshold values	Formulae
1	Universal Threshold	$\delta_u = \alpha \sqrt{2 \log N}$
2	Universal Threshold level dependent	$\delta_{uld} = \alpha_j \sqrt{2 \log n_j}$
3	Universal modified threshold level dependent	$\delta_{umld} = \alpha_j \frac{\sqrt{2 \log n_j}}{\sqrt{n_j}}$
4	Modified Unified Threshold	$\delta_{mou} = \alpha_j \frac{\sqrt{2 \log n_j}}{\log(j+1)}$
5	Universal modified threshold level dependent	$\delta_{umld} = \alpha_j \frac{\sqrt{2 \log n_j}}{\sqrt{n_j}}$
6	Exponential Threshold level dependent	$\delta_{exp} = 2^{(j-J/2)} \alpha_j \sqrt{2 \log n_j}$
7	Minimax threshold	$\delta_{mini} = 0.3936 + 0.1829 * (\log n_j / \log 2)$
8	Adaptive threshold Selection	$\delta_{adp} = \alpha_j \sqrt{w_b}$

Where  $w_b$  signify the  $b^{\text{th}}$  coefficient wavelet square, selected from  $W = [w_1, w_2, \dots, w_N]$  matrix. The  $n_j$  is the length of the signal in  $j$ th dimension, whereas  $\alpha$  is the standard deviation (SD) rely on

median-absolute deviation (MAD). For each threshold value selection rule, the original length of the signal defined by  $N$ .

Later, distinct combination of  $(f_n)$  and  $(\delta)$  are further utilized to evaluate the different performance parameters in a proposed methodology.

### 4.3 CONVENTIONAL NOISE ESTIMATOR

The conventional noise estimator is formulated by Donoho and Johnstone for estimating the noise level ( $\alpha$ ) in time–frequency domain [132,133]. In conventional noise estimator, the detail coefficients of wavelet transform at finest level are considered as they are mostly influenced by noise. The value of conventional noise estimator is further utilized in the thresholding technique to perform denoising of ECG signal. The mathematical modelling of conventional noise estimator is focused on median absolute deviation (MAD) and is expressed by Eq. (4.7)

$$\alpha = z \times (\text{median}|x_{jk}|) \quad (4.7)$$

where  $z$  indicates the constant value rely on distinct probability distribution functions and  $x_{jk}$  represents the detail coefficients at finest level. The median of coefficients are taken to limit the effect of outliers. The value  $\alpha$  is utilized in different categories of threshold value selection that are further applied in determining the distinct threshold functions. The nature of ECG signal having discontinuities, distortion and interference are dependent on the selected threshold value selection for estimating the noise. After the computation of threshold value selection, distinct threshold functions are appraised to eradicate the noise content from the ECG signal using conventional estimator.

Implementation of Conventional estimator offers some limitations like

- i. Low efficiency – Conventional estimator exhibit low efficiency that predicts 37% for Gaussian probability distribution.
- ii. Dispersion – Conventional estimator depicts dispersion in symmetric distribution that leads to random errors in the reconstructed signal.

To overcome these limitations a new noise estimator ( $\alpha^*$ ) has been proposed that successively eliminates the noise from the detailed coefficients.

#### 4.4 PROPOSED METHODOLOGY FOR DENOISED SYSTEM

The input ECG signal from Physio Bank ATM database, MIT-BIH Arrhythmia ‘v5’ of 100 record consisting of 1536 samples has been used for proposed work [28]. The entire process of implementation using proposed estimator is elaborated in Fig. 4.1

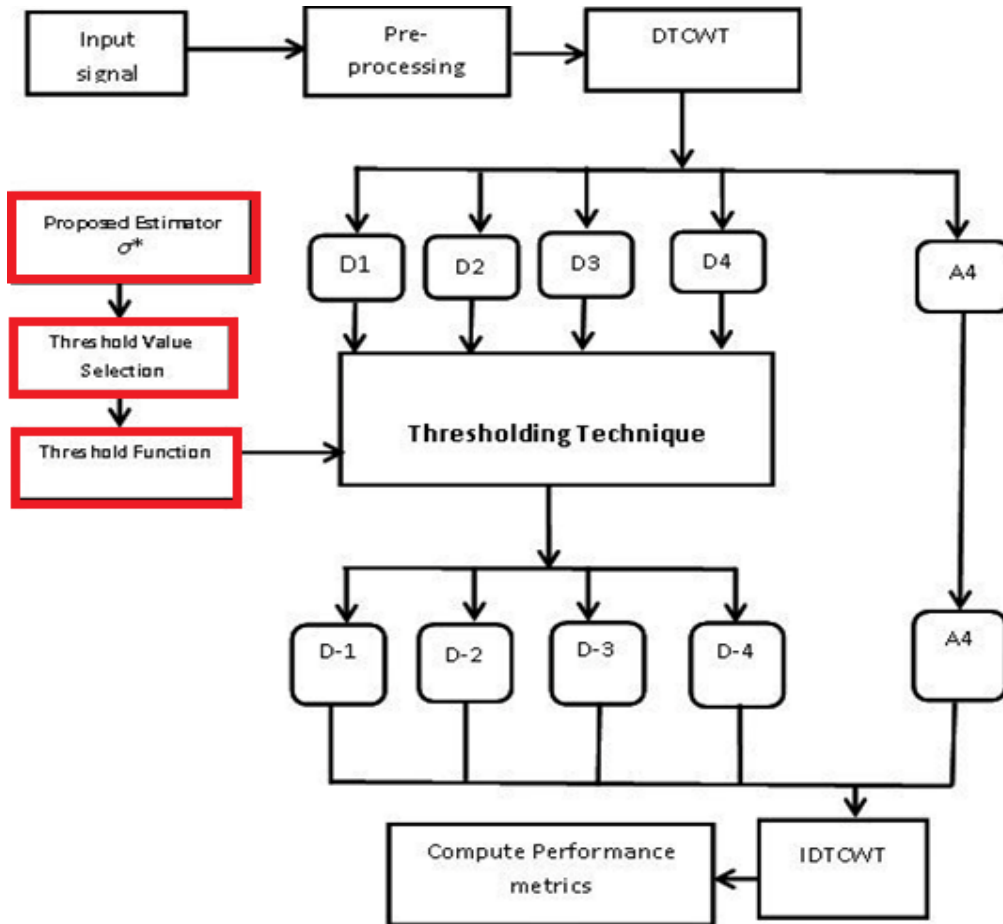


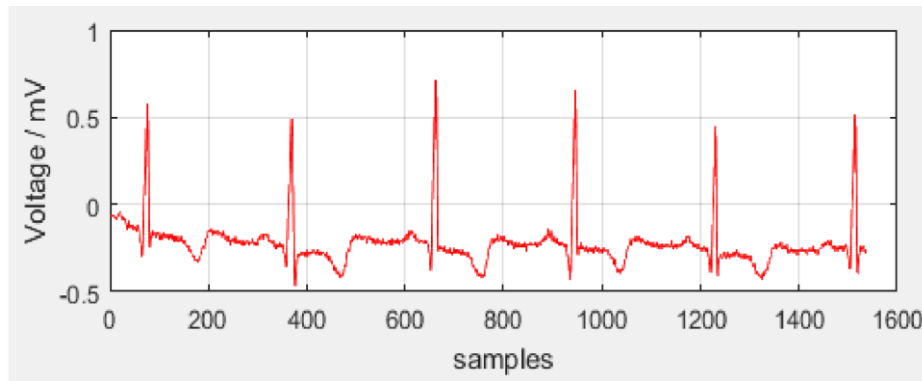
Figure 4.1 Proposed Methodology

Initially, the raw input ECG signal is fed to pre-processing stage to remove low frequency noise from the signal followed by implementation of DTCWT technique on preprocessed signal to extract detail and approximation coefficients. Later, thresholding process is employed on detail coefficients by utilizing distinct threshold value selection and threshold functions. The selection of threshold value is optimized using proposed estimator. This thresholding technique delivers



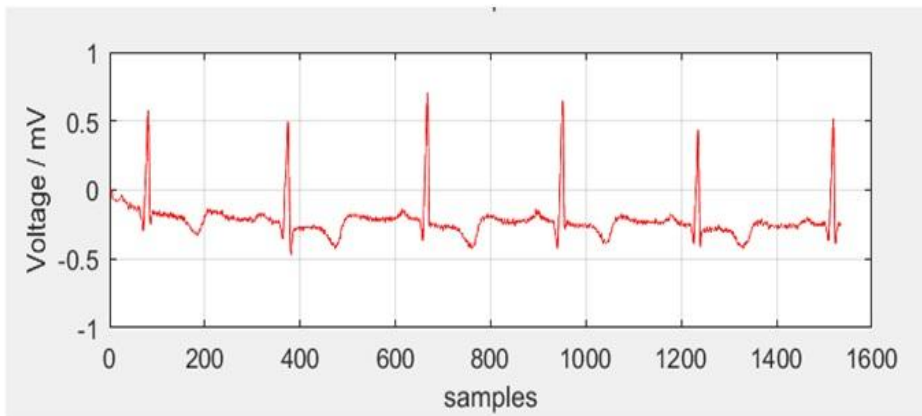
modified detail coefficients at each decomposition level by suppressing noise content. An IDTCWT procedure is applied on modified detail and approximation coefficients to attain reconstructed signal. Finally, different performance metrics are computed for validation of proposed methodology.

Fig 4.2 depicts the input ECG signal having morphological irregularities due to the contamination of distinct noises.



**Figure 4.2** Input ECG signal

The first step include the filtering by taking into account the filter order ( $N$ ) = 10 and window length  $(N+1) = 11$  to eliminate the low frequency (baseline wander) noise using a FIR High Pass filter (Blackman window). The Preprocessed signal is obtained after elimination of low frequency baseline wander noise is shown in Fig. 4.3.



**Figure 4.3** Removal of Low frequency component from ECG signal

After filtering the 4<sup>th</sup> level signal decomposition is performed (as already explained in Chapter-3) using Dual tree complex wavelet transform (DTCWT) technique to decompose the signal into high frequency detail coefficients and low frequency approximation coefficients. The detail and approximation coefficients are shown in Fig 4.4 and Fig.4.5. In this multilevel decomposition detailed coefficients are extracted at each level comprising of 768 coefficients at level 1 followed by 384, 192 and 96 coefficients at subsequent level (2,3 and 4) while 96 coefficients are obtained at 4<sup>th</sup> level of decomposition for Arrhythmia ‘v5’100 record.

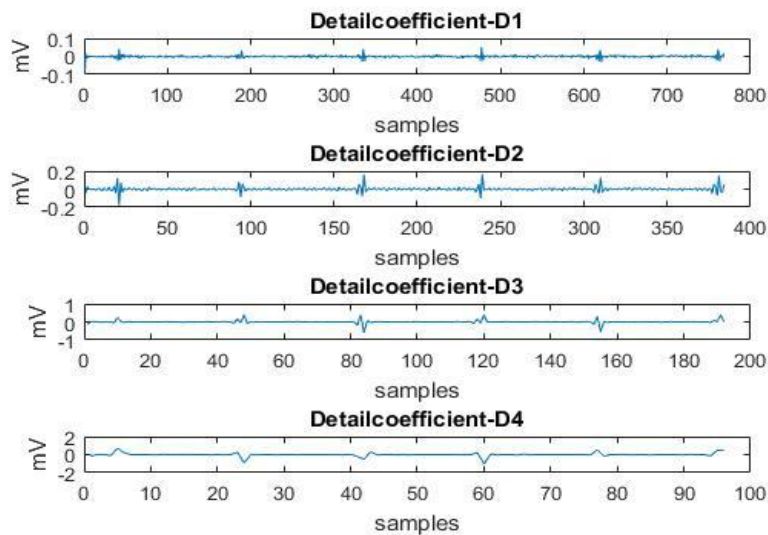


**Figure 4.4** Detail coefficients at 4<sup>th</sup> level decomposition

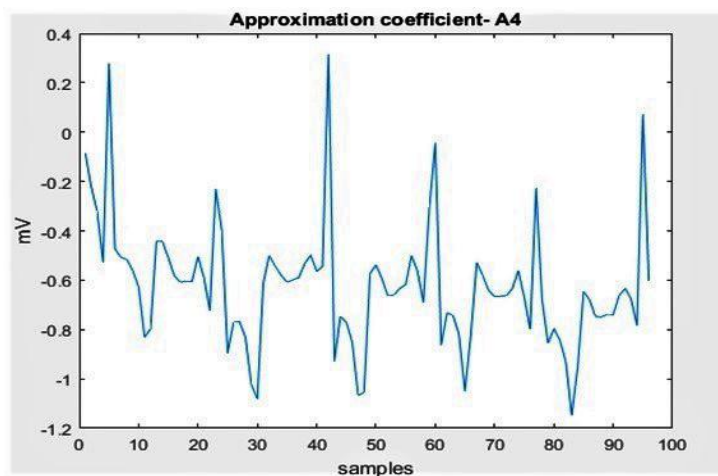


**Figure 4.5** Approximation coefficients

Thresholding technique consists of distinct threshold value selection and different threshold function which is further optimized using proposed noise estimator that effectively limit the substantial variation in the amplitude of the ECG signal occurred due to the existence of noise contents.

### ***PROPOSED NOISE ESTIMATOR***

In 1990, a powerful correlation coefficient was suggested with a high degree of breakdown based upon the regression model of the least median of squares (LMdS) [143]. The coefficient of correlation of LMdS provides exceptionally high estimation of the relation. In order to address the problem, a new correlation coefficient using weighted least squares by consolidating the LMdS with the M estimator is introduced. In 2011, further rendering of correlation coefficient relies on the middle utilizing scale estimator without employing iterative algorithms median absolute deviation (MAD) is introduced and recognized as Median-Product (MP) correlation coefficient [83]. The mean of standard correlation coefficient is replaced by the median and utilization of MAD for coefficient computation. Nonetheless, MAD exhibit few downsides, especially the low efficiency as 37% at the Gaussian distribution and depicts scattering of symmetric conveyance. On comparison to other schemes the strong correlation coefficient takes requires less time for computation. The usage of MAD can be enhanced to vigorous scale estimator in order to boost the efficiency of robust correlation.

The key delivery of this research intends to strengthen the robust correlation coefficient by proposing a noise estimator that yields excellent performance by addressing the limitation of existing estimator. The proposed noise estimator has a high point of breakdown and is more effective under normal conditions. The proposed noise estimator ( $\alpha^*$ ) is modelled by Eq.4.8.

$$\alpha^* = z \times \text{median}\left(\frac{|x_{jk}|}{2}\right) \quad (4.8)$$

The proposed noise estimator ( $\alpha^*$ ) focuses on two parameters that have been defined as the amplitude downscaling factor (2), in order to prevent the occurrence of spurious high frequency information at the output, and the z value that rely on various distribution functions for the suppression of transient noise.

Thresholding technique is applied on the detail coefficients at finest level. This thresholding procedure is applied at each level of detail coefficients (D1, D2, D3 and D4) to attain modified detail coefficients (D-1, D-2, D-3 and D-4) respectively. An IDTCWT strategy is applied on modified detail coefficients and approximation coefficients to obtain denoised ECG signal as illustrated in Fig 4.6.

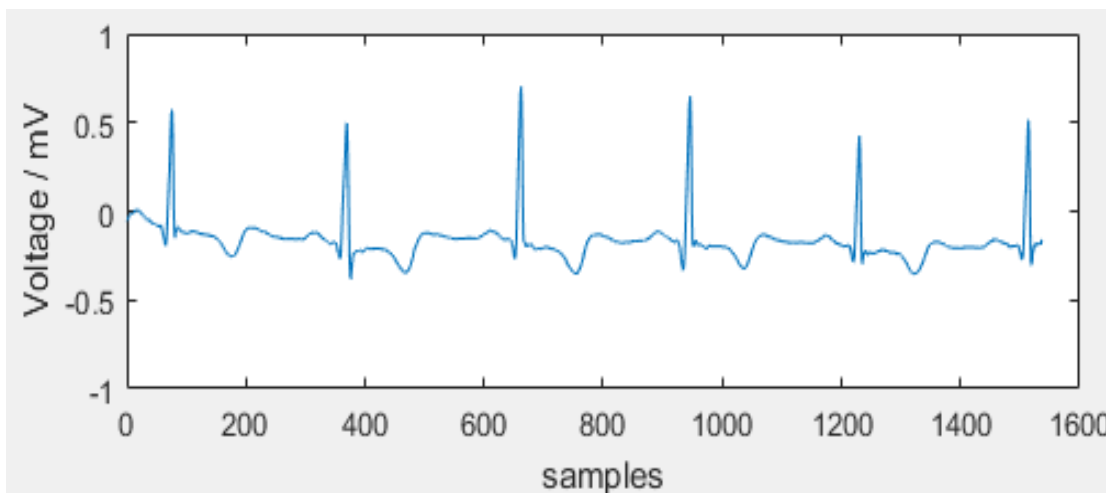


**Figure 4.6** Denoised ECG signal

This proposed methodology is effective in denoising the ECG signal that is further validated in next section by evaluating the different performance parameters that signifies the quality of reconstructed signal.

## 4.5 RESULTS AND DISCUSSION

Distinct ( $\delta$ ) and ( $f_n$ ) are implemented to denoise the ECG using conventional ( $\alpha$ ) and proposed noise estimator ( $\alpha^*$ ). Various performance metrics are evaluated to achieve optimal thresholding using best combination of distinct ( $\delta$ ) and ( $f_n$ ) followed by curve fitting to examine the relationship between conventional and proposed estimator. Later, results of proposed approach are compared with state-of-the-art- methods.

### 4.5.1 Results for conventional estimator

The different performance parameters using conventional estimator are evaluated by considering the combination of distinct ( $\delta$ ) and ( $f_n$ ). The  $z$  value for conventional estimator is predicted by considering Gaussian probability distribution.

Table 4.2 tabulates the SNR evaluation for different combination of ( $\delta$ ) and ( $f_n$ ) using conventional estimator for ‘v5’100 record and further applied on all records of “MIT-BIH Arrhythmia database”.

**Table 4.2.** Evaluation of SNR values for Conventional estimator

S. No.	Threshold Function	$\delta_u$	$\delta_{uld}$	$\delta_{umltd}$	$\delta_{mou}$	$\delta_{mini}$	$\delta_{adp}$	$\delta_{expld}$	$\delta_{eur}$
1.	Hard	28.77	26.86	43.62	30.81	28.21	37.45	34.96	26.86
2.	Soft	26.76	22.55	38.31	28.22	25.38	31.09	28.788	22.55
3.	Semi Soft	10.15	10.78	9.90	10.06	10.30	10.05	10.07	10.78
4.	Trimmed	24.31	21.67	26.90	24.98	25.36	27.48	26.27	24.31
5.	Non-Negative Garrote	28.33	25.90	<b>45.67</b>	30.81	27.49	34.93	42.59	25.90
6.	Hyperbolic	14.09	13.91	14.23	14.13	14.15	14.20	14.23	13.91

Table 4.2 depicts that maximum (**45.67 dB**) SNR is attained using “*Non - negative Garrote threshold function with universal modified level-dependent threshold value selection*” among all possible combinations of ( $\delta$ ) and ( $f_n$ ). Table 4.3 tabulates the evaluation of Mean square error (MSE) for distinct ( $\delta$ ) and ( $f_n$ ).

**Table 4.3.** Evaluation of MSE values for Conventional estimator

S. No.	Threshold Function	$\delta_u$	$\delta_{uld}$	$\delta_{umltd}$	$\delta_{mou}$	$\delta_{mini}$	$\delta_{adp}$	$\delta_{expld}$	$\delta_{eur}$
1.	Hard	8.54e-05	7.86e-05	2.78e-06	5.32e-05	9.69e-05	1.15e-05	2.04e-05	1.32e-04
2.	Soft	1.35e-04	1.20e-04	1.33e-06	9.66e-05	1.85e-04	4.98e-05	8.48e-05	3.56e-04
3.	Semi Soft	0.006	0.005	0.006	0.006	0.006	0.006	0.006	0.005
4.	Trimmed	2.37e-04	4.36e-04	1.30e-04	2.03e-04	1.86e-04	1.14e-04	1.51e-04	2.37e-04
5.	Non-Negative Garrote	9.41e-05	1.64e-04	<b>1.73e-06</b>	5.32e-05	1.14e-04	2.06e-05	3.52e-06	1.64e-04
6.	Hyperbolic	0.002	0.0026	0.0024	0.0025	0.0025	0.0024	0.0024	0.0026

Table 4.3 signify that the low (**1.73e-06**) MSE value is achieved using “*Non - negative Garrote threshold function with universal modified level-dependent threshold value selection*” that signifies its effectiveness for ECG denoising. PRD for distinct ( $\delta$ ) and ( $f_n$ ) is tabulated in Table 4.4.

**Table 4.4** Evaluation of PRD values for Conventional estimator

S.No.	Threshold Function	$\delta_u$	$\delta_{uld}$	$\delta_{umltd}$	$\delta_{mou}$	$\delta_{mini}$	$\delta_{adp}$	$\delta_{expld}$	$\delta_{eur}$
1.	Hard	0.03	0.04	0.006	0.02	0.03	0.01	0.01	0.04
2.	Soft	0.04	0.07	0.012	0.03	0.05	0.02	0.03	0.07
4.	Semi Soft	0.31	0.28	0.31	0.31	0.30	0.31	0.31	0.28
3.	Trimmed	0.06	0.08	0.04	0.05	0.06	0.04	0.04	0.06
5.	Non-Negative Garrote	0.03	0.05	<b>0.005</b>	0.02	0.03	0.01	0.007	0.05
6.	Hyperbolic	0.19	0.20	0.19	0.19	0.19	0.19	0.19	0.20

From Table 4.4, it has been observed that minimum value of PRD (**0.005**) is achieved using “*Non-negative Garrotte threshold function with universal modified level-dependent threshold value selection*” that determines its efficacy for denoising process as compared to other threshold functions and threshold value selection.

Computational assessment of different performance metrics in Table 4.2, 4.3 and 4.4 revealed that “*Non-negative Garrotte threshold function with universal modified level-dependent threshold value selection*” delivers high SNR, low MSE and small PRD using conventional estimator.

#### 4.5.2 Results for Proposed Estimator

Different performance parameters (SNR, MSE and PRD) are computed to determine the efficiency of proposed noise estimator for denoising process. Table 4.5 tabulates the computation of SNR for different ( $\delta$ ) and ( $f_n$ ) for proposed estimator.

**Table 4.5.** Evaluation of SNR values for proposed estimator

S.No	Threshold Function	$\delta_u$	$\delta_{uld}$	$\delta_{umld}$	$\delta_{mou}$	$\delta_{mini}$	$\delta_{adp}$	$\delta_{expld}$	$\delta_{eur}$
1.	Hard	33.21	28.34	46.27	38.62	30.78	44.76	41.00	28.34
2.	Soft	29.08	25.74	44.17	31.71	27.91	35.97	33.50	25.74
3.	Semi Soft	10.02	10.26	9.87	9.98	10.14	9.89	9.97	10.26
5.	Trimmed	25.32	23.68	27.42	26.13	24.82	26.65	27.45	23.68
3.	Non-Negative Garrote	30.54	27.74	<b>54.98</b>	34.40	29.35	41.01	38.04	27.74
4.	Hyperbolic	14.16	14.08	14.23	14.20	14.14	14.22	14.21	14.08

From Table 4.5 it has been observed that the high value of SNR (54.98 dB) has been obtained from “*Non-negative Garrotte threshold function with universal modified level-dependent*”

*threshold value selection*” using proposed noise estimator. Similarly MSE and PRD are computed for proposed noise estimator and are tabulated in Table 4.6 and 4.7 respectively.

**Table 4.6.** Evaluation of MSE for proposed estimator

S. No.	Threshold Function	$\delta_u$	$\delta_{uld}$	$\delta_{umld}$	$\delta_{mou}$	$\delta_{mini}$	$\delta_{adp}$	$\delta_{expld}$	$\delta_{eur}$
1.	Hard	3.06e-05	9.38e-05	1.51e-06	8.81e-06	5.36e-05	2.14e-06	5.09e-06	9.38e-05
2.	Soft	7.92e-05	1.71e-04	2.45e-06	4.32e-05	1.03e-04	1.62e-05	2.86e-05	1.71e-04
3.	Semi Soft	0.006	0.006	0.006	0.006	0.006	0.006	0.006	0.006
4.	Trimmed	1.88e-04	2.74e-04	1.16e-04	1.56e-04	2.11e-04	1.38e-04	1.15e-04	2.74e-04
5.	Non -Negative Garrote	5.66e-05	1.07e-04	<b>2.03e-07</b>	2.33e-05	7.44e-05	5.07e-06	1.00e-05	1.07e-04
6.	Hyperbolic	0.002	0.002	0.002	0.002	0.002	0.002	0.002	0.002

**Table 4.7.** Evaluation of PRD for proposed estimator

S. No.	Threshold Function	$\delta_u$	$\delta_{uld}$	$\delta_{umld}$	$\delta_{mou}$	$\delta_{mini}$	$\delta_{adp}$	$\delta_{expld}$	$\delta_{eur}$
1.	Hard	0.02	0.03	0.004	0.01	0.02	0.005	0.008	0.03
2.	Soft	0.03	0.05	0.006	0.02	0.04	0.01	0.021	0.05
3.	Semi Soft	0.31	0.30	0.32	0.31	0.31	0.31	0.006	0.30
4.	Trimmed	0.05	0.06	0.04	0.04	0.05	0.04	0.04	0.06
5.	Non-Negative Garrote	0.02	0.04	<b>0.003</b>	0.01	0.03	0.008	0.001	0.04
6.	Hyperbolic	0.19	0.19	0.19	0.19	0.19	0.19	0.19	0.19

Table 4.6 and 4.7 depicts the MSE and PRD values respectively for proposed estimator for distinct threshold value selection and threshold functions. It signifies that least value of MSE (**2.03e-07**) and PRD (**0.003**) has been obtained from “*Non - negative Garrote threshold function with universal modified level-dependent threshold value selection*” which reveals its effectiveness



to denoise the ECG signal. For further validation, the combination of distinct ( $\delta$ ) and ( $f_n$ ) are applied on the (100-107) record of “MIT-BIH Arrhythmia database” for computation of SNR as tabulated in Table 4.8.

**Table 4.8.** SNR computation of distinct threshold value selection and threshold function using proposed estimator

Threshold functions	Value selection	ECG Samples							
		100	101	102	103	104	105	106	107
Hard	$\delta_u$	33.21	36.19	33.98	31.50	35.26	28.64	25.44	40.67
	$\delta_{uld}$	33.76	36.67	34.33	31.92	35.66	29.18	25.84	41.15
	$\delta_{umld}$	46.27	49.90	47.12	48.13	47.41	47.39	32.81	42.68
	$\delta_{expl}$	41.00	45.97	43.64	41.16	43.84	39.43	25.66	42.57
	$\delta_{min}$	30.78	33.92	32.56	30.60	33.16	27.34	18.30	37.32
	$\delta_{mon}$	38.62	41.20	38.52	36.63	40.21	33.86	29.52	45.75
	$\delta_{adp}$	44.76	44.80	48.89	38.54	49.33	51.11	44.27	44.45
	$\delta_{Heur}$	28.34	31.38	30.18	27.96	30.95	22.36	14.01	33.75
Soft	$\delta_u$	26.98	31.94	30.14	28.56	31.34	25.15	18.57	36.51
	$\delta_{uld}$	29.31	32.17	30.36	28.74	31.57	25.35	18.88	36.75
	$\delta_{umld}$	44.17	52.07	50.56	48.71	51.26	45.55	35.59	51.62
	$\delta_{expl}$	33.50	36.95	35.13	32.84	35.13	30.36	18.28	35.18
	$\delta_{min}$	27.91	30.83	29.30	27.66	30.06	24.37	14.03	32.51
	$\delta_{mon}$	32.02	34.52	32.56	30.79	33.83	27.55	21.65	39.13
	$\delta_{adp}$	35.97	36.84	38.09	31.15	40.33	39.34	28.55	36.12
	$\delta_{Heur}$	25.74	28.71	26.80	25.42	27.49	24.58	11.84	28.93
Non-Negative Garrote	$\delta_u$	30.50	33.49	31.81	29.72	32.90	26.38	21.50	38.42
	$\delta_{uld}$	27.74	30.63	29.35	27.29	30.25	23.68	12.76	31.93
	$\delta_{umld}$	<b>54.98</b>	<b>58.73</b>	<b>55.43</b>	<b>53.03</b>	<b>53.84</b>	<b>52.23</b>	<b>40.83</b>	<b>55.92</b>
	$\delta_{expl}$	38.04	42.26	40.72	37.86	40.87	35.35	21.67	39.88
	$\delta_{min}$	29.35	32.22	31.10	29.11	31.85	25.65	15.51	35.47
	$\delta_{mon}$	34.40	37.20	35.01	32.87	36.37	29.86	25.69	41.93
	$\delta_{adp}$	41.01	41.64	44.37	35.09	46.86	46.45	37.95	41.15
	$\delta_{eur}$	27.74	30.63	29.35	27.29	30.25	23.68	12.76	31.93
Hyperbolic	$\delta_u$	14.16	12.83	14.05	7.46	17.47	16.12	11.90	19.60
	$\delta_{uld}$	14.08	12.81	13.98	7.43	17.33	15.76	10.32	19.40

	$\delta_{\text{umld}}$	14.23	12.87	14.11	7.48	17.57	16.42	12.36	19.65
	$\delta_{\text{expl}}$	14.21	12.86	14.10	7.47	17.53	16.35	11.94	19.56
	$\delta_{\text{min}}$	14.14	12.83	14.04	7.45	17.44	16.08	11.09	19.50
	$\delta_{\text{mon}}$	14.20	12.85	14.08	7.47	17.52	16.28	12.14	19.63
	$\delta_{\text{adp}}$	14.22	12.86	14.11	7.47	17.56	16.42	12.34	19.59
	$\delta_{\text{Heur}}$	14.08	12.81	13.98	7.43	17.33	15.76	10.32	19.40
	$\delta_{\text{u}}$	25.32	29.01	24.73	25.57	26.08	22.14	15.19	31.73
	$\delta_{\text{uld}}$	23.68	27.71	23.33	25.12	24.39	20.63	11.44	28.00
Trimmed	$\delta_{\text{umld}}$	27.27	31.07	26.19	27.55	26.31	24.36	17.25	33.24
	$\delta_{\text{expl}}$	26.25	30.31	25.42	26.79	26.61	23.24	14.84	31.23
	$\delta_{\text{min}}$	24.82	28.64	24.41	25.52	25.59	21.74	12.92	30.11
	$\delta_{\text{mon}}$	26.06	29.74	25.30	26.02	26.67	22.92	16.15	32.41
	$\delta_{\text{adp}}$	26.65	30.36	25.79	26.79	27.25	24.31	17.20	31.51
	$\delta_{\text{eur}}$	23.68	27.71	23.33	25.12	24.39	20.63	11.44	28.00
Semi-Soft	$\delta_{\text{u}}$	10.02	10.00	11.20	4.46	14.81	15.49	12.45	16.83
	$\delta_{\text{uld}}$	10.26	10.12	11.52	4.58	15.06	16.76	18.80	16.86
	$\delta_{\text{umld}}$	9.87	9.92	11.00	4.41	14.34	14.68	11.19	16.60
	$\delta_{\text{expl}}$	9.97	9.94	11.08	4.45	14.57	15.19	13.55	16.60
	$\delta_{\text{min}}$	10.14	10.03	11.24	4.50	14.77	15.65	15.20	16.74
	$\delta_{\text{mon}}$	9.98	9.96	11.16	4.44	14.63	15.06	11.57	16.71
	$\delta_{\text{adp}}$	9.89	9.94	11.04	4.46	14.44	14.65	11.09	16.62
	$\delta_{\text{Heur}}$	10.26	10.12	11.52	4.58	15.06	16.76	18.80	16.86

Table 4.8 determines that high value of SNR is obtained from the “*Non - negative Garrotte threshold function with universal modified level-dependent threshold value selection*” among all other combination of ( $\delta$ ) and ( $f_n$ ) for (100-107) record of Arrhythmia database.

Therefore, proposed noise estimator using “Non- Negative Garrotte threshold function with universal modified level-dependent threshold value selection” show its superiority to achieve best performance results among other threshold value selection and functions in terms of SNR, MSE and PRD. Later, Comparative analysis of proposed noise estimator ( $\alpha^*$ ) with conventional

estimator ( $\alpha$ ) has been done in Table 4.9 to analyse the efficiency and effectiveness of proposed estimator to attain denoised ECG signal.

**Table 4.9.** Comparative Analysis of conventional and proposed estimator

Record	SNR (dB)		MSE		PRD	
	Conventional	Proposed	Conventional	Proposed	Conventional	Proposed
‘V5’ 100	45.67	<b>54.98</b>	1.73e-6	<b>2.03e-7</b>	0.005	<b>0.003</b>
‘MLII’ 103	47.92	<b>53.04</b>	2.65e-6	<b>2.77e-7</b>	0.004	<b>0.003</b>

In table 4.9 comparative analysis of conventional and proposed estimator for two records i.e. ‘V5’100 and ‘MLII’103 has been performed. The result reveals that the proposed estimator outperforms in all aspects by delivering highest SNR, lowest MSE and smallest PRD to attain clean ECG signal as compared to conventional noise estimator. The table further signifies that 20.38% and 10.68% of SNR improvement is achieved by employing proposed noise estimator for ‘V5’100 and ‘MLII’103 as implemented on same platform of conventional estimator.

### 4.5.3 Optimal Threshold Tuning

Threshold tuning is executed by varying the threshold value and threshold function at each level of decomposition to attain denoised ECG signal. In this thesis *eight distinct* set of threshold value selection rules along with *six different* threshold functions are implemented and evaluated on “MIT-BIH arrhythmia database”. An Extensive empirical analysis of conventional as well as proposed noise estimator has been performed for different combinations of threshold value selection and threshold functions. The best combination of distinct threshold value selection and threshold function using proposed noise estimator is applied to attain denoised ECG signal as shown in Fig. 4.7.

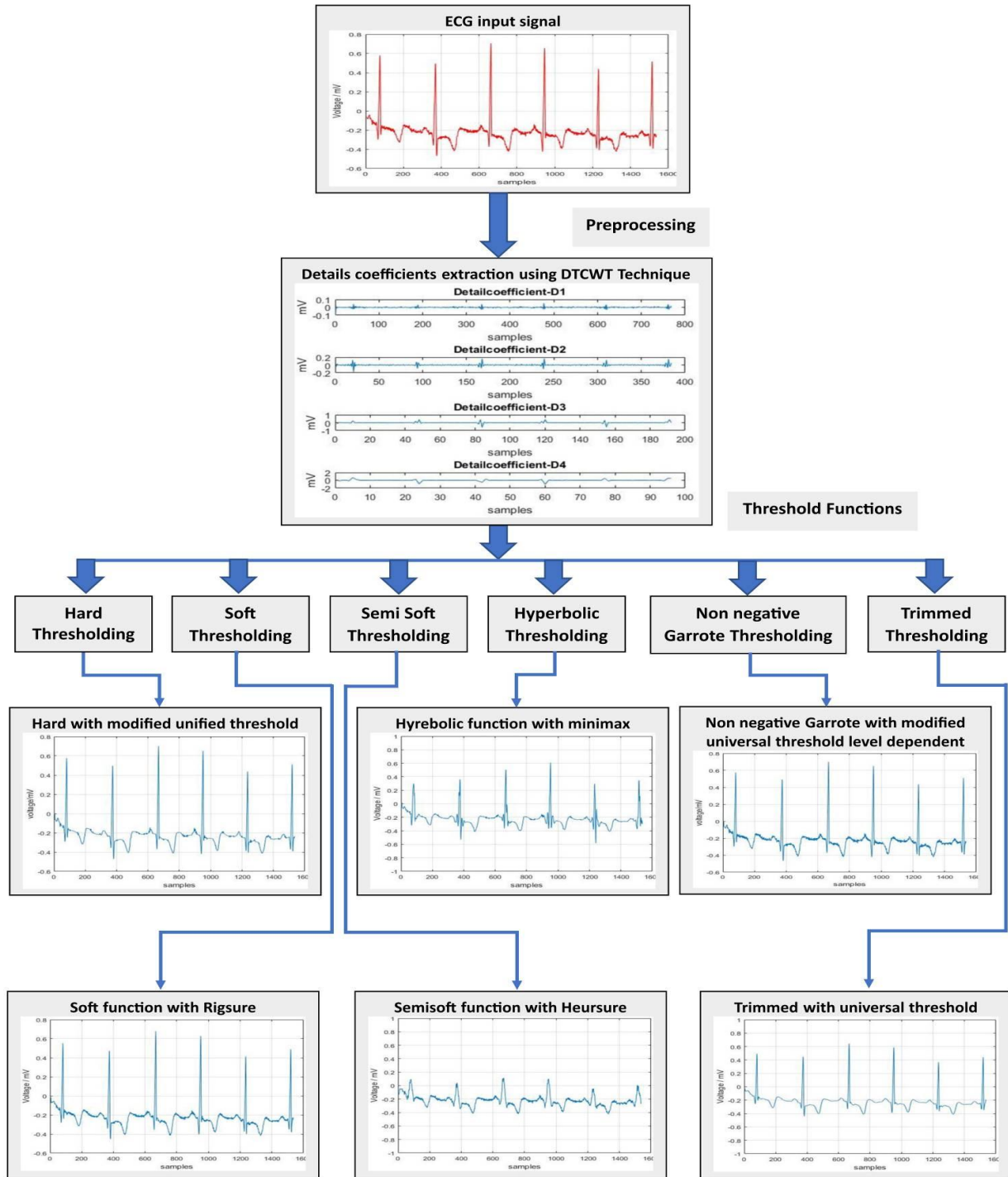


**Figure 4.7** Block diagram summarizing the results of different threshold value and threshold functions using proposed estimator

The performance outcomes show that the optimal threshold tuning is achieved by using “*Non - negative Garrote threshold function with universal modified level-dependent threshold value selection*”. The non-negative Garrote estimator exhibit path of pAtrially linear solution and is the least square scale variant that built it reliable, flexible and simple to measure. Aliasing in signal processing is an effect that makes diverse signal to become indistinguishable when sampled, resulted to the distortion in the reconstructed signal from original signal. This optimal threshold tuning successively overcomes this effect that make it vigorous to artifacts than other existing techniques.

For better interpretation the proposed noise estimator using optimal threshold tuning is implemented for 100-109 record of “MIT-BIH arrhythmia database” and later compared with some eminent techniques such as DWT and DT-WT [142] as depicted in Table 4.10.

**Table 4.10.** SNR Comparison of 100 -109 records arrhythmia database

<b>Record</b>	<b>Charri <i>et al.(2017)</i> DWT</b>	<b>Charri <i>et al.(2017)</i> DT-WT</b>	<b>Proposed Technique DTCWT (Gaussian distribution)</b>
100	42.65	45.83	<b>54.98</b>
101	48.41	49.39	<b>58.22</b>
102	45.49	49.87	<b>55.43</b>
103	52.20	55.41	<b>58.73</b>
104	54.13	57.51	<b>62.09</b>
105	62.82	66.18	<b>69.77</b>
106	47.45	51.89	<b>52.23</b>
107	54.57	55.52	<b>55.92</b>
108	43.32	48.16	<b>59.70</b>
109	51.25	53.76	<b>53.89</b>

Table 4.10 shows that the proposed noise estimator using optimal threshold tuning delivers high SNR value for all defined record 100-109 of MIT-BIH arrhythmia database.

Curve fitting for conventional and proposed noise estimator using optimal threshold tuning is predicated in next section.

#### 4.5.4 Curve Fitting

Curve fitting is the process of formulating a curve to have best fit for variable data series [144]. The prime motive of curve fitting is to determine the parameter of mathematical model that defines the data in such a manner that it minimizes the difference between data and model. In this work, the curve fitting plot for conventional and proposed noise estimator is analyzed for different records of MIT-BIH Arrhythmia database while considering SNR as shown in Fig. 4.8

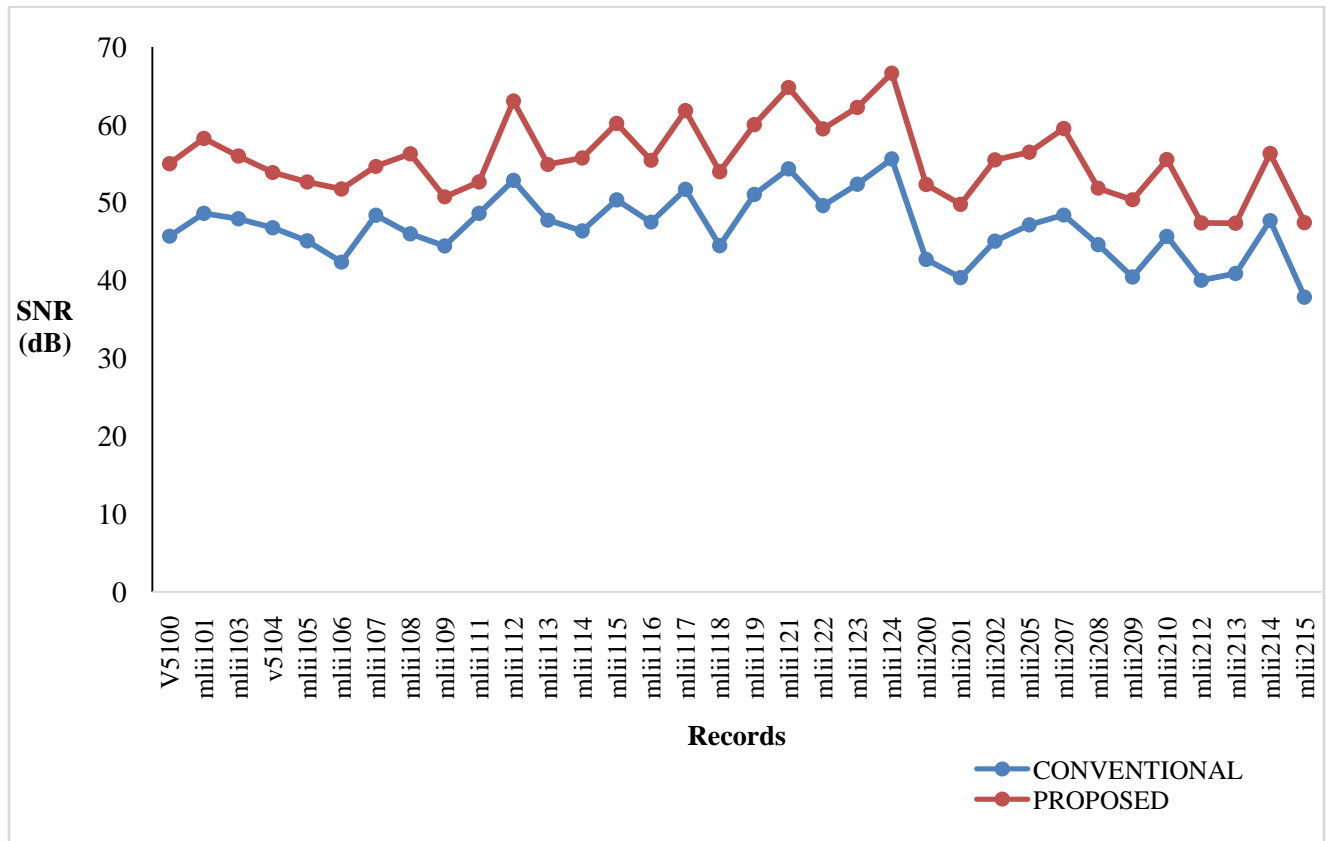


Figure 4.8 Curve Fitting Plot

Fig 4.8 represents the behaviour of conventional and proposed estimator for different records of ECG signal. Both conventional and proposed noise estimator have almost same curve pattern that defines their linear relationship with respect to each other. Further, 0.947, Pearson Correlation coefficient has been computed that depicts the strong positive relationship between conventional

and proposed estimator. The calculated correlation coefficient is closer to 1.0 which signifies that both conventional and proposed noise estimator is nearly on the verge of perfect positive relationship.

#### 4.5.5 Comparison with State-of-the-Art- Work

Comparison of proposed noise estimator using optimal threshold tuning has been done with other state of art techniques to examine its efficiency to attain denoised ECG signal as tabulated in Table 4.11

**Table 4.11** Comparison of Proposed estimator with State-of-the-Art-Work

S. No.	Technique	SNR (dB)
1.	Hybridizing $\beta$ -hill climbing + wavelet transform (2018) [102]	16.7
2.	Wavelet transform with Genetic Algorithm (2018) [103]	19.3
3.	Fourier decomposition method (2020) [106]	23.3
4.	Eigen value decomposition method (2020) [106]	12.9
5.	Empirical mode decomposition Wavelet transform based on extended Kalman filter (2020) [106]	10.3
6.	Proposed Robust noise estimator	<b>54.98</b>

Table 4.11 shows that the proposed noise estimator using optimal threshold tuning attains high SNR value than other state of art techniques which further signifies its reliability for removal of different noises from the ECG signal.

## 4.6 SUMMARY

In this chapter an empirical analysis of conventional and proposed noise estimator for Gaussian distribution function is performed by exhausting all combinations of threshold value selection and

threshold functions. An optimal threshold tuning is achieved utilizing “Non-negative Garrotte threshold function with universal modified threshold level-dependent threshold value selection”. Implementing the proposed noise estimator with optimal threshold tuning depicts the significant improvement in SNR by 20.38% as compared to conventional estimator by successively eliminating the spurious high frequency from the reconstructed signal. Later, person correlation coefficient for conventional and proposed estimator is 0.947 which depicts the linear relationship between both estimators. This work is further extended by taking ( $2^n$ ) down scaling factor in robust noise estimator to analyze its impact on the quality reconstructed signal utilizing different distribution functions in next chapter.



# **CHAPTER 5**

## **DISTRIBUTION MODELING FOR ECG DENOISING SYSTEM DESIGN**

# CHAPTER 5

## Distribution Modeling for ECG Denoising System Design

Noise estimation algorithms are vital components of many advanced human computer interaction systems [145]. It is used in the denoising approach in order to enhance the quality of a signal that is distorted due to distinct noises. The algorithm for the noise estimation is relying on a trade-off between signal distortion and residual noise [146]. Different noise estimation methods have been developed for reduction of noise that includes Minimum Statistics (MS) noise estimation approach for non-stationary signals to monitor varying noise levels. The noise estimation is calculated as the minimum values of the smoothed power approximation of the noisy signal, multiplied by a factor that compensates for the bias [147]. Nevertheless, the MS algorithm also appears to skew the noise estimation below that of the actual noise level [148]. It therefore leaves residual noise in the signal that causes the characteristic noise variation in highly non-stationary, noisy environments. This noise can be estimated by using various probability distribution functions.

### 5.1 INTRODUCTION

Contamination of signal by the additive white Gaussian noise (AWGN) is counted as the classic signal processing problem. Signal disruptions caused by noise are usual during the phase of acquisition, transmission and reproduction. Several researches in the last two decades are concentrated in noise reduction in order to enhance the signal quality being processed. Distinct approaches using the wavelet thresholding are effective especially for the elimination of additive white Gaussian noise. The Hard and soft strategies for denoising are suggested by Donoho and Johnstone [133]. These methods eradicate certain wavelet coefficients which contain the valuable information. The key problem with both the approaches is the selection of a appropriate threshold

value. The concept of threshold independent of coefficient is described by Donoho and Johnston rely on two factors i.e. noise power and signal size. However, the implementation of such a theoretical finding is in fact very doubtful when a small signal of finite size is being handled. Furthermore, most signals display a non-uniform spatial energy distribution that motivates non-uniform threshold selection. Linear filtering is an efficient technique for additive noise reduction, while non-linear filters are useful for processing multiple and function dependent noise.

A probability distribution is a function of statistics that depicts all possible values that a random variable can hold within a defined range [149]. This range is constituted from entire minimum and maximum possible values. Probability distribution helps to identify the thermal noise and transient noise from the signal and estimate the peak-to-peak value of noisy signal [150]. A random noise consists of infinite summation of sinusoidal waves at distinct frequency level. In addition, applying the threshold limits without model fitting for non-stationary ECG signal exhibit a significant difference between the data sets of similar parameters measured over a different period of time [86]. This problem encouraged the researcher to examine different probability distribution functions. The probability distribution portrays the scope of conceivable qualities that an arbitrary variable can accomplish and the probability that the estimation of the irregular variable is inside any subset of that range. A probability distribution provides vital information about the data, how the values are changing, regardless of whether they are aggregated or dispersive and whether they are symmetrically arranged on the X-axis or not. The different probability distribution functions that are considered in this research work are Gaussian, Normal and Exponential Distribution Functions.

*Gaussian distribution Functions* : The Gaussian distribution has a bell-shaped curve and the measurements is expected to be equal above and below the mean value. The values of mean, median and mode for Gaussian distribution have equal. [149].

The facts on which the reference range, mean  $\pm$  standard deviation (SD ( $\sigma$ )) relies that the lower end of abnormal values and upper end of normal values frequently overlap. The mean  $\pm$ SD conserves the reference range according to the coefficient values measurement. A Gaussian distribution is well approximated for the distribution of many of the coefficient values since practically all the values which an analyzer may believe are within the three standard deviations

that mean  $\pm 1$  SD include 68.2% of all value, mean  $\pm 2$  SD include 95.5% of all values and mean  $\pm 3$  SD 99.7% of all values are approximated. [149].

The Gaussian distribution function is mathematically modeled by Eq. 5.1

$$f(x) = ae^{-\frac{(x-b)^2}{2\sigma^2}} \quad (5.1)$$

where  $a$  is the peak curve height,  $b$  is the peak centre (position) and  $\sigma$  is the standard deviation that controls the Gaussian RMS width/width of the bell. The parameter  $a$  is set equal to  $\frac{1}{\sigma(\sqrt{2\pi})}$

such that the total curve area is equal to 1.

*Normal Distribution Function:* Using normal distribution, the real-valued random variables are described that grouped around a singular mean value as a principal approximation. Due to certain reasons the normal distribution is known as the most relevant probability distribution than others: Firstly, according to central limit theorem, the mean of a large number of random variables is normally distributed under certain conditions [151]. Furthermore, the Normal distribution is remarkably systemically tractable i.e. for explicitly evaluating a significant number of outcomes that comprise this distribution. This normal distribution is independent of the original distribution form.

The Normal distribution probability density function (pdf) is expressed as Eq. 5.2

$$\int_{-\infty}^{\infty} ge^{-\frac{(x-c)^2}{2s^2}} dx = gs\sqrt{2\pi} \quad (5.2)$$

The value of mean ( $\mu = 0$ ) and variance ( $\sigma^2 = 1$ ) for Standardized Normal distribution as described by Eq. 5.3

$$p(x) = \frac{1}{\sqrt{2\pi}} e^{-x^2/2} \quad (5.3)$$

Normal distribution is symmetrical about its mean and is non-zero over the entire real line. The normal distribution is classified when the values lie within the 2 standard deviations of the mean which represents 95% of the value [152].

*Exponential Distribution Function:* It defines the probability distribution of the time between events in a Poisson point process in which continual and independent happening of events at a constant average rate. Exponential distribution of continuous random variable  $X$  exist if its probability density function  $f_X(x|\lambda)$  is defined as

$$f_X(x|\lambda) = \begin{cases} \lambda e^{-\lambda x} & \text{for } x > 0 \\ 0 & \text{for } x < 0 \end{cases} \quad (5.4)$$

where  $\lambda > 0$  is known as distribution rate. Usually, the exponential distribution is used to model the time before anything happens in the process. The exponential distribution is a continuous analogue of the geometric distribution and possessing memory less property [153]. Such probability distribution functions are examined in order to analyze their impact on output metrics and on the essence of the recovered signal.

## 5.2 THE PROPOSED DENOISED APPROACH

The robust noise estimator is implemented to yield a clean ECG signal employing the proposed methodology as illustrated in Fig 5.1. It consists of raw input signal obtained from “MIT BIH arrhythmia database” of ‘V5’ 100 record of Physio Bank ATM [28]. The proposed methodology comprises of filtering stage, DTCWT technique, thresholding procedure, proposed estimator with  $2^n$  scaling factor, Different distribution functions and Inverse DTCWT to accomplish the denoising the process for non-stationary ECG signal. Individual block of proposed estimator has crucial significance to attain clean signal without losing the valuable information.

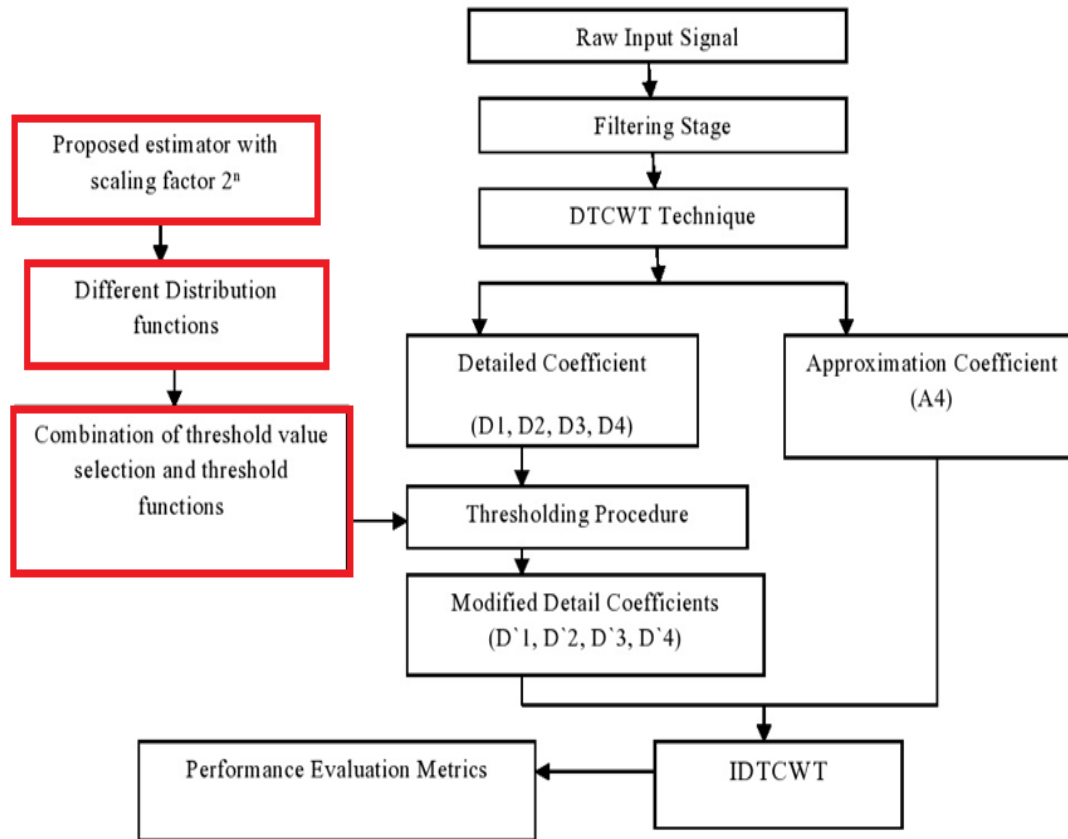


**Figure 5.1** Methodology Adopted for ECG denoising using Different Distribution Functions

The input raw ECG signal is supplied to the filtering block to eliminate low frequency baseline wander noise followed by the implementation of DTCWT technique that performs multilevel decomposition for extraction of detail (D1, D2, D3, and D4) and approximation coefficients (A4). In another step, the procedure of thresholding is carried out on detail coefficients by specifying the various ( $\delta$ ) and ( $f_n$ ) using the proposed noise estimator employing different distribution functions.

***Proposed Noise Estimator with  $2^n$  scaling factor :***

A robust noise estimator ( $\alpha^*$ ) has been proposed that supervise the trade-off between signal distortion and residual noise for eradicating the estimated noise in highly non-stationary noisy environment.

The proposed noise estimator is mathematically modeled by Eq. 5.5.

$$\alpha^* = z \times \text{median}\left(\frac{|x_{jk}|}{2^n}\right) \quad (5.5)$$

The Proposed robust noise estimator ( $\alpha^*$ ) is dependent on two factors-

- i. **2<sup>n</sup> down scaling factor**- The high frequency detail coefficients are prominently influential to the noise. The presence of these artifacts brings the overall change in amplitude of an ECG signal due to the accommodation of desired information by fairly high amplitude noise. To mitigate the affect these noises, downscaling of amplitude by 2<sup>n</sup> factor is done that further assists in the reduction of outliers by taking the median of the corresponding coefficients.
- ii. **z parameter dependent on distinct distribution functions**- The different probability distribution functions are determined for measurement of signal that contain random noise and gross errors. This probabilistic framework determines whether the estimator is deviated from the fundamental process resulting in a change in the underlying probability distribution of the signal. The different probability distribution functions are exploited to perform data (samples) rectification and modeling enhancing the performance of robust noise estimator by reducing the Mean Square Error (MSE).

The proposed estimator ( $\alpha^*$ ) along with best combination of threshold value selection and threshold functions delivers modified detail coefficients (D`1, D`2, D`3, D`4) at each level of decomposition. The process of IDTCWT is applied on modified detail coefficients and approximation coefficients to attain reconstructed signal.

### 5.3 RESULTS AND DISCUSSION

The distinct probability distribution functions are executed by varying the  $n^{\text{th}}$  value of downscaling factor 2<sup>n</sup> for analyzing the impact on ECG denoising using proposed robust noise estimator. Various performance metrics are computed for different samples of ECG to identify the

best suited probability distribution function with finer value of scaling factor. The performance evaluation of proposed methodology is accessed on “MIT- BIH arrhythmia” database [28].

### 5.3.1 Results of varying Distribution Functions

Computation of different performance metrics using proposed technique for different distribution functions (Gaussian, Normal and exponential) are examined. An exhaustive empirical analysis is performed to obtain an efficient probability distribution function for ECG denoising using optimal thresholding.

*Normal distribution function* : The distinct performance metrics has been evaluated for proposed estimator with  $n = 1$  using Normal distribution function. Table 5.1 depicts the SNR evaluation of proposed estimator using Normal distribution for different ( $\delta$ ) and ( $f_n$ ).

**Table 5.1.** SNR Evaluation of Proposed estimator with  $n = 1$  using Normal distribution

S.No	Threshold Function	$\delta_u$	$\delta_{uld}$	$\delta_{umld}$	$\delta_{mou}$	$\delta_{mini}$	$\delta_{adp}$	$\delta_{expld}$	$\delta_{heur}$
1.	Hard	35.61	28.95	50.26	47.84	33.54	28.95	43.74	35.61
2.	Soft	30.19	26.55	46.07	37.65	28.88	26.55	35.11	30.19
3.	Semi Soft	10.00	10.19	9.86	9.88	10.08	10.19	9.94	10.00
4.	Trimmed	25.67	24.48	27.46	26.85	25.21	24.14	27.09	25.67
5.	Non-Negative Garrote	32.14	28.24	<b>58.23</b>	42.23	30.54	28.24	40.13	32.14
6.	Hyperbolic	14.18	14.10	14.26	14.23	14.16	14.10	14.22	14.18



Table 5.2 shows the MSE evaluation of proposed estimator with  $n = 1$  using Normal distribution for different threshold function and threshold value selection.

**Table 5.2.** MSE Evaluation of Proposed estimator with  $n = 1$  using Normal distribution

S. No.	Threshold Function	$\delta_u$	$\delta_{uld}$	$\delta_{umld}$	$\delta_{mou}$	$\delta_{mini}$	$\delta_{adp}$	$\delta_{expld}$	$\delta_{Heur}$
1.	Hard	1.76e-05	8.17e-05	6.03e-07	4.88e-06	2.83e-05	1.05e-06	2.70e-06	8.17e-05
2.	Soft	6.14e-05	1.41e-04	1.58e-06	3.09e-05	8.30e-05	1.10e-05	1.97e-05	1.41e-04
3.	Semi Soft	0.006	0.006	0.006	0.006	0.006	0.006	0.006	0.006
4.	Trimmed	1.73e-04	2.28e-04	1.15e-04	2.43e-04	1.93e-04	1.32e-04	1.25e-04	2.47e-04
5.	Non Negative Garrote	3.92e-05	9.60e-05	<b>9.63e-08</b>	1.40e-05	5.65e-05	3.04e-06	6.22e-06	9.60e-05
6.	Hyperbolic	0.002	0.002	0.002	0.002	0.002	0.002	0.002	0.002

The PRD evaluation of Proposed estimator with  $n = 1$  using Normal distribution is depicted in Table 5.3 for different threshold function and threshold value selection.

**Table 5.3.** PRD Evaluation of Proposed estimator with  $n = 1$  using Normal distribution

S.No	Threshold Function	$\delta_u$	$\delta_{uld}$	$\delta_{umld}$	$\delta_{mou}$	$\delta_{mini}$	$\delta_{adp}$	$\delta_{expld}$	$\delta_{Heur}$
1.	Hard	0.01	0.03	0.003	0.008	0.02	0.004	0.006	0.03
2.	Soft	0.03	0.04	0.005	0.02	0.03	0.01	0.017	0.04
3.	Semi Soft	0.31	0.30	0.32	0.31	0.31	0.32	0.31	0.30
4.	Trimmed	0.05	0.05	0.04	0.06	0.05	0.04	0.04	0.06
5.	Non Negative Garrote	0.002	0.003	<b>0.001</b>	0.014	0.002	0.006	0.009	0.003
6.	Hyperbolic	0.19	0.19	0.19	0.19	0.19	0.19	0.19	0.19

The performance evaluation of proposed estimator for  $n = 1$  using Normal distribution depicts that “Non-Negative Garrote threshold function with universal modified threshold level-dependent

value selection” among all possible combinations of threshold value selection and threshold functions that delivers 58.23 dB of SNR , 9.63e-08 of MSE and 0.001 of PRD.

*Exponential distribution* : The performance of proposed estimator with  $n = 1$  using Exponential distribution function is evaluated. Table 5.4 tabulates the evaluation of SNR value of proposed estimator using Exponential distribution for different threshold function and threshold value selection.

**Table 5.4.** SNR Evaluation of Proposed estimator with  $n = 1$  using Exponential distribution

S. No.	Threshold Function	$\delta_u$	$\delta_{uld}$	$\delta_{umld}$	$\delta_{mou}$	$\delta_{mini}$	$\delta_{adp}$	$\delta_{expld}$	$\delta_{eur}$
1.	Hard	31.90	27.76	45.08	36.95	29.02	41.98	38.83	28.10
2.	Soft	28.53	24.73	42.73	30.21	25.04	33.76	32.09	23.87
3.	Semi Soft	10.01	9.83	9.75	9.83	10.08	9.72	9.84	10.12
4.	Trimmed	23.47	22.34	26.35	25.12	23.45	25.84	27.14	22.09
5.	Non-Negative Garrote	29.76	26.78	<b>53.12</b>	31.89	28.45	39.89	36.43	26.04
6.	Hyperbolic	14.11	14.06	14.21	14.18	14.16	14.19	14.20	14.04

Table 5.5 tabulates the MSE values of proposed estimator with  $n = 1$  using Exponential distribution for different threshold function and threshold value selection.

**Table 5.5.** MSE Evaluation of Proposed estimator with  $n=1$  using Exponential distribution

S. No.	Threshold Function	$\delta_u$	$\delta_{uld}$	$\delta_{umld}$	$\delta_{mon}$	$\delta_{mini}$	$\delta_{adp}$	$\delta_{expld}$	$\delta_{eur}$
1.	Hard	4.82e-05	10.65e-05	2.01e-06	9.10e-06	6.06e-05	3.12e-06	6.14e-06	10.45e-05
2.	Soft	8.72e-05	1.89e-04	3.10e-06	5.12e-05	2.03e-04	2.23e-05	3.16e-05	2.10e-04
3.	Semi Soft	0.007	0.007	0.006	0.006	0.007	0.006	0.007	0.006
4.	Trimmed	2.28e-04	3.12e-04	2.16e-04	2.62e-04	2.32e-04	1.89e-04	1.67e-04	3.17e-04
5.	Non-Negative Garrote	6.26e-05	2.08e-04	<b>3.12e-07</b>	2.67e-05	7.98e-05	6.12e-06	2.01e-05	1.89e-04
6.	Hyperbolic	0.003	0.003	0.003	0.003	0.003	0.003	0.003	0.003

Table 5.6 depicts the PRD value of proposed estimator with  $n = 1$  using Exponential distribution for different  $(\delta)$  and  $(f_n)$ .

**Table 5.6** PRD Evaluation of Proposed estimator with  $n = 1$  using Exponential distribution

S.No.	Threshold Function	$\delta_u$	$\delta_{uld}$	$\delta_{umld}$	$\delta_{mou}$	$\delta_{mini}$	$\delta_{adp}$	$\delta_{expld}$	$\delta_{eur}$
1.	Hard	0.03	0.03	0.005	0.02	0.04	0.005	0.009	0.03
2.	Soft	0.04	0.05	0.006	0.02	0.04	0.01	0.023	0.06
3.	Semi Soft	0.33	0.31	0.33	0.32	0.31	0.33	0.008	0.33
4.	Trimmed	0.07	0.08	0.05	0.04	0.05	0.05	0.06	0.08
5.	Non-Negative Garrote	0.03	0.04	<b>0.004</b>	0.02	0.04	0.008	0.002	0.05
6.	Hyperbolic	0.20	0.19	0.19	0.20	0.19	0.19	0.20	0.20

The performance evaluation of proposed estimator with  $n = 1$  using Exponential distribution depicts an efficient performance for “*Non- Negative Garrote threshold function with universal modified threshold level-dependent value selection*” delivering SNR value of 53.12 dB , MSE as  $3.12e-07$  and PRD as 0.004.

*Gaussian distribution function:* The empirical performance analysis of proposed noise estimator with  $n =1$  using Gaussian distribution for “*Non- Negative Garrote threshold function with universal modified threshold level-dependent value selection*” as tabulated in Table 5.7.

**Table 5.7.** Performance Analysis of Proposed estimator with  $n = 1$  using Gaussian distribution

SNR (dB)	MSE	PRD
54.98	$2.03e-7$	0.003

The proposed estimator with  $n = 1$  using Gaussian distribution function yields 54.98 dB SNR ,  $2.03e-7$  MSE and 0.003 PRD values.

### Comparative Analysis of Proposed Noise Estimator using Different Distribution Functions

Performance assessments of conventional and proposed estimator are computed using distinct distribution functions (Gaussian, Normal and Exponential) as tabulated in Table 5.8.

**Table 5.8.** Comparison Table of performance metrics using different distribution functions

Different Distribution Functions	SNR		MSE		PRD	
	Conventional	Proposed	Conventional	Proposed	Conventional	Proposed
Gaussian distribution	45.67	54.98	$1.73e-6$	$2.03e-07$	0.005	0.003
Normal distribution	48.65	<b>58.23</b>	$8.75e-07$	<b><math>9.63e-08</math></b>	0.003	<b>0.001</b>
Exponential distribution	44.05	53.12	$2.52e-06$	$3.12e-07$	0.006	0.004

The proposed estimator with  $n = 1$  using normal distribution delivers significant outcomes in terms of SNR, MSE, and PRD as compared to conventional estimator. The SNR and PRD values obtained using different distribution functions employing the proposed methodology are shown in Fig 5.2. Comparative analysis of SNR for conventional and proposed estimator using different distribution depicts that the proposed estimator using Normal distribution offers 58.23 dB relative to 54.98dB with Gaussian distribution function and 53.12 dB with Exponential distribution function. The value of PRD is 0.001 as compared to 0.003 and 0.004 from the Gaussian as well as Exponential Distribution function.

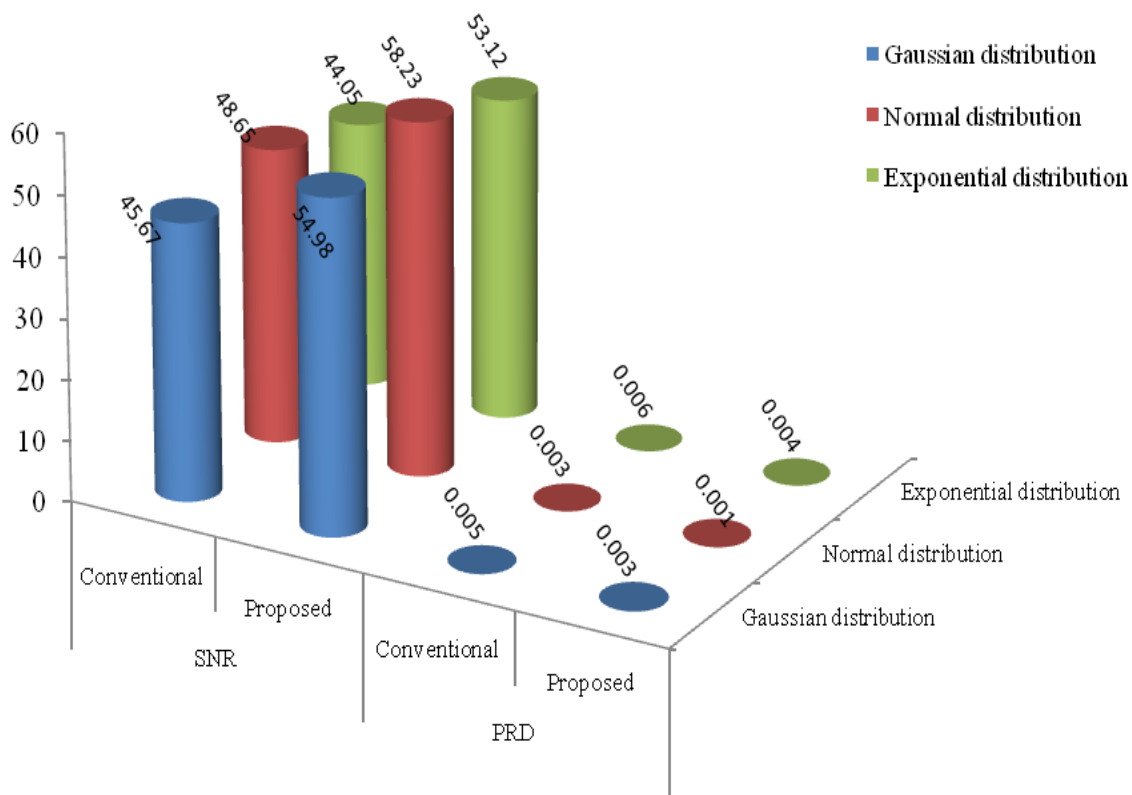


**Figure 5.2** Performance analysis for different distribution function using conventional and proposed estimator

From Figure 5.2 it is demonstrated that the proposed estimator employing Normal distribution outperforms when compared to the Gaussian and exponential distribution in terms of SNR, MSE and PRD. Several issues in engineering domain are focussed on the Gaussian distribution function

of the data is well justified. Nominal, however, is useless if the estimators were derived under distributional assumptions in the noise. The proposed estimator has a high breakdown point, which under normal assumption is 50% more effective.

To *validate* the proposed methodology, the performance parameters are computed for proposed estimator with  $n = 1$  using Normal and Gaussian distribution for all 96 records of “MIT/BIH Arrhythmia database” as tabulated in Table 5.9.

**Table.5.9.** Performance Evaluation for MIT-BIH Arrhythmia Database for Normal and Gaussian distribution functions with proposed estimator

Record	Lead	Normal Distribution			Gaussian Distribution		
		SNR	MSE	PRD	SNR	MSE	PRD
100	MLII	58.56	1.78E-07	0.001	55.25	3.83E-07	0.003
100	V5	58.23	9.63E-08	0.001	54.98	2.04E-07	0.003
101	MLII	61.33	3.21E-07	8.58E-04	58.22	1.89E-07	0.001
101	V1	52.60	1.68E-07	0.002	49.09	3.77E-07	0.004
102	V5	59.34	1.02E-07	0.001	55.43	2.00E-07	0.003
102	V2	62.90	7.00E-08	7.16E-04	61.12	1.06E-08	8.79E-04
103	MLII	65.69	8.39E-08	9.23E-04	58.73	4.18E-07	0.001
103	V2	55.70	1.50E-07	0.001	53.03	2.77E-07	0.003
104	V5	56.80	2.48E-07	0.001	53.84	4.91E-07	0.002
104	V2	65.92	7.84E-08	1.03E-05	62.09	9.46E-08	7.16E-04
105	MLII	54.97	4.89E-07	0.001	52.64	8.35E-07	0.002
105	V1	70.02	9.95E-08	0.001	69.77	2.12E-07	0.002
106	MLII	54.27	5.14E-07	0.001	52.23	1.05E-06	0.002
106	V1	44.35	3.70E-07	0.006	40.83	8.32E-07	0.009
107	MLII	57.07	1.39E-06	0.001	54.62	2.45E-06	0.003
107	V1	57.11	8.18E-07	0.001	55.92	1.27E-06	0.003

108	MLII	59.61	1.26E-07	1.00E-03	56.23	2.74E-07	0.002
108	V1	62.85	1.33E-07	7.20E-04	59.70	2.74E-07	0.001
109	MLII	53.05	2.11E-06	0.002	50.71	3.62E-06	0.003
109	V1	56.30	5.87E-07	0.001	53.89	1.12E-06	0.002
111	MLII	55.06	1.80E-07	0.001	52.62	3.15E-07	0.002
111	V1	53.40	3.21E-07	0.002	50.41	6.39E-07	0.003
112	MLII	66.59	1.85E-07	4.68E-04	63.02	4.20E-07	7.07E-04
112	V1	63.97	1.81E-07	6.33E-04	60.69	3.85E-07	9.24E-04
113	MLII	57.38	3.55E-07	0.001	54.87	6.33E-07	0.002
113	V1	66.43	3.66E-08	4.77E-04	63.06	7.95E-08	7.03E-04
114	V5	59.11	6.82E-08	1.10E-03	55.70	1.49E-07	0.001
114	MLII	59.45	6.69E-08	1.10E-03	56.06	1.46E-07	0.001
115	MLII	63.55	1.47E-07	6.64E-04	60.13	3.24E-07	9.85E-04
115	V1	60.78	7.88E-08	9.15E-04	57.05	1.86E-07	0.001
116	MLII	58.02	2.04E-06	1.30E-03	55.40	3.74E-06	0.001
116	V1	59.39	5.05E-07	1.10E-03	55.90	1.13E-06	0.001
117	MLII	65.10	2.31E-07	5.56E-04	61.78	4.95E-07	8.14E-04
117	V2	61.14	2.37E-07	8.77E-04	57.90	5.01E-07	0.001
118	MLII	57.30	2.13E-06	1.40E-03	53.95	4.61E-06	0.002
118	V1	54.86	1.48E-06	1.80E-03	51.91	2.91E-06	2.54E-03
119	MLII	62.85	5.02E-07	7.20E-04	59.99	9.70E-07	1.00E-03
119	V1	61.07	2.16E-07	8.84E-04	57.51	4.92E-07	1.30E-03
121	MLII	68.10	1.01E-07	3.94E-04	64.77	2.16E-07	5.77E-04
121	V1	65.79	1.30E-07	5.13E-04	62.03	3.09E-07	7.91E-04
122	MLII	62.51	4.27E-07	7.49E-04	59.44	8.66E-07	1.10E-03
122	V1	59.30	5.05E-07	1.10E-03	55.97	1.09E-06	1.60E-03
123	MLII	65.12	2.75E-07	5.55E-04	62.20	5.38E-06	7.76E-03

123	V5	60.23	1.71E-07	9.73E-04	56.76	3.82E-06	1.45E-03
124	MLII	70.14	7.37E-09	3.11E-04	66.60	1.66E-07	4.68E-03
124	V4	67.63	8.19E-08	4.15E-04	64.01	1.88E-07	6.30E-04
200	MLII	55.47	5.03E-07	1.70E-03	52.29	1.04E-06	2.40E-03
200	V1	54.03	5.07E-08	2.00E-03	50.60	1.12E-07	3.00E-03
201	MLII	53.03	3.24E-07	2.20E-03	49.75	6.88E-07	3.30E-03
201	V1	50.71	5.51E-07	2.90E-03	47.39	1.18E-06	4.30E-03
202	MLII	58.73	5.66E-08	1.20E-03	55.47	1.20E-07	1.70E-03
202	V1	54.49	9.47E-08	1.90E-03	50.86	2.18E-07	2.86E-03
203	MLII	46.41	5.66E-06	4.80E-03	43.09	1.21E-05	7.00E-03
203	V1	41.01	2.94E-06	8.90E-03	37.56	6.53E-06	1.32E-02
205	MLII	59.93	1.96E-07	1.00E-03	56.45	4.36E-07	1.50E-03
205	V1	65.18	7.90E-08	5.51E-04	61.80	1.72E-07	8.13E-04
207	MLII	63.10	6.68E-08	6.99E-04	59.48	1.54E-07	1.10E-03
207	V1	63.96	7.25E-08	6.34E-04	60.33	1.67E-07	9.63E-04
208	MLII	54.20	1.09E-06	2.00E-03	51.82	1.88E-06	2.60E-03
208	V1	53.16	6.19E-07	2.20E-03	51.40	9.30E-07	2.70E-03
209	MLII	53.81	3.53E-07	2.00E-03	50.34	7.86E-07	3.00E-03
209	V1	39.79	7.21E-07	0.010	36.77	1.45E-06	0.014
210	MLII	58.58	1.09E-07	0.001	55.49	2.22E-07	1.70E-03
210	V1	46.94	3.09E-07	0.004	43.50	6.83E-07	6.70E-03
212	MLII	50.03	1.08E-06	0.003	47.36	2.00E-06	4.30E-03
212	V1	52.21	1.10E-06	0.002	49.91	1.87E-06	3.20E-03
213	MLII	49.68	5.35E-06	0.003	47.32	9.20E-06	4.30E-03
213	V1	52.55	4.32E-06	0.002	50.08	7.64E-06	0.003
214	MLII	58.88	2.57E-07	0.001	56.28	4.68E-07	0.002
214	V1	55.63	5.63E-07	0.001	53.13	9.99E-07	0.002



215	MLII	50.93	5.54E-07	0.002	47.40	1.25E-06	0.004
215	V1	58.50	1.69E-07	0.001	55.11	3.69E-07	0.002
217	MLII	57.46	5.81E-07	0.001	54.26	1.22E-06	0.002
217	V1	59.04	2.44E-07	0.001	55.95	4.97E-07	0.002
219	MLII	59.62	5.91E-07	0.001	56.41	1.24E-06	0.002
219	V1	61.76	3.08E-07	8.17E-04	58.51	6.51E-07	1.20E-03
220	MLII	62.53	2.69E-07	7.48E-04	59.81	5.04E-07	1.00E-03
220	V1	61.59	1.11E-07	8.33E-04	58.01	2.53E-07	1.30E-03
221	MLII	57.52	2.27E-07	1.30E-03	54.42	4.63E-07	1.90E-03
221	V1	55.95	1.76E-07	1.60E-03	52.53	3.88E-07	2.40E-03
222	MLII	53.30	1.32E-07	2.20E-03	50.08	2.77E-07	3.10E-03
222	V1	65.05	4.21E-08	5.59E-04	61.62	9.28E-08	8.30E-04
223	MLII	64.86	1.48E-07	5.71E-04	61.23	3.41E-07	8.68E-04
223	V1	61.89	1.23E-07	8.04E-04	58.88	2.47E-07	1.14E-03
228	MLII	51.10	6.73E-07	2.80E-03	47.93	1.40E-06	4.00E-03
228	V1	55.76	7.08E-07	1.60E-03	52.36	1.55E-06	2.40E-03
230	MLII	57.73	3.39E-07	1.30E-03	54.43	7.26E-07	1.90E-03
230	V1	53.89	4.28E-07	2.00E-03	51.04	8.24E-07	2.80E-03
231	MLII	55.64	2.91E-07	1.70E-03	52.59	5.88E-07	2.35E-03
231	V1	57.99	7.30E-08	1.30E-03	54.47	1.64E-07	1.89E-03
232	MLII	46.86	8.33E-07	4.50E-03	43.44	1.83E-06	6.73E-03
232	V1	52.83	2.24E-07	2.30E-03	49.47	4.86E-07	3.36E-03
233	MLII	57.69	6.42E-07	1.30E-03	55.23	1.13E-06	1.73E-03
233	V1	54.32	7.05E-07	1.90E-03	51.71	1.28E-06	2.60E-03
234	MLII	53.37	3.50E-07	2.10E-03	49.99	7.62E-07	3.17E-03
234	V1	49.48	2.22E-07	3.40E-03	46.05	4.90E-07	5.00E-03

---

Table 5.9 depicts that average value of SNR obtained using proposed methodology for Normal distribution is (57.69 dB) and (54.58 dB) for Gaussian distribution. This signifies that proposed technique using normal distribution outperforms to achieve ECG denoising in comparison with Gaussian distribution. For further computations, normal distribution function is considered as it improves the performance of proposed technique.

### 5.3.2. Proposed results by introducing Downscaling Factor ( $2^n$ )

An efficient approach for ECG signal denoising using a proposed robust noise estimator empowered with  $2^n$  downscaling factor for optimal thresholding is executed. The proposal is for eliminating the high frequency noises and concurrently preserving the signal complexes with a robust noise estimator that is scaled by  $2^n$  factor. In order to determine its substantial impact on signal quality, the proposed estimator is assessed for distinct values of  $n = 1, 2, 3$  and  $4$ .

**Table 5.10.** Proposed noise estimator downscaled by  $2^n$  using normal distribution

S.No.	$2^n$ Factor	SNR	MSE	PRD	PSNR
1.	$2^1$	58.23	9.64e-08	0.001	70.160
2.	$2^2$	68.75	8.566e-09	3.65e-04	80.68
3.	$2^3$	<b>80.72</b>	<b>5.45e-10</b>	<b>9.21e-05</b>	<b>92.63</b>
4.	$2^4$	92.75	3.41e-11	2.30 e-05	104.68

Table 5.10 showed that there is considerable enhancement in the signal quality by increasing the value of  $n$  from 1 to 3 but for the value  $n = 4$ , the PSNR value is exceeding the normal range (1 to 100 dB) resulted into the disappearance of signal originality.

Fig.5.3 shows the proposed robust noise estimator for distinct value of  $n$  using Normal distribution function.

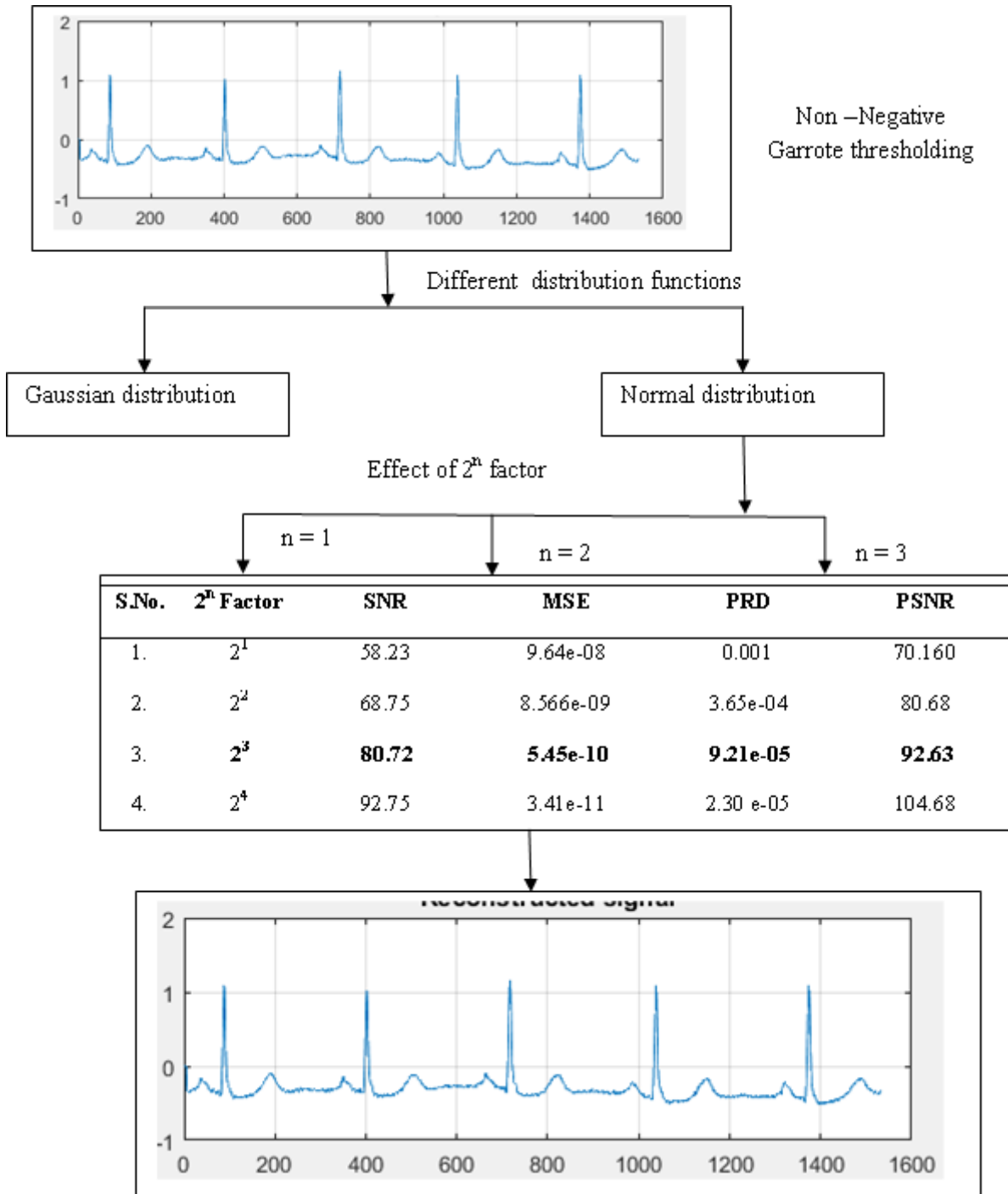


**Figure 5.3** Proposed robust noise estimator for distinct value of  $n$

It is depicted from Fig.5.3 that the proposed robust noise estimator with  $2^3$  factor using Normal distribution function demonstrates 80.720dB SNR,  $5.45e-10$  MSE,  $9.21e-05$  PRD and 92.63dB PSNR on comparison to the proposed estimator with  $2^1$  factor that offers 58.23dB SNR,  $9.64e-08$  MSE, 0.001 PRD and 70.16 dB PSNR . This performance evaluation determines the considerable noise reduction and improving the signal quality by delivering 38.63 % SNR improvement. The performance metrics PSNR is evaluated for 100-107 records employing distinct distribution functions to validate the proposed robust noise estimator with  $2^3$  scaling factor as tabulated in Table 5.11.

**Table 5.11.** PSNR Evaluation of Proposed Estimator using  $2^3$  factors for 100-107 record

PSNR (dB)	100	101	102	103	104	105	106	107
<b>Gaussian Distribution</b>	88.81	86.54	87.42	86.57	85.37	89.47	82.78	74.61
<b>Normal Distribution</b>	92.63	89.04	91.23	90.35	89.11	93.24	85.34	77.70

Table 5.11 states a substantial improvement in the ECG signal quality using Normal distribution attaining the average value of PSNR (88.58 dB) as opposed to the typical PSNR value (85.19 dB) attained from Gaussian distribution for 100-107 records.

**Comparative Analysis of Proposed Noise Estimator by varying Downscaling Factor ( $2^n$ )**

Table 5.12 contrasts the computational assessment of the proposed estimator with  $2^n$  scaling factor for both distribution functions with other state-of-the-art -approaches.

**Table 5.12.** Comparison with State-of-the- art- Techniques

S.No.	Authors	Techniques	SNR (dB)	MSE	PRD
1.	Zubair AR <i>et al.</i> ,2018) [101]	DWT + Garrote	41.79		
2.	TYadav and R Mehra.2016 [154]	Daubechies (DB) technique based on wavelet filtering	52.07	-	-
3.	K.Salih <i>et al.</i> ,2015 [155]	Adaptive filtering using Moving average filter.	-	4.9e-04	-
4.	Priyaa KD <i>et al.</i> ,2016 [156]	Wavelet wiener filter	-	0.1440	-
5.	Charri <i>et al.</i> ,2017 [142]	DT-WT	45.83	-	-
6.	<b>Proposed Technique</b>	<b>DTCWT with <math>2^3</math> factor (Gaussian Distribution)</b>	76.890	1.313e-09	1.43e-04
7.	<b>Proposed Technique</b>	<b>DTCTW with <math>2^3</math> factor (Normal Distribution)</b>	<b>80.720</b>	<b>5.44e-10</b>	<b>9.21e-05</b>

Analysis of Table 5.12 depicted that the proposed method delivers high SNR, small PRD and low MSE as compared to state-of-art work by removing the distinct noises from the ECG signal and enhancing the signal quality by high PSNR value. The proposed estimator employing  $2^3$  downscaling factor and taking  $z$  value for Normal distribution function delivers finer outcomes which signify the signal enhancement that claims it superiority to perform denosing in regard to other existing technique.

An Optimal Threshold System Design is framed that precisely identifies the heart related problems.

## 5.4 OPTIMAL THRESHOLD SYSTEM DESIGN

An Optimal Threshold System Design is framed that include an efficient DTCWT technique for removal of artifacts followed by design of robust noise removal system using optimal threshold tuning by varying the threshold value ( $\delta$ ) and its function ( $f_n$ ) at each level of decomposition followed by probability distribution modelling for Electrocardiogram System Design to enhance the quality of reconstructed signal followed by detection of different peaks and their intervals for successive computation of Heart Rate as illustrated in Fig.5.4.

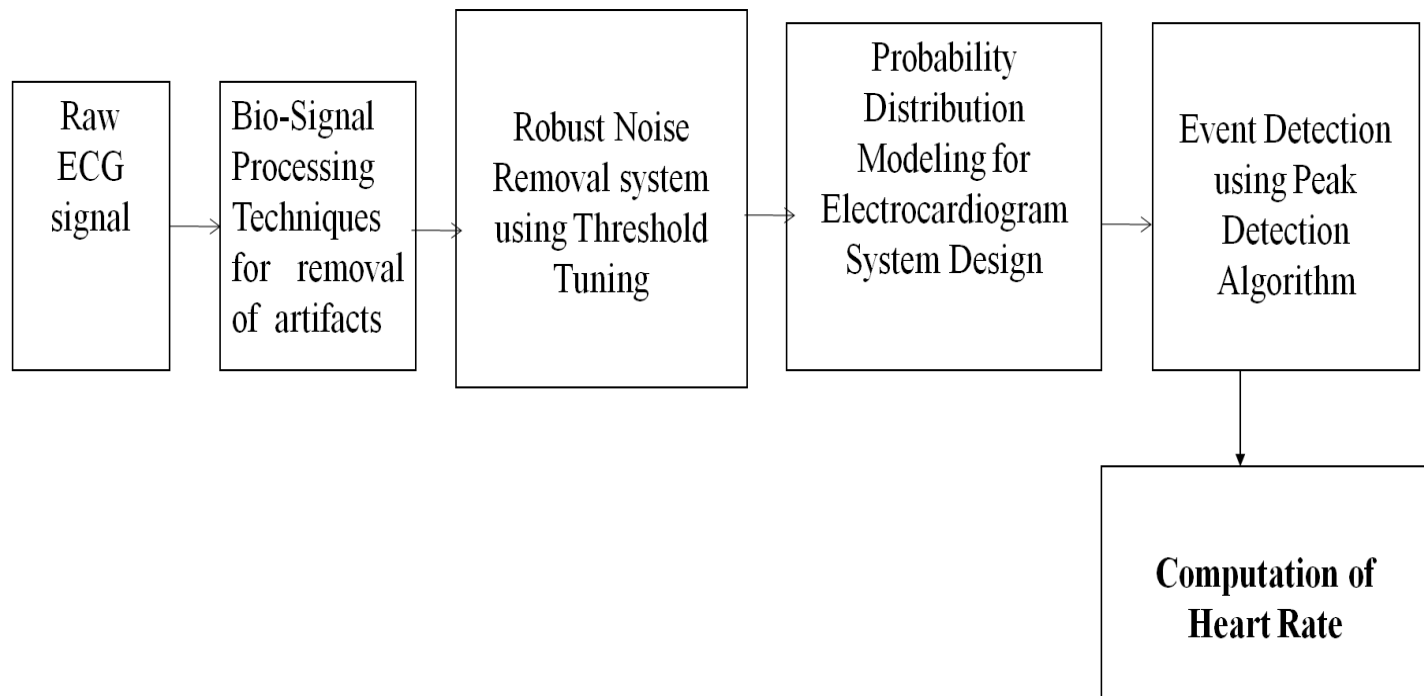


**Figure 5.4** Optimal Threshold System Design

Different peaks and their intervals are detected for different records of ECG signal employing Optimal Threshold System are tabulated in Table 5.13

**Table 5.13.** Event Detection employing Optimal Threshold System

<b>Database</b>	<b>R wave</b>	<b>P wave</b>	<b>Q wave</b>	<b>S wave</b>	<b>T wave</b>	<b>RR interval</b>	<b>PR interval</b>	<b>QRS interval</b>	<b>ST interval</b>
<b>MLII 100</b>	0.8782	-0.2146	-0.5532	-0.4858	-0.2898	0.7988	0.1689	0.0449	0.2898
<b>MLII101</b>	1.0856	-0.1356	-0.4159	-0.4481	-0.1291	0.8931	0.1617	0.0894	0.2289
<b>V5102</b>	0.8659	-0.1765	-0.3013	-0.0259	-0.0952	0.8257	0.3256	0.1672	0.2694
<b>MLII103</b>	1.7937	-0.2401	-0.5953	-0.5442	0.03644	0.8458	0.1650	0.0510	0.2461
<b>V5104</b>	0.9677	-0.1335	-0.2808	-0.3000	-0.0309	0.8111	0.2727	0.1532	0.2778
<b>MLII105</b>	1.1798	-0.1105	-0.3843	-0.4974	-0.2039	0.7117	0.1505	0.1532	0.1921
<b>MLII106</b>	2.0040	0.0496	-0.4593	-0.6701	0.4890	1.0157	0.1139	0.1597	0.2222
<b>MLII107</b>	0.8659	-0.1765	-0.3013	-0.0259	0.0952	0.8257	0.3256	0.1672	0.2694
<b>MLII108</b>	0.0412	-0.1645	-0.2461	-0.1012	-0.0954	0.9849	0.3875	0.1835	0.3278
<b>MLII109</b>	0.4057	-0.3110	-0.6543	-0.8502	-0.2376	0.7844	0.2514	0.1375	0.2708

Table 5.13 represents the values of distinct peaks and their intervals for different record of ECG signal employing Optimal Threshold System.

Later Heart rate is computed for distinct records of “MIT-BIH Arrhythmia database” using Eq. (3.15) as shown in Table 5.14.

**Table 5.14.** Computation of Heart Beat Rate

<b>Record</b>	<b>Age and Sex</b>	<b>Heart Rate computation (Robust Optimal Thresholding System Design)</b>	<b>Heart Rate mentioned in MIT-BIH Arrhythmia Database (Gold Standard)  Normal sinus rhythm</b>
MLLII 100	69 & Male	75	70-89
MLII101	75 & Female	67	55-79
V5102	64 & Female	72	72-78
MLII103	Age not recorded & Male	71	62-92
V5104	66 & Female	74	69-82
MLII105	73 & Female	84	78-102
MLII106	24 & Female	59	49-87
MLII107	63 & Male	73	68-82
MLII108	67 & Female	64	44-78
MLII109	64 & Male	83	77-101

Table 5.14 determines the heart rate value for distinct records and are validated by realizing the outcomes with defined range of “MIT-BIH Arrhythmia database” (gold standard) that signifies the resultant value lies within the defined range which predicts its accuracy to examine the different signals more precisely.

## **5.5 SUMMARY**

In this chapter different probability distribution modelling is performed and signals are analysed by implementing robust noise estimator with  $2^n$  downscaling factor. Proposed noise estimator



with  $2^n$  downscaling factor employing normal distribution modeling yields (80.72) dB SNR, (92.63) dB PSNR,  $(5.45e-10)$  MSE and  $(9.21e-05)$  PRD that signifies the significant noise reduction by enhancing signal quality subsequently. An Optimal Threshold System is designed for computation of accurate Heart rate to examine the different ECG signals more precisely.

## **CHAPTER 6**

# **CONCLUSION AND FUTURE SCOPE**

# **CHAPTER 6**

## **CONCLUSION AND FUTURE SCOPE**

### **6.1 CONCLUSION**

The main aim of this dissertation is to develop an Optimal Threshold System Design for accurate computation of Heart rate to diagnose cardiac arrhythmias. The electrocardiogram signal which is non-stationary in nature and provide crucial information for the diagnosis of heart abnormalities. The ECG acquisition and transmission are complex processes that are abruptly influenced by different noise and artifacts. The ECG treatment methods are analyzed especially noise reduction techniques for precise extraction of important information from the signal are discussed in Chapter 1.

An exhaustive review of the literature on removal of artifacts, event detection and noise estimation methods on ECG is conducted. The second chapter addresses the conceptual and fundamental aspects of ECG configuration in the literature review. The effective outcomes are demonstrated by various noise reduction techniques using filter and adaptive filtering. The literature also suggests the thresholding strategies employing noise estimator for noise elimination is the efficient approach using wavelet transform. The literature also emphasizes on the event detection process especially QRS detection is undertaken by numerous researchers in their research. Comprehensive analysis of machine learning approaches with various event detection of ECG has been conducted.

The Proposed models in third chapter describe the implementation of various Bio-signal processing methods for the eradication of artifacts and noise contents from the raw input ECG signal. A Cascade Digital filter is proposed employing best performance filters of Frequency domain and Optimal filtering yielding 7.75 dB SNR improvement on comparison with state of art methods but offers some limitations such as large memory requirement and computational

complexity. To tackle this problem different time-frequency domain filtering techniques such as MTD and DTCWT are exploited that reduces the computational complexity with less memory requirement. The performance evaluation of different filtering techniques determines that DTCWT strategy is most effective that delivers high SNR (27.75 dB), low MSE (1.0777e-04) and small PRD (0.041) among specified techniques (Cascade filtering, Mallet tree decomposition) and other state of art techniques to achieve the denoising goal for non-stationary ECG signal. Once the artifacts are eliminated, detection of principal peaks and their intervals are carried out using Peak Detection Algorithm (PDA) to extract the crucial information for accurate analysis of ECG interpretation. The outcome shows that DTCWT perceive its efficiency for computation of  $R-R$  interval as collate to MIT-BIH Arrhythmia Database (Gold standard).

The fourth chapter deals with the estimation of noise and enhancement of signal quality. A robust noise estimation approach is proposed using optimal threshold tuning. An empirical analysis of conventional and proposed noise estimator for Gaussian distribution function is performed by exhausting all combinations of threshold value selection and threshold functions. An optimal threshold tuning is achieved by Non-negative Garrotte threshold function with universal modified threshold level-dependent threshold value selection. Implementing the proposed noise estimator with optimal threshold tuning depicts the significant improvement in SNR by 20.38% as compared to conventional estimator. The proposed noise estimation approach depicts high SNR (54.98 dB) and low MSE (2.03e-07) and small PRD (0.003). Later, Pearson correlation coefficient for conventional and proposed estimator is computed with 0.947 value is achieved that depicts the linear relationship between both estimators.

In fifth chapter the proposed noise estimator is empowered with  $2^n$  downscaling factor utilizing (Gaussian, Exponential and Normal) distribution functions to handle the tradeoff between signal distortion and residual noise. Different values of  $n$  (1, 2, 3 and 4) are analyzed to perceive its impact on the reconstructed signal quality. The computational results show that proposed noise estimator equipped by  $2^3$  downscaling factor employing normal distribution that yields a high SNR (80.72 dB), sharp PSNR (92.63dB), low MSE (5.45e-10) and small PRD (9.21e-05) which signifies the considerable reduction of noise by subsequently improving the signal quality.

Finally, An Optimal Threshold System is designed for computation of accurate Heart rate for distinct ECG signals for precise detection and diagnosis of Cardiac Arrhythmia that assists cardiologists for better prognosis of patients.

## **6.2 FUTURE SCOPE**

From time to time, researchers face new challenges to come up with more efficient and sophisticated methods and algorithms in place of existing methods. Although we have proposed cascade digital filter and new noise estimator for estimation of heart rate in this research work, but one can take into account the following potential future contributions for further advancements:

- i. The Optimal Thresholding System Design is further utilized for detection of different Heart related diseases by deep analysis of ECG signal.
- ii. Machine learning techniques can also be explored out for fusion of multimodal physiological signals.
- iii. FPGA and ASIC based Hardware implementation for wearable and portable ECG module can be developed for real time continuous monitoring.

# **LIST OF PUBLICATIONS**

## LIST OF PUBLICATIONS

### Journals:

1. Navdeep Prashar, Meenakshi Sood, Shruti Jain, "Dual-Tree Complex Wavelet Transform Technique based Optimal Threshold Tuning System to Deliver Denoised ECG Signal", *Transactions of the Institute of Measurement and Control*, vol.42, no.4, pp 854-869, 2020  
**(SCI) [I F-1.956]**
2. Navdeep Prashar, Meenakshi Sood, Shruti Jain, "Design and Implementation of a Robust Noise Removal System in ECG signals using Dual- Tree Complex Wavelet Transform," *Journal of Biomedical Signal Processing and Control*, vol.63, pp 1-12, 2020.  
**(SCI) [I F-3.13]**
3. Navdeep Prashar, Meenakshi Sood, Shruti Jain, "A Novel Cardiac Arrhythmia Processing using Machine Learning Techniques," *International Journal of Image and Graphics*, vol.20, no.3, pp.1-17, 2020  
**(ESCI / Scopus Indexed)**
4. Navdeep Prashar , Meenakshi Sood , Shruti Jain, "Design and Performance Analysis of Cascade Digital Filter for ECG Signal Processing," *International Journal of Innovative Technology and Exploring Engineering*, vol.8, no.8, pp.2659-2665, 2019. **(Scopus Indexed)**
5. Navdeep Prashar, Meenakshi Sood, Shruti Jain, "Semiautomatic Detection of Cardiac Diseases employing Dual Tree Complex Wavelet Transform", *Periodicals of Engineering and Natural Sciences*, vol.6, no., 2, pp.129-140, 2018. **(Scopus Indexed)**
6. Navdeep Prashar, Jyotsna Dogra, Meenakshi Sood, Shruti Jain, "Removal of electromyography noise from ECG for high performance biomedical systems," *Network Biology*, vol.8, no.1, pp.12-24, 2018. **(Clarivate\Web of Science)**

## Conferences:

1. Navdeep Prashar, Meenakshi Sood, Shruti Jain, "Morphology Analysis and Time Interval Measurements using Mallat Tree Decomposition for CVD Detection," In Proc.2nd International Conference on Advanced Informatics for Computing Research,2018. **(Scopus)**
2. Navdeep Prashar, Shruti Jain, Meenakshi Sood, Jyotsna Dogra, "Review of Biomedical System for High Performance Applications," In Proc. 4<sup>th</sup> IEEE International Conference on signal processing and control, 2017, pp.300-304. **(Scopus)**



# REFERENCES

## REFERENCES

- [1] W. H. Organization, “Global status report on non-communicable diseases 2014,” 2014.
- [2] S. L. Joshi, R. A. Vatti, R. V. Tornekar, “A survey on ecg signal denoising techniques,” In Proc.IEEE International conference on Communication Systems and Network Technologies (CSNT), 2013, pp.60–64.
- [3] W. Zhang, X. Wang , L.Ge , Z. Zhang Z, “Detection of ECG Signal Based on Multiresolution Sub-band Filter”, In Proc. IEEE Engineering in Medicine and Biology 27th Annual Conference, 2006,pp.2714-2717.
- [4] A. J. Moss, S. Stern, *Noninvasive electrocardiology: clinical aspects of Holter monitoring*. Philadelphia: W.B. Saunders, 1996.
- [5] Wikipedia:electrocardiography.[Online].Available:<http://en.wikipedia.org/wiki/Electrocardiography> [Accessed: November 12, 2019].
- [6] R. U. Acharya, J. S. Suri, J. A. E. Spaan, and S. M. Krishnan, *Advances in Cardiac Signal Processing*. Germany: Springer, 2007.
- [7] M. G. Khan, *Rapid ECG Interpretation*. London: Saunders, 2003
- [8] L.Cromwell, F. J. Weibell, E. A. Pfeiffer, *Biomedical Instrumentation and Measurements*. New Delhi: PHI Learning Private Limited, 2009
- [9] Diagram of the human heart. Available:<https://en.wikipedia.org/wiki/Heart#/media/File> [Accessed: March 22, 2020].
- [10] M. K. Das, S. Ari, “Analysis of ECG signal denoising method based on S- transform,” *Innovation and Research in Biomedical Engineering (IRBM)*, vol. 34, no. 6, pp. 362-370, 2013.
- [11] M.A. Hasan , M.D. Mamun, “Hardware approach of R-peak detection for the measurement offetal and maternal heart rates,”*Journal of Applied Research and Technology*, vol.10, no.6,pp.835-844, 2012.
- [12] B. Surawicz , R. Childers, B. J. Deal, and L.S Gettes, “AHA/ACCF/HRS Recommendations for the Standardization and Interpretation of the Electrocardiogram,”*Journal of the American College of Cardiology*, vol. 53, pp. 976-981,2009.

- [13] M.G.Tsipouras, D.I. Fotiadis and D. Sideris, “Arrhythmia classification using the R-R-interval duration signal”, In Proc. IEEE Computers in Cardiology,2002,pp. 485-488.
- [14] R.M.Rangayyan, *Biomedical Signal Analysis: A Case-study Approach*. New York: Wiley-Interscience,2001.
- [15] R. S. Khandpur, *Handbook of Biomedical Instrumentation*. New Delhi: Tata McGraw Hill, 2010.
- [16] A. Ibaida ,I.Khaili, D.AI-Shammary DA., “Embedding Patients Confidential Data in ECG Signal for Health Care Information System”, In Proc. 32nd Annual International Conference of the IEEE Engineering in Medicine and Biology, 2010,pp. 3891-3894.
- [17] Price, Dallas., "How to read an electrocardiogram (ECG). Part 1: Basic principles of the ECG. The normal ECG," *South Sudan Medical Journal*, vol.3, no.2, pp.26-31, 2010.
- [18] N.V. Thakor, “Electrocardiographic monitors,” in *Encyclopedia of Medical Devices and Instrumentation*, Webster J. G., Ed., New York: Wiley, 1988,pp. 1002–1017.
- [19] E.F. Carpio, J.F.Gomez , R. Sebastian, A. Lopez-Perez , E.Castellanos , J. Almendral , J.M. Ferrero and B. Trenor , “Optimization of Lead Placement in the Right Ventricle During Cardiac Resynchronization Therapy,” *Frontiers in Physiology*, vol.10, 2019.
- [20] F. Gritzali, G. Frangakis, G. Papakonstantinou, “Noise estimation in ecg signals,” in Proc.of the Annual International Conference of the IEEE Engineering in Medicine and Biology Society,1988 ,pp. 152– 153.
- [21] E.Castillo, E., D.P. Morales, A. García, F.Martínez-Martí, L. Parrilla, and A.J. Palma, “Noise suppression in ECG signals through efficient one-step wavelet processing techniques,”*Journal of Applied Mathematics*, 2013.
- [22] R.W. Flegal, K. Furie, A Go, K Greenlund, N Haase, S.M. Hailpern,“Heart disease and stroke statistics-2008” update: a report from the American Heart Association Statistics Committee and Stroke Statistics Subcommittee, *Circulation*.117:e25–146,2008.
- [23]C.M. Albert, W. G. Stevenson, “The Future of Cardiovascular Biomedicine: Arrhythmias and Electrophysiology”, *Circulation*, vol.133, no 25, pp.2687-2696,2016.
- [24] Brian Olshansky MD, *Arrhythmias in Integrative Medicine*, 4<sup>th</sup> ed., Philadelphia, PA: Elsevier 2018.
- [25]L. J. Gessman, R. Trohman, *Cardiac Arrhythmias in Critical Care Medicine*, 3<sup>rd</sup> ed., Philadelphia, PA: Elsevier 2008.

- [26] J. Pan, W. J. Tompkins, "A real time QRS detection algorithm," *IEEE Trans. Biomed. Eng.*, vol. 32, pp. 230-236, 1985.
- [27] Andrew A Grace, Dan M Roden, "Systems biology and cardiac arrhythmias," *Lancet(London, England)* , vol.380,no. 9852,pp 1498-508,2013
- [28]PhysioBankAtm.Available:<https://www.physionet.org/physiobank/database/html/mitdbdir/records.htm> [Accessed: December 28, 2019].
- [29] Elgendi, Mohamed, Björn Eskofier, Socrates Dokos, and Derek Abbott. "Revisiting QRS detection methodologies for portable, wearable, battery-operated, and wireless ECG systems," *PloS one*,vol.9, no. 1,2014.
- [30] M.P.Chawla, H.K. Verma, Vinod Kumar, "Artifacts and noise removal in electrocardiograms using independent component analysis," *International Journal of Cardiology*, pp 278-281,2008.
- [31] Sundarrajan Rangachari, Philipos C. Loizou , "A noise-estimation algorithm for highly non-stationary environments,"*Speech Communication*, vol.48 ,no.2 ,pp 220–231,2006.
- [32] R. Gupta, S.Singh, K.Garg, S.Jain, "Indigenous Design of Electronic Circuit for Electrocardiograph," *International Journal of Innovative Research in Science, Engineering and Technology*, vol.3, no.5, pp-12138-12145, 2014.
- [33] A. Dhiman, A. Singh, S. Dubey, S.Jain, "Design of Lead II ECG Waveform and Classification Performance for Morphological features using Different Classifiers on Lead II,"*Research Journal of Pharmaceutical, Biological and Chemical Sciences (RJPBCS)*, vol7,no.4, pp-1226- 1231,2016.
- [34] S. Palanivel, R. Sukanesh ,"Experimental studies on intelligent, wearable and automated wireless mobile tele-alert system for continuous cardiac surveillance,"*Journal of Applied Research and Technology*, vol.11,no.1,pp133-143, 2013.
- [35] N.V. Thakor and Yi-Sheng Zhu, "Application of Adaptive Filtering to ECG Analysis: Noise Cancellation and Arrhythmia Detection," *IEEE Transaction on Biomedical Engineering*, vol.38, no.8,pp- 783-794,1991.
- [36] R. Jane R., N.V.Thakor, P. Laguna, and P. Caminal, "Adaptive Baseline Wander Removal in the ECG: Comparative Analysis with Cubic Spline Technique,"In Proc. IEEE Computers in Cardiology, 1992, pp.143-146.
- [37] S Pei , C. Tseng , " Adaptive IIR notch filter based on least mean p-power error criterion,"*IEEE Trans Circuit and Systems II : Analog Digit Signal Processing* ,vol.40,no.8,525-8, 1993.

- [38] S. Pei, CC. Tseng , "Elimination of AC interference in electrocardiogram using IIR notch filter with transient suppression," *IEEE Trans Biomed Eng.* , vol. 42,no.11,pp.1128-32,1995.
- [39]A.Sander, A. Voss , G. Griessbach , "An Optimized Filter System For Eliminating 50 Hz Interference from High Resolution ECG," *Biomedizinische Technik. Biomedical Engineering*,vol.40,no.4,pp.82-87,1995.
- [40] D.L. Donoho, "De-noising by soft thresholding ," *IEEE Transaction on Information Theory*, vol. 41,no.3,pp. 613-627,1995.
- [41] PS.Hamilton , "A comparison of adaptive and nonadaptive filters for reduction of power line interference in the ECG,"*IEEE Trans Biomed Eng.*,vol 43,no.3,pp.105-109,1996.
- [42] N.E.Huang , Z. Shen , S.R.Long, M.C.Wu, H.H.Shih , Q.Zheng, C.Tung,H. Liu,"The empirical mode decomposition and hilbert spectrum for nonlinear and nonstationary time series analysis," *Proceedings of the Royal Society of London. Series A: mathematical, physical and engineering sciences*, vol.454, no.1971, pp.903-995, 1998.
- [43] S.Olmos , P. Laguna," Steady-state MSE convergence of LMS adaptive filters with deterministic reference inputs with applications to biomedical signals," *IEEE Trans Signal Processing*,vol.48,no.82,pp.2229-41,2000.
- [44] S.S.Dhillon , S. Chakrabarti,"Power line interference removal from electrocardiogram using a simplified lattice based adaptive IIR notch filter,"*In Proc. 23rd Annual International Conference of the IEEE Engineering in Medicine and Biology Society*, 2001,vol.4,pp. 3407-3412.
- [45] A. K. Ziarani , Adalbert Konrad, "A Nonlinear Adaptive Method of Elimination of Power Line Interference in ECG Signals," *IEEE Transactions on Biomedical Engineering*, vol. 49,no.6,pp. 540-547,2002.
- [46] Y.V.R. Rao, N. Venkateswaran. "Allpass lattice structure based second order digital IIR notch filter for removing DC and very low frequencies," *In Proc. TENCON 2003 IEEE Conference on Convergent Technologies for Asia-Pacific Region*, 2003, vol. 4, pp. 1384-1385.
- [47] Y-W. Bai, W-Y. Chu, C-Y.Chen, Y-T. Lee, Y-C. Tsai, and C-H.Tsai , "Adjustable 60Hz noise reduction by a notch filter for ECG signals," *In Proc. 21st IEEE Instrumentation and Measurement Technology Conference* , 2004,vol.3,pp. 1706-1711.
- [48] M.S.Chavan , R.A. Agrawala , M.D.U. plane, " Digital Elliptic Filter Application for noise Reduction in ECG Signal", *In Proc. 4th Wseas International Conference on Electronics, Control & Signal Processing* ,2005,pp. 58-63.
- [49] L.Chmelka , J. Kozumplik , "Wavelet-Based Wiener Filter for Electrocardiogram Signal Denoising," *In Proc. Computers in cardiology*,2005 ,pp. 771-774.

- [50] A. Pomsathit , P. Wattanaluk , O. Sangaroon and C. Benjangkaprasert , " Variable step-size algorithm for lattice form structure adaptive IIR notch filter," In Proc. International conference on communications, Circuits and Systems, 2006,pp. 332–335.
- [51] S. M. M. Martens, M. Mischi, S. G. Oei and J. W. M. Bergmans, "An Improved Adaptive Power Line Interference Canceller for Electrocardiography," *IEEE Transactions on Biomedical Engineering*, vol. 53, no. 11, pp. 2220-2231,2006.
- [52] M.A.Tinati and B. Mozaffary, "A Wavelet Packets Approach to Electrocardiograph Baseline Drift Cancellation," *International Journal of Biomedical Imaging*, 2006.
- [53] K.J.Kim, J.H. Ku , I.Y. Kim, S.I. Kim and S.W. Nam, "Notch filter design using the  $\alpha$ -scaled sampling kernel and its application to power line noise removal from ECG signals," In Proc. International Conference on Control Automation and Systems, 2007,pp. 2415–2418.
- [54] Alfaouri Mikhled and Khaled Daqrouq,"ECG Signal Denoising By Wavelet Transform Thresholding,"*American Journal of Applied Sciences*, vol.5,no.3 ,pp. 276-281,2008
- [55] Wei. Zhang , Ge.Linin Ge, "A Method for Reduction of Noise in the ECG," In Proc. 2nd International Conference on Bioinformatics and Biomedical Engineering,2008,pp. 2119-2122.
- [56] C. Saritha , V. Sukanya and Y. Narasimha Murthy, "ECG Signal Analysis using Wavelet Traansforms," *Bulg. J. Phys.*, vol.35,no.1,pp. 68-77,2008.
- [57] Lin Yue-Der and Yu Hen Hu, "Power Line Interference Detection and Suppression in ECG Signal Processing,"*IEEE Transaction on Biomedical Engineering*, 2008, vol.55, no.1, pp.354-357.
- [58] M.Dai ,S.L. Lian , "Removal of baseline wander from dynamic electrocardiogram signals," In Proc. 2nd International Congress on Image and Signal Processing,2009, pp. 1–4.
- [59] Mohammad Zia Ur Rahman, Rafi Ahamed Shaik, D.V.Rama koti Reddy, "Denoising ECG Signals using Transform Domain Adaptive Filtering Technique," In Proc. *Annual IEEE India Conference*,2009,pp.1-4.
- [60] Al-Qawasmi Abdel-Rehman, Khaleed Daqrouq,"ECG Signal Enhancement using Wavelet Transform," *WEAS Transaction on Biology and Medicine*," vol.7,no.2, pp. 62-70,2010.
- [61] J. Piskorowski , "Digital Q-varying notch IIR filter with transient suppression," *IEEE Transaction on Instrumentation and Measurement*, vol. 59(4),pp. 866–72,2010.
- [62] A. Bhavani Sankar , D. Kumar , K. Seethalakshmi, "Performance study of various adaptive filter algorithms for noise cancellation in respiratory signals," *Signal Process: An International Journal (SPIJ)*,vol.4, no.5,pp.267–78,2010.

- [63] C.B. Mbachu , G.N. Onoh, V.E. Idigo, E.N. Ifeagwu S.U. Nnebe, “ Processing ECG Signal with Kaiser Window-Based FIR Digital Filters,”*International Journal of Engineering Science and Technology*,vol.3,no.8 ,pp.6775 – 6783,2011.
- [64] M. Khan M, F. Aslam , T. Zaidi T,S.A. Khan, “Wavelet Based ECG denoising Using Signal-Noise Residue Method”, In Proc. 5th International Conference on Bioinformatics and Biomedical Engineering , pp.1-4, 2011.
- [65] A. Awal ,S.S. Mostafa and M. Ahmad, “Performance Analysis of Savitzky-Golay Smoothing Filter Using ECG Signal ,” *International Journal of Computer and Information Technology*, vol.1, no.2,pp 90-95,2011.
- [66] R. Vullings , B. de Vries , J.W. Bergmans , “An adaptive Kalman filter for ECG signal enhancement,” *IEEE Trans Biomed Eng.*, vol.58, no.4.pp.1094–1103, 2011.
- [67] N.K. Dewangan , Manoj K Kowar and Kiran Dewangan, 2011, “A Comparative Study of Denoising of ECG Signals using Wavelet Transform,” *Global Journal of Modern Biology and Technology*, vol.1,no.3,pp. 1-3,2011.
- [68] J. Piskorowski ,“Powerline interference removal from ECG signal using notch filter with non-zero initial conditions”, In Proc. IEEE International Symposium on Medical Measurements and Applications Proceedings, 2012,pp. 1–3.
- [69] L. Smital , M. Vitek , J. Kozumplík , I. Provazník I , “ Adaptive wavelet wiener filtering of ECG signals,” *IEEE Trans Biomed Eng.* , vol.60,no.2,pp.437–45,2013.
- [70] C.B. Mbachu , A.W. Nwosu , “Measurement of Electrocardiographic Signals for Analysis of Heart Conditions and Problems,”*American Journal of Engineering Research (AJER)* ,Vol. 3, no.10, pp. 61-67,2014.
- [71] S. Kocoń and J. Piskorowski , “ Time-varying IIR multi-notch filter based on all-pass filter prototype,” In Proc. 19th International Conference on Methods and Models in Automation and Robotics (MMAR),2014, pp. 112–118.
- [72] H.K. Jayant ,K.P.S. Rana, V. Kumar, S.S. Nair, and P. Mishra , “ Efficient IIR notch filter design using Minimax optimization for 50Hz noise suppression in ECG,” In Proc. International Conference on Signal Processing, Computing and Control (ISPCC), 2015, pp. 290-295.
- [73] N. Razzaq, S. A. Sheikh, M. Salman and T. Zaidi, "An Intelligent Adaptive Filter for Elimination of Power Line Interference From High Resolution Electrocardiogram," *IEEE Access*, vol. 4, pp. 1676-1688, 2016.

- [74] C. Tseng, and S. Lee, "Power line interference removal in ECG using bernstein-polynomial-based FIR notch filter," In Proc. IEEE 6th Global Conference on Consumer Electronics (GCCE),2017,pp. 1–2.
- [75] B.U.Kohler, C. Hennig, R. Orglmeister, R., "The principles of software QRS detection", *IEEE Engineering in Medicine and Biology Magazine*, vol.21, no.1, pp. 42 – 57,2002.
- [76] I.K. Daskalov, I.A. Dotsinsky and I.I. Christov, "Developments in ECG Acquisition, Preprocessing, Parameter Measurement, and Recording," *IEEE Engineering in Medicine and Biology*, vol.17,no.2,pp. 50-58,1998.
- [77] S.Z. Mahmoodabadi , A. Ahmadian and M.D. Abolhasani , "ECG Feature Extraction using Daubechies Wavelets". In Proc. fifth IASTED International Conference, Visualization, Imaging, And Image Processing, 2005, pp. 343-348.
- [78] S. Sumathi S., M. Y. Sanavullah, "Comparative Study of QRS Complex Detection in ECG based on Discreter Wavelet Transform,"*International Journal of Recent Trends in Engineering*, vol2,no.5, pp. 273-277,2009.
- [79] S. Banerjee, M. Mitra, "ECG Signal Denoising and QRS Complex Detection by Wavelet Transform Based Thresholding,"*Sensors & Transducers Journal*, vol.119,no.8,pp. 207-214,2010.
- [80] K.V.L. Narayana, A. Bhujanga Rao , "Wavelet Based QRS Detection in ECG using MATLAB,"*Innovative Systems Design and Engineering*, vol.2, no.7, pp.60-69, 2011.
- [81] P. Sasikala, D. R. S. D. Wahida Banu , "Extraction of P wave and T wave in Electrocardiogram using Wavelet Transform," *International Journal of Computer Science and Information Technologies*, vol.2,no.1,pp.489-493,2011.
- [82] N.K. Dewangan , Manoj K Kowar , "ECG Signal Denoising and QRS Complex Detection using Multi Resolution Sub-band Filter and Thresholding Technique,"*Global J. of Mod. Bio. & Tech.*, vol.3, no.1, pp.15-20, 2013.
- [83] A.Z.M. Shafiullah, J.A. Khan, "A new robust correlation estimator for bivariate data,"*Bangladesh Journal of Scientific Research*, vol. 24,no. 2 ,pp. 97-106,2011.
- [84] M.Z.U. Rahman , R.A. Shaik, D.V.R.K.Reddy , "Efficient and simplified adaptive noise cancelers for ECG sensor based remote health monitoring,"*IEEE Sensors J.*, vol.12, no.3, pp.566–73, 2012.
- [85] H.S. Niranjana Murthy, M. Meekashi , "ECG Signal Denoising and Ischemic Event Feature Extraction using Daubechies Wavelets," *International Journal of Computer application*,vol. 67,no.2,pp.29-33,2013.



- [86] A. Jablonski , T. Barszcz M. Bielecka ,P. Breuhaus, “Modeling of probability distribution functions for automatic threshold calculation in condition monitoring systems”,*Measurement*,vol.46,no.1,pp.727-738,2013.
- [87] M. AlMahamdy M, H.B. Riley, “Performance study of different denoising methods for ECG signals,” *Procedia Comput Sci*,vol.37,pp. 325–32,2014.
- [88] U. Seljuq , F. Himayun , H. Rasheed, “ Selection of an optimal mother wavelet basis function for ECG signal denoising,” In Proc. 17th IEEE International Multi Topic Conference 2014, pp. 26-30, 2014.
- [89] F.M. Ghombavani, K. Kiani ,“A powerful novel method for ECG signal de-noising using different thresholding and Dual Tree Complex Wavelet Transform,” In Proc. 2nd International Conference on Knowledge–Based Engineering and Innovation(KBEI), 2015,pp. 966-971.
- [90]Can He, Jianchun Xing, Juelong Li, Qiliang Yang, Ronghao Wang , “A New Wavelet Threshold Determination Method Considering interscale Correlation in Signal Denoising,”*Mathematical Problems in Engineering*, 2015..
- [91] B. Singh , P. Singh , S. Budhiraja , “Various approaches to minimise noises in ECG signal: A survey,” In Proc. Fifth International Conference on Advanced Computing & Communication Technologies, 2015, pp. 131–137.
- [92] R.G. Afkhami , G. Azarnia , M.A. Tinati, “ Cardiac arrhythmia classification using statistical and mixture modeling features of ECG signals,” *Pattern Recognition Letters*,vol.70,pp. 45–51,2016.
- [93] J. Jebaraj , R. Arumugam , “ Ensemble empirical mode decomposition-based optimised power line interference removal algorithm for electrocardiogram signal,” *IET Signal Processing*,vol.10,no.6 ,pp.583–91,2016.
- [94] T. Niederhauser , Thomas Niederhauser, T. Marisa, Lukas Kohler, Andreas Haeberlin, Reto A Wildhaber, Roger Abächerli, Josef Goette, Marcel Jacomet, Rolf Vogel," A baseline wander tracking system for artifact rejection in long-term electrocardiography,” *IEEE Transactions on Biomedical Circuits and Systems*,vol10,no.1,pp: 255–65,2016.
- [95] Y.Gong , P. Gao , L. Wei , C. Dai , L. Zhang , Y. Li , “ An enhanced adaptive filtering method for suppressing cardiopulmonary resuscitation artefact,” *IEEE Transactions on Biomedical Engineering*, vol.64, no.2,pp.471–8,2017.
- [96] J. Rodrigues , D. Belo , H. Gamboa , “Noise detection on ECG based on agglomerative clustering of morphological features,” *Computer in Biology and Medicine* , vol.87, pp. 322–34,2017

- [97] S. Nagai, D. Anzai , J. Wang , “ Motion artefact removals for wearable ECG using stationary wavelet transform,” *Healthcare Technology Letters* , vol.4,no.4,pp. 138–41,2017.
- [98] Shanti Chandra ,Amblika Sharma , Girish Kumar Singh, “Feature extraction of ECG signal ,” *Journal of Medical Engineering & Technology* ,vol. 42, no. 4,pp 306-316, 2018.
- [99] S.Kumar, D. Panigrahy , P.K.Sahu ., “ Denoising of Electrocardiogram (ECG) signal by using empirical mode decomposition (EMD) with non-local mean (NLM) technique,” *Biocybernetics Biomedical Engineering*, vol. 38,no.2,pp.297–312,2018.
- [100] H.He , Y. Tan , “A novel adaptive wavelet thresholding with identical correlation shrinkage function for ECG noise removal,” *Chinese Journal of Electronics*, vol.27,no3,pp.507–13,2018
- [101] A.R. Zubair, Y.K. Ahmed and K.A. Akande , “Electromyography Noise Suppression in Electrocardiogram Signal Using Modified Garrote Threshold Shrinkage Function”, *African Journal of Computing & ICT*, vol.11,no.3,pp. 85 – 94,2018.
- [102]Zaid Abdi Alkareem Alyasseri,Ahamad Tajudin Khader,Mohammed Azmi Al-Betar,Ammar Kamal Abasi,Sharif Naser Makhadmeh, “Hybridizing  $\beta$ -hill climbing with wavelet transform for denoising ECG signals,” *Information Sciences*, Vol. 429, pp. 229-46,2018.
- [103] Alan S. Said Ahmad , Majd S. Matti , Omar A.M. ALhabib and Sabri Shaikhow, “Denoising of Arrhythmia ECG Signals”, *International Journal of Medical Research & Health Sciences*,vol.7,no.3,pp.83-93,2018.
- [104] Di Wang ,Yujuan Si ,Weiyi Yang ,Gong Zhang andTong Liu, “A Novel Heart Rate Robust Method for Short-Term Electrocardiogram Biometric Identification,” *Applied Sciences* ,vol.9,no.1,pp.201,2019.
- [105] Li W., “Wavelets for electrocardiogram: overview and taxonomy, ” *IEEE Access*, vol.7,pp. 25627-25649,2019.
- [106] Amit Singhal,PushpendraSingh,BinishFatimah,Ram Bilas Pachori, “An efficient removal of power-line interference and baseline wander from ECG signals by employing Fourier decomposition technique,” *Biomedical Signal Processing and Control*,vol. 57, 2020.
- [107]Kozlikova, Katarina, “Biological Signals In Medical Diagnostics,” In Proc. AIP Conference Proceedings, pp.147-150,2010.
- [108]John Enderle, Joseph Bronzino, Susan M. Blanchard, *Introduction to Biomedical Engineering*. Connecticut: Elsevier Academic Press,2005.
- [109] M. Haïssaguerre , N. Derval , F. Sacher, L. Jesel, I. Deisenhofer, L.de Roy, J.L. Pasquié, A. Nogami, D.Babuty, S. Yli-Mayry and C. De Chillou,, “Sudden cardiac arrest associated with early repolarization,” *New England Journal of Medicine*, vol.358, no.19, pp.2016-2023,2008.

- [110] M.R.Sabuncu, Ender Konukoglu, "Alzheimer's Disease Neuroimaging Initiative, Clinical prediction from structural brain MRI scans: a large-scale empirical study." *Neuroinformatics*, vol. 13, no.1, pp. 31-46,2015.
- [111] H. Pulliainen, H.Niela-Vilén, E.Ekholm, S. Ahlqvist-Björkroth , "Experiences of interactive ultrasound examination among women at risk of preterm birth: a qualitative study," *BMC Pregnancy Childbirth*, vol.19,no.1,pp. 338,2019
- [112] Mesin,Luca. , *Introduction to biomedical signal processing*. ilmiolibro self publishing,2017.
- [113] Ganapathy, Nagarajan, Ramakrishnan Swaminathan, and Thomas M. Deserno. "Deep learning on 1-D biosignals: a taxonomy-based survey," *Yearbook of medical informatics*, vol.27, no.1, pp. 98,2018.
- [114] Litwin, Louis. "FIR and IIR digital filters." *IEEE potentials*,vol.19, no.4,pp. 28-31,2000.
- [115] B. Sharma, Jenkin Suji, "Analysis of various window techniques used for denoising ECG signal." In Proc. IEEE 2016 Symposium on Colossal Data Analysis and Networking (CDAN), 2016, pp. 1-5.
- [116] John G. Proakis, Dimitris G. Manolakis, *Digital signal processing: Principles, algorithms, and applications*. India: Pearson education, 2007.
- [117] N. B. Jones, J. D. McK. Watson, *Digital Signal Processing: Principles, Devices and Applications*. London: Institution of Engineering and Technology, 1990.
- [118] S. O. Gilani, Y. Ilyas, M. Jamil, "Power line noise removal from ECG signal using notch, band stop and adaptive filters," In Proc. International Conference on Electronics, Information, and Communication (ICEIC), 2018, pp. 1-4.
- [119] U.E. Ayten, R. A. Vural, T. Yildirim, "Low-pass filter approximation with evolutionary techniques," In Proc. 7th International Conference on Electrical and Electronics Engineering (ELECO), 2011, pp. 125-129.
- [120] R. W. Daniels, *Approximation Methods for Electronic Filter Design*. New York : Tata McGraw-Hill, 1974.
- [121] Paulo S.R. Diniz , *Adaptive Filtering Algorithms and Practical Implementation*. Switzerland: Springer, 2008.
- [122] S. Sharma, R. P. Narawaria., "Noise Reduction from ECG Signal using Adaptive Filter Algorithm", *International Journal of Engineering Research & Technology (IJERT)*, Vol. 3,no.7,2014.

- [123] S. Kasar , A, Mishra , M. Joshi, “Performance of Digital filters for noise removal from ECG signals in Time domain,” *International Journal of Innovative Research in Electrical, Electronics, Instrumentation and Control Engineering*, Vol. 2,no.4,pp.1352-1355,2014.
- [124] K.K. Patro, R. Kumar, “De-Noising of ECG raw Signal by Cascaded Window based Digital filters Configuration”, In Proc. IEEE Power, Communication and Information Technology Conference (PCITC) Siksha ‘O’,2015.
- [125] B. Harshal Shingne and Dhanashri H. Gawali, “FPGA based Design and Implementation of Cascaded FIR Filter for ECG Signal Processing”, In Proc. IDES joint International conferences on IPC and ARTEE, 2017.
- [126] A. Katunin, “Application of time-frequency distributions in diagnostic signal processing problems: a case study,” *Diagnostyka*, vol. 17, no. 2, pp. 95–103, 2016.
- [127] A. S. Alfahoum, A. Alfraihat, “Methods of EEG Signal Features Extraction Using Linear Analysis in Frequency and Time-Frequency Domains,” *International Scholarly Research Notices*, no. 3, 2014.
- [128] N. H. Chandra, A. S. Sekhar, “Fault detection in rotor bearing systems using time frequency techniques,” *Mechanical Systems and Signal Processing*, vol. 72, pp. 105–133, 2016.
- [129] P.S.Addison, "Wavelet transforms and the ECG: a review," *Physiological measurement*, vol.26, no. 5, 2005.
- [130] Qibin Zhao, Liqing Zhan, “ECG Feature Extraction and Classification Using Wavelet Transform and Support Vector Machines,” In Proc. International Conference on Neural Networks and Brain,2005, vol. 2, pp. 1089-1092.
- [131] Too, Jingwei, A. R. Abdullah, N. Mohd Saad, N. Mohd Ali, and H. Musa. "A detail study of wavelet families for EMG pattern recognition," *International Journal of Electrical and Computer Engineering*,vol. 8, no. 6 ,2018.
- [132] V. Naga Prudhvi Raja , T. Venkateswarlu , “Denoising of medical images using dual tree complex wavelet transform”,*Procedia Technology*,vol.4,pp.238 – 244,2012.
- [133] Donoho, David L., and Jain M. Johnstone, "Ideal spatial adaptation by wavelet shrinkage," *biometrika*,vol 81, no. 3,pp. 425-455,1994.
- [134] H. Kaur , Rajini, “ECG Signal Denoising with Savitzky-Golay Filter and Discrete Wavelet Transform (DWT)”, *International Journal of Engineering Trends and Technology (IJETT)*,vol.36,no.5,pp 266-269,2016.

- [135] Dejan Stantic, Jun Jo, “Multiscale Wavelet Method for Heart Abnormality Detection Within IoTs Environment”, In Proc. International Conference on Web Intelligence, Mining and Semantics, 2018, pp 1-11.
- [136] Dejan Stantic, “Abnormality Detection from ECG Signals Using Multiscale Wavelet Analysis”, Ph.D thesis, Griffith University, Australia, 2016.
- [137] G.G. Tsaneva , K. Tcheshmedjiev K, “ Denoising of Electrocardiogram Data with Methods of Wavelet Transform”, In Proc. International Conference on Computer Systems and Technologies, 2013 ,pp. 9- 16.
- [138] Lu Jing-yi, Lin Hong, Ye Dong and Zhang Yan-sheng, “A New Wavelet Threshold Function and Denoising Application,” *Mathematical Problems in Engineering* , 2016.
- [139] Zhang, Yang, Weifeng Ding, Zhifang Pan, and Jing Qin, "Improved wavelet threshold for image de-noising," *Frontiers in neuroscience*, vol.13, 2019.
- [140] C. He, J. C. Xing, Q. L. Yang, “Optimal wavelet basis selection for wavelet denoising of structural vibration signal,” *Applied Mechanics and Materials*, vol. 578, pp. 1059–1063, 2014.
- [141] J.-Y. Tang, W.-T. Chen, S.-Y. Chen, W. Zhou, “Wavelet based vibration signal denoising with a new adaptive thresholding function,” *Journal of Vibration and Shock*, vol. 28, no. 7, pp. 118–121, 2009.
- [142] O.El. B’charri, Latif R, Elmansouri K, Abenaou A, Jenkal W, “ ECG signal performance de-noising assessment based on threshold tuning of dual-tree wavelet transform,” *Biomedical Engineering*, pp.16-26, 2017.
- [143] Abdullah MB , “On a robust correlation coefficient,” *The Statistician*, vol. 39, no.4, pp. 455-460, 1990.
- [144] William M. Kolb, *Curve Fitting for Programmable Calculators*. Syntec, 1984.
- [145] S. Lee, C. Lim, J.-H. Chang, “A new a priori SNR estimator based on multiple linear regression technique for speech enhancement,” *Digital Signal Processing*, vol. 30, no. 7, pp. 154–164, 2014.
- [146] Soojeong Lee, Gangseong Lee, “Noise Estimation and Suppression Using Nonlinear Function with A Priori Speech Absence Probability in Speech Enhancement,” *Journal of Sensors*, vol. 2016, pp.1-7, 2016.

- [147] R. Martin, “Noise power spectral density estimation based on optimal smoothing and minimum statistics,” *IEEE Transactions on Speech and Audio Processing*, vol. 9, no. 5, pp. 504–512, 2001.
- [148] S. Rangachari, P. C. Loizou, “A noise-estimation algorithm for highly non-stationary environments,” *Speech Communication*, vol. 48, no. 2, pp. 220–231, 2006.
- [149] P. Wilson, H. Alan Mantooh, *Model-based engineering for complex electronic systems*. Newnes:Elsevier,2013.
- [150] Art Kay, *Introduction and Review of Statistics in Operational Amplifier Noise*.UK: Elsevier, 2012.
- [151] Chris Tsokos, Rebecca Wooten, *Normal Probability in the Joy of Finite Mathematics*. USA: Elsevier 2016
- [152] Dixon, W. J., and Massey, F. J., *Introduction to Statistical Analysis*. NewYork: McGraw-Hill, New York,1983.
- [153] A.Hassairi, A.Roula,“Exponential probability distribution on symmetric matrices,” *Statistics & Probability Letters*, Vol. 145, Pages 37-42, 2019.
- [154] T. Yadav T, R. Mehra , “Denoising and SNR Improvement of ECG Signals Using Wavelet Based Techniques,” In Proc. 2nd International Conference on Next Generation Computing Technologies (NGCT) ,2016, pp678-682.
- [155] S.K. Salih , S. A. Aljunid , S. M. Aljunid , O. Maskon, “Adaptive Filtering Approach for Denoising Electrocardiogram Signal Using Moving Average Filter,” *Journal of Medical Imaging and Health Informatics*, Vol. 5, pp.1065-1069, 2015.
- [156] K.D.Priyaa ,G.S. Rao, P.S.V.S. Rao,“Comparative Analysis of Wavelet Thresholding Techniques with Wavelet-Wiener Filter on ECG Signal,” In Proc. 4th International Conference on Recent Trends in Computer Science & Engineering , 2016,vol87,pp178 -183.

# **APPENDICES**

## APPENDICES

### 1.1 DESCRIPTION OF MIT-BIH ARRHYTHMIA RECORDS

**1. Record 100 (MLII, V5; Sex- Male, Age -69)**

Rhythm	Rate	Episodes	Duration
Normal Sinus	70-89	1	30:06

**2. Record 101 (MLII, V1; Sex- Female, Age- 75)**

Rhythm	Rate	Episodes	Duration
Normal Sinus	55-79	1	30:06

**3. Record 102 (V5, V2; Sex- Female, Age- 84)**

Rhythm	Rate	Episodes	Duration
Normal Sinus	72-78	2	1:22
Paced Rhythm	68-78	3	28.44

**4. Record 103 (MLII, V2; Sex-Male, Age - not recorded)**

Rhythm	Rate	Episodes	Duration
Normal Sinus	62-92	1	30:06

**5. Record 104 (V5, V2; Sex- Female, Age- 66)**

Rhythm	Rate	Episodes	Duration
Normal Sinus	69-82	22	3:52



Paced Rhythm    70-78        23        26.13

The rate of paced rhythm is close to that of the underlying sinus rhythm, with some fusion beats from pacemakers. PVCs are multiform. This record exists with many bursts of muscle noise.

**6. Record 105 (MLII, V1; Sex- Female, Age- 73)**

Rhythm	Rate	Episodes	Duration
Normal Sinus	78-102	1	30:06

Uniformity of PVCs. The primary characteristics of this record are high-grade noise and artifact.

**7. Record 106 (MLII, V1; Sex- Female, Age -24)**

Rhythm	Rate	Episodes	Duration
Normal Sinus	49-82	21	22:36
Ventricular bigeminy	55-103	18	7:15
Ventricular trigeminy	57-90	1	0:13
Ventricular tachycardia	121	1	0:02

Multiformity of PVCs and signal are acquired with low frequency noise component.

**8. Record 107 (MLII, V1; Sex - Male, Age -63)**

Rhythm	Rate	Episodes	Duration
Normal Sinus	68-82	1	30:06

Complete blockage of heart is present. The PVCs are multiform.

**9. Record 108 (MLII, V1; Sex- Female, Age- 87)**

Rhythm	Rate	Episodes	Duration
Normal Sinus	44-78	1	30:06

First degree AV obstruction and sinus arrhythmia arise borderline with multiformity of PVCs. The lower channel experiences noise and baseline shifts.

**10. Record 109 (MLII, V1; Sex- Male, Age- 64)**

Rhythm	Rate	Episodes	Duration
Normal Sinus	77-101	1	30:06

. The PVCs indicate multiformity with presence of first degree AV block in the record.

**11. Record 111 (MLII, V1; Sex-Female, Age- 47)**

Rhythm	Rate	Episodes	Duration
Normal Sinus	64-82	1	30:06

Exhibit AV block of first degree and presence of short bursts of both baseline shifts and muscle noise.

**12. Record 112 (MLII, V1; Sex-Male, Age- 54)**

Rhythm	Rate	Episodes	Duration
Normal Sinus	74-91	1	30:06

There is existence of S-T segment depression in the upper channel.

**13. Record 113 (MLII, V1; Sex-Female, Age- 24)**

Rhythm	Rate	Episodes	Duration
Normal Sinus	48-87	1	30:06

Wandering atrial pacemaker varies the rate of normal sinus rhythm.

**14. Record 114 (V5, MLII; Sex-Female, Age- 72)**

Rhythm	Rate	Episodes	Duration
Normal Sinus	51-82	2	30:01
SVTA	102-122	1	0:05

The PVCs are uniform

**15. Record 115 (MLII, V1; Sex-Female, Age -39)**

Rhythm	Rate	Episodes	Duration
Normal Sinus	50-84	1	30:06

**16. Record 116 (MLII, V1; Sex-Male, Age- 68)**

Rhythm	Rate	Episodes	Duration
Normal Sinus	74-86	1	30:06

**17. Record 117 (MLII, V2; Sex- Male, Age- 69)**

Rhythm	Rate	Episodes	Duration
Normal Sinus	48-66	1	30:06

**18. Record 118 (MLII, V1; Sex-Male, Age- 69)**

Rhythm	Rate	Episodes	Duration
Normal Sinus	54-91	1	30:06

The PVCs are multiform.

**19. Record 119 (MLII, V1; Sex-Female, Age- 51)**

Rhythm	Rate	Episodes	Duration
Normal Sinus	61-84	49	22:36
Ventricular bigeminy	52-91	37	3:55
Ventricular trigeminy	56-77	17	3:34

The PVCs are uniform.

**20. Record 121 (MLII, V1; Sex-Female, Age- 83)**

Rhythm	Rate	Episodes	Duration
Normal Sinus	55-83	1	30:06

Noise contents are present in the record.

**21. Record 122 (MLII, V1; Sex- Male, Age- 51)**

Rhythm	Rate	Episodes	Duration
Normal Sinus	67-97	1	30:06

The low amplitude high frequency noise is present throughout the lower channel.

**22. Record 123 (MLII, V5; Sex-Female, Age- 63)**

Rhythm	Rate	Episodes	Duration
Normal Sinus	41-65	1	30:06

Uniformity and interpolation of the PVCs.

**23. Record 124 (MLII, V4; Sex-Male, Age- 77)**

Rhythm	Rate	Episodes	Duration
Normal Sinus	47-64	6	28:36
Nodal (junctional) rhythm	56-64	2	0:30
Ventricular trigeminy	51-59	2	0:22
Idioventricular rythm	53-61	3	0:37

The junctional escape beats follows the multiform PVCs.

**24. Record 200 (MLII, V1; Sex-Male, Age- 64)**

Rhythm	Rate	Episodes	Duration
Normal Sinus	69-111	70	15:58
Ventricular bigeminy	60-108	71	3:52
Ventricular tachycardia	90-141	7	0:15

In the upper channel there are sporadic bursts of high frequency noise, and in the lower channel there is extreme noise and artifact along with multiformity of PVCs.

**25. Record 201 (MLII, V1; Sex-Male, Age- 68)**

Rhythm	Rate	Episodes	Duration
Normal Sinus	31-61	16	12:57
SVTA	124	1	0:02
Atrial fibrillation	56-149	3	10:06
Nodal (junctional) rhythm	37-60	3	0:24
Ventricular trigeminy	49:56	12	6:37

Uniformity and late-cycle of PVCs. In the following episodes of ventricular trigeminy there is occurrence of Junctional escape beats.

**26. Record 202 (MLII, V1; Sex-Male, Age- 68)**

Rhythm	Rate	Episodes	Duration
Normal Sinus	49-69	3	19:31
Atrial flutter	101-143	71	3:52
Atrial fibrillation	90-141	7	0:15

The PVCs are uniform and late-cycle.

**27. Record 203 (MLII, V1; Sex-Male, Age- 43)**

Rhythm	Rate	Episodes	Duration
Normal Sinus	63-173	1	2:43
Atrial flutter	61-180	2	5:14
Atrial fibrillation	54-180	20	21:32
Ventricular trigeminy	100-116	1	0:04
Ventricular tachycardia	124-189	21	0:33

Multiformity of PVCs. The upper channel experiences changes in the QRS morphology due to axis shifts. Both channels have considerable noise including muscle artifact shifts and baseline shifts.

**28. Record 205 (MLII, V1; Sex -Male, Age- 59)**

Rhythm	Rate	Episodes	Duration
Normal Sinus	80-99	7	29:43
Ventricular Tachycardia	79-216	6	0:23

**29. Record 207 (MLII, V1; Sex- Female, Age- 89)**

Rhythm	Rate	Episodes	Duration
Normal Sinus	57-90	10	22:20
SVTA	108-130	1	0:52
Ventricular bigeminy	49-83	4	2:38
Idioventricular rythm	29-71	1	1:49
Ventricular Tachycardia	118-119	2	0:03
Ventricular Flutter	143-358	6	2:24

The predominant rhythm is normal sinus with AV block at first degree and left bundle branch block. There are instances where the block of conduction switches to a pattern of the right bundle branch. Multiformity of PVCs is examined. The Idioventricular rhythm appears following the longest ventricular fluttering sequence. The record ends during the SVTA episode.

**30. Record 208 (MLII, V1; Sex -Female, Age- 23)**

Rhythm	Rate	Episodes	Duration
Normal Sinus	91-134	27	24:43
Ventricular trigeminy	79-129	26	5:22

Uniformity of PVCs are examined. The couplets are often seen in a bigeminal pattern, many of which include a fusion PVC. Each triplets consist of two PVCs and a fusion PVC.

**31. Record 209 (MLII, V1; Sex -Male, Age- 62)**

Rhythm	Rate	Episodes	Duration
Normal Sinus	82-116	11	28:23
SVTA	106-171	10	1:42

**32. Record 210 (MLII, V1; Sex –Male, Age- 89)**

Rhythm	Rate	Episodes	Duration
--------	------	----------	----------

Atrial fibrillation	63-158	9	29:30
Ventricular bigeminy	69-109	5	0:23
Ventricular trigeminy	85-114	1	0:07
Ventricular tachycardia	103-161	2	0:06

The PVCs are multiform.

**33. Record 212 (MLII, V1; Sex-Female, Age- 32)**

Rhythm	Rate	Episodes	Duration
Normal Sinus	63-108	1	30:06

There is right bundle branch block that occurs when the heart rate reaches around 90 bpm.

**34. Record 213 (MLII, V1; Sex-Male, Age- 61)**

Rhythm	Rate	Episodes	Duration
Normal Sinus	101-113	22	29:01
Ventricular bigeminy	102-116	19	1:00
Ventricular tachycardia	110-117	2	0:04

The PVCs are multiform and typically late-cycle, also leading to PVC fusion. The morphology of fusion PVCs in ranges from almost normal to nearly identical to that of PVCs.

**35. Record 214 (MLII, V1; Sex -Male, Age- 53)**

Rhythm	Rate	Episodes	Duration
Normal Sinus	49-92	13	28:53
Ventricular trigeminy	71-87	10	1:08
Ventricular tachycardia	126-150	2	0:05

Multiformity of PVCs. There are two instances of rising artifact amplitude, and one instance of slippage of tape.



**36. Record 215 (MLII, V1; Sex- Male, Age- 81)**

Rhythm	Rate	Episodes	Duration
Normal Sinus	81-124	3	30:03
Ventricular tachycardia	174-177	2	0:02

Multiformity of PVCs. Tape slippage has two very brief occurrences (each in span of less than one second).

**37. Record 217 (MLII, V1; Sex -Male, Age- 65)**

Rhythm	Rate	Episodes	Duration
Atrial fibrillation	69-103	24	4:12
Paced rhythm	65-76	33	25:10
Ventricular bigeminy	68-91	9	0:42
Ventricular tachycardia	103	1	0:02

The PVCs are multiform.

**38. Record 219 (MLII, V1; Sex- Male, Age- not recorded)**

Rhythm	Rate	Episodes	Duration
Normal sinus	38-75	8	6:01
Atrial fibrillation	51-103	10	23:47
Ventricular bigeminy	71-88	2	0:08
Ventricular trigeminy	74-94	1	0:10

Some transitions from atrial fibrillation to normal sinus rhythm are persistent delays of up to 3 seconds along multiformity of PVCs.

**39. Record 220 (MLII, V1; Sex -Female, Age- 87)**

Rhythm	Rate	Episodes	Duration
Normal Sinus	58-74	9	29:50
SVTA	113-150	8	0:16

**40. Record 221 (MLII, V1; Sex -Male, Age- 83)**

Rhythm	Rate	Episodes	Duration
Atrial fibrillation	47-110	12	29:17
Ventricular bigeminy	88-101	1	0:03
Ventricular trigeminy	69-92	8	0:42
Ventricular tachycardia	122-130	2	0:04

Multiformity of PVCs is examined, But one type is considerably more common than the other.

**41. Record 222 (MLII, V1; Sex -Female, Age- 84)**

Rhythm	Rate	Episodes	Duration
Normal Sinus Rythm	49-84	32	15:57
Atrial bigeminy	57-98	3	1:28
SVTA	121-148	4	0:08
Atrial flutter	123-148	42	7:03
Atrial fibrillation	69-163	24	1:44
Nodal (junctional) Rhythm	47-122	31	3:45

The nodal escape beats are usually accompanied by episodes of paroxysmal atrial flutter / fibrillation. High-frequency noise / artifact intervals are present in both channels.

**42. Record 223 (MLII, V1; Sex -Male, Age- 73)**

Rhythm	Rate	Episodes	Duration
Normal sinus	75-94	11	23:23
Atrial fibrillation	74-106	7	4:19
Ventricular bigeminy	67-92	3	0:38
Ventricular trigeminy	76-118	7	1:46

Multiformity of PVCs are examined. The two longest ventricular tachycardia episodes are sluggish (100 to 105 bpm), and bidirectional.

**43. Record 228 (MLII, V1; Sex -Female, Age- 80)**

Rhythm	Rate	Episodes	Duration
Normal Sinus	54-80	21	24:17
Ventricular bigeminy	50-88	20	5:48

There is block of AV at first degree. There are three brief tape slippage events, with a cumulative time of 2.2 seconds.

**44. Record 230 (MLII, V1; Sex- Male, Age- 32)**

Rhythm	Rate	Episodes	Duration
Normal Sinus	63-99	104	17:45
Pre-excitation(WPW)	59-93	103	12:21

**45. Record 231 (MLII, V1; Sex -Female, Age- 72)**

Rhythm	Rate	Episodes	Duration
Normal Sinus	49-69	6	18:26
Pre-excitation(WPW)	34-38	5	11:40

AV conduction is very abnormal with 2:1 AV block intervals, Mobitz II block instances, and the right bundle branch block that appears to be connected to the pace. The couplet could be a ventricular one.

**46. Record 232 (MLII, V1; Sex- Female, Age- 76)**

Rhythm	Rate	Episodes	Duration
Sinus bradycardia	24-28	1	30:06

Sick sinus syndrome is aligned with the rhythm. The underlying sinus bradycardia, first degree AV block, and recurrent ectopic atrial runs at levels between 80 and 90 bpm are present. The length of multiple long pauses is up to 6 seconds.

**47. Record 233 (MLII, V1; Sex -Male, Age-57)**

Rhythm	Rate	Episodes	Duration
Normal sinus	98-110	36	28:03
Ventricular bigeminy	88-122	28	1:48
Ventricular trigeminy	106-122	1	0:04
Ventricular tachycardia	120-141	6	0.11

The PVCs are multiform.

**48. Record 234 (MLII, V1; Sex -Female, Age- 56)**

Rhythm	Rate	Episodes	Duration
Normal Sinus	84-99	2	29:40
SVTA	91-147	1	0:26

The PVCs are uniform.

These records were exported as .mat format and loaded for processing in MATLAB.

**2.1 FIR FILTERS**

A non- recursive FIR filters are characterized by Eq. (1)

$$H(z) = b_0 + b_1 z^{-1} + b_2 z^{-2} + \dots + b_n z^{-n} \tag{1}$$

where  $b_0, b_1, \dots, b_n$  are filter coefficients .

## 2.2 IIR FILTERS

The IIR system consists of infinite impulse response. IIR filters are generally executed utilizing structures having feedback that describe the IIR filter as a function of present and past values of the excitation as well as the past value of the response.

Recursive IIR filters are determined by Eq. (2)

$$H(z) = \frac{a_0 + a_1 z^{-1} + a_2 z^{-2} + a_3 z^{-3} \dots + a_n z^{-n}}{1 - b_1 z^{-1} + b_2 z^{-2} + b_3 z^{-3} \dots + b_n z^{-n}} \quad (2)$$

where  $a_0, a_1, \dots, a_n$  and  $b_0, b_1, \dots, b_n$  are filter coefficients.

## 2.3 WINDOWING TECHNIQUE

- a. Rectangular window(RW): In this window function the filter have finite values with in a definite interval ranging from  $-M$  to  $M$ . RW function is given by Eq. (3)

$$w(n) = 1, |n| < M$$

$$= 0, \text{ otherwise} \quad (3)$$

- b. Kaiser window (KW): In this window the side lobe level can be monitored by varying the parameter  $\alpha$  with respect to main lobe peak. KW function is defined by Eq.(4)

$$w(n) = \frac{I_0\left(\pi\alpha\sqrt{1-\left(\frac{2n}{M-1}-1\right)^2}\right)}{I_0(\pi\alpha)} \quad 0 < n < M-1 \quad (4)$$

$$= 0 \quad \text{Otherwise}$$

- c. Hamming window (HW): HW function is used to minimize the maximum side lobe. The window function is characterized by Eq.(5)

$$w(n) = \alpha - \beta \cos(2\pi n/(M-1)) \quad 0 \leq n \leq M-1 \quad (5)$$

- d. Hanning window (HaW): HaW function is defined in Eq. (6)

$$w(n) = 0.5[1 - (\cos(2\pi n)/(M-1))] \quad 0 \leq n \leq M-1 \quad (6)$$

e. Blackman window(BW) : BW exhibits wider main lobe width than that of HW and is defined by Eq. (7)

$$w(n) = 0.42 - 0.5 \cos(2\pi n/(N-1)) + 0.08 \cos(4\pi n/(N-1)) \quad 0 \leq n \leq M-1 \quad (7)$$

Using inverse Fourier transform, the desired frequency response specification  $G_d(\omega)$  and the corresponding unit sample response  $g_d(n)$  are determined by Eq.(8)

$$G_d(\omega) = \sum_{i=0}^{\infty} g_d(n) e^{-j\omega n} \quad (8)$$

Where

$$g_d(n) = \int_{-\pi}^{\pi} G_d(\omega) e^{j\omega n} d\omega \quad (9)$$

The impulse response  $g_d(n)$  is of infinite duration as define in Eq.(9). So, at some point truncation is performed, say  $n = M - 1$  to obtain a FIR filter having length  $M$  (i.e. 0 to  $M-1$ ). This can be achieved by multiplying  $g_d(n)$  with a the Rectangular window function as defined in Eq. (10).

The impulse response of FIR filter

$$g(n) = g_d(n) w(n) \quad (10)$$

that implies

$$g(n) = \begin{cases} g_d(n) & n = 0, 1, 2, \dots, M-1 \\ 0 & \text{otherwise} \end{cases} \quad (11)$$

The product of the window function  $w(n)$  with  $g_d(n)$  is similar to convolution of  $G_d(\omega)$  with  $W(\omega)$ , where  $W(\omega)$  is the Fourier transform of the window function  $w(n)$  as defined in Eq.(12)

$$W(\omega) = \sum_{i=0}^{\infty} w(n) e^{-j\omega n} \quad (12)$$

The frequency response of the truncated FIR filter  $G(\omega)$  is obtained by the convolution of  $G_d(\omega)$  with  $W(\omega)$

$$G(\omega) = \frac{1}{2\pi} \int_{-\pi}^{\pi} G_d(v)W(\omega - v)dv \quad (13)$$

The Fourier transform of  $g(n)$  also delivers the frequency response  $G(\omega)$  as defined in Eq.(14)

$$G(\omega) = \sum_{i=0}^{\infty} g(n)e^{-j\omega n} \quad (14)$$

But performing direct truncation of the Fourier series  $g_d(n)$  to  $M$  terms to attain  $g(n)$  causes the ripples in the characteristic frequency response  $H(\omega)$ . This arises due to the non-uniform convergence of Fourier series at discontinuity. The Oscillatory behavior close to filter's band edge is known as Gibbs phenomenon. Thus, Eq. 14 represent the frequency response  $G(\omega)$  have ripples in frequency domain.

For significant reduction of these ripples, the multiplication of  $g_d(n)$  with  $w(n)$  containing a taper and decays slowly to zero rather than instantly as occurred in rectangular window. The  $g(n)$  represented in time domain is similar to convolution function  $G(\omega)$  in frequency domain, that observe the effect of smoothing  $G_d(\omega)$ .

## 2.4 APPROXIMATION METHODS

- a. Butterworth Approximation (BA) –In pass band Butterworth approximation filter depicts the flat frequency response and known to be filter of maximally flat magnitude. The gain  $G_n(\omega)$  for  $n^{\text{th}}$  order low pass Butterworth filter as a function of discrete frequency  $\omega$  is given by Eq.(15)

$$G_n(\omega)^2 = \frac{1}{1 + \left(\frac{j\omega}{j\omega_c}\right)^{2N}} \quad (15)$$

Butterworth filter design gives monotonic amplitude response in both passband and stopband and slightly exhibit non-linear phase response.

- b. Chebyshev I Approximation (ChA) - Chebyshev I approximation filters have steeper roll-off as compared to Butterworth filters but exhibits ripples in passband . The gain  $G_n(\omega)$  for  $n^{\text{th}}$  order low pass Chebyshev I filter is defined in Eq. (16)

$$G_n(\omega)^2 = \frac{1}{1 + \epsilon^2 T_n^2\left(\frac{j\omega}{j\omega_c}\right)} \quad (16)$$

Where  $\epsilon$  is the ripple characterization parameter

And  $T_n^2$  is the Chebyshev function of degree N.

Chebyshev filter design provides decent selectivity with moderate complexity and has non linear phase response that leads to phase distortion.

- c. Elliptic Approximation (EA) - Elliptic approximation design exhibit equiripple for both passband and stopband. It provides the fastest transition from passband to stopband. The gain  $G_n(\omega)$  for  $n^{\text{th}}$  order low pass Elliptic filter is defined in Eq. (17)

$$G_n(\omega)^2 = \frac{1}{1 + \epsilon^2 R_n^2\left(\xi \frac{j\omega}{j\omega_c}\right)} \quad (17)$$

Where  $R_n$  is  $n^{\text{th}}$  order elliptical rational function and  $\xi$  is the selectivity factor derived from stopband attenuation

## 2.5 FAMILIES OF DISCRETE WAVELET TRANSFORM

- a. Daubechies - Daubechies is the first wavelet family that constructs compactly orthogonal wavelets with a pre-assigned degree of smoothness to build discrete wavelet practicable. The Daubechies family wavelets are designated as dbN, such that N is the order and db is called as wavelet ‘family name’. Different classes of Daubechies wavelet are classified as db4, db5, db6, db7, db8. Fig 1 represents the Daubechies db6 wavelet.
- b. Biorthogonal - This type of wavelet exhibits linear phase property, which is needed for signal and image reconstruction. In bior two wavelets are used one for decomposition and the other for reconstruction of signal. A biorthogonal wavelet is a wavelet where the associated wavelet transform is invertible but not necessarily orthogonal. Designing biorthogonal wavelets allow more degree of freedom than orthogonal wavelets. One additional degree of freedom is the possibility to construct symmetric wavelet functions. Biorthogonal wavelet is further classified as bior3.5, bior3.7 and bior3.9.



- c. Reverse Orthogonal- This family is derived from the wavelet pairs of biorthogonal that are further classified as rbio4.4, rbio5.5, rbio6.8.
- d. Coiflets –This type of wavelet has almost symmetric graphs which are similar to daubechies wavelet as they found to have large number of missing moments. Coiflets wavelet is further classified in to coif4 and coif 5.
- e. Symlets- The symlets are proposed by Daubechies is nearly symmetrical wavelet derived by modifying the db family. Symlets are the modified version of Daubechies wavelets with increased symmetry. Symlets are further classified as sym4, sym5, sym6 and sym9.